Winter Leaf Yellowing in 'Hass' Avocado

A thesis

submitted in partial fulfilment

of the requirements for the degree

of

Master of Science in Biological Sciences

at

The University of Waikato

by

ANDRIES J. MANDEMAKER

THE UNIVERSITY OF
WAIKATO
Te Whare Wānanga o Waikato

January 2007

Abstract

The New Zealand avocado industry is worth $39.7 million in exports of 'Hass' avocados. Crop yields grew steadily from 1996 to 2001 to reach an average of 8/86 tonnes/ha. Since then however, crop yields have remained steady. To increase returns to growers, crop yields must increase. Avocado leaves in New Zealand become yellow in winter and it is hypothesised that chilling, followed by photoinhibition, is leading to photooxidation. Leaf yellowing leads to reduced photosynthetic capacity and early leaf abscission, at a time when carbon fixation and carbohydrate reserves are needed to support developing flowers, subsequent fruit set and vegetative flush, in addition to the existing mature crop.

The focus of this research was to determine the underlying causes of yellowing in 'Hass' avocado leaves during winter. It is suspected that it is a result of the creation of free-radical oxygen that causes photooxidation of leaf components under excess light during low temperature conditions, such as experienced on clear winter mornings in the Bay of Plenty.

An orchard in Katikati, in the Bay of Plenty, New Zealand was selected has it had a history of leaf yellowing. Two open flow, differential gas exchange measurement systems, The CIRAS-1 and the CMS-400 were used to monitor leaf photosynthetic performance over the course of the 2006 winter, with particular focus on the month of August. Chlorophyll *a* fluorescence was measured with a Walz Mini-PAM, leaf colour with a Minolta Chroma meter CR-200b and chlorophyll content with Minolta SPAD chlorophyll meter (in addition to traditional extraction techniques).

There was conclusive evidence that the cold nights resulted in decreased net photosynthesis over the winter, with the depression starting in May and ending around the middle of August, dates that coincide closely with the period when days with mean temperatures <10°C occurred. The decrease in photosynthesis appears to be due to a direct effect on the carbon reduction pathway and in unusual in that full recovery seems to occur at the same time during the day. No photodamage of significance was found and

the avocado seems to be highly protected against high light when photosynthesis is inhibited. This investigation found that leaf yellowing is not caused by photodamage following depressed photosynthesis.

A new hypothesis is proposed which suggests that leaf yellowing is produced by the re-allocation of nitrogen from leaves during cold weather during flowering. It is suggested that the chilled leaves are seen as unproductive, old or shaded leaves by the plant and nutrient resources are re-allocated away from these leaves.

A foliar application of 1% low biuret urea and 0.5% magnesium sulphate is currently used by avocado growers to restore leaf colour in leaves that have become yellow over winter. An experiment was carried out on yellowed leaves on 23rd August 2006 to determine the effectiveness of the treatment. This study concluded that the treatment was able to restore some leaf colour, but had no effect on leaf photosynthetic function.

Acknowledgements

Don't be afraid to go out on a limb… that's where the fruit is.

Anonymous

Dedicated to the memory of Derek Smith

Table of Contents

List of Figures

List of Tables

1 Introduction

1.1 The New Zealand avocado industry

The New Zealand economy is driven by exports from the primary sector. Horticultural exports have grown from $100 million to over $2 billion since 1980 and the New Zealand avocado industry is an important part of this export led industry.

The largest growing area for avocados in New Zealand is along the Bay of Plenty coastline, predominantly between Waihi and Te Puke, contributing approximately 1,789 ha and 62% of the total avocado crop in New Zealand. The Far North and Whangarei regions contribute the majority of the remaining crop, with relatively minor plantings throughout the rest of New Zealand (South Auckland, Gisbourne, Taranaki). Only the 'Hass' cultivar is exported from New Zealand and exports were worth $39.7 Million in the 2005/06 season (Avocado Industry Council, 2006). New Zealand avocados are exported to Australia and the United States, with small volumes heading to Korea and Japan in an attempt to extend marketing opportunities. New export markets in Europe are currently being developed. It should be noted however, that total New Zealand avocado production is insignificant by world standards (about 1%).

1.1.1 Limitations on growth and sustainability of the New Zealand avocado industry

The New Zealand avocado industry has set goals for growth and sustainability including an average yield target of 15 tonnes/ha. The targets can be met in part through increased production per hectare as well as by sustainable increases in planted area. Land area planted in productive avocado trees (5 years and older) has increased rapidly from 946 ha in 1997 to 2902 ha in 2006 (Avocado Industry Council, 2006). Productivity per hectare more than doubled between 1996 and 2001, from 3.65 tonnes/ha to 8.86 tonnes/ha, due to

greater commercialisation of avocado growing operations and the industry wide adoption of phosphorus acid injections as a treatment and preventative of *P. cinnimomi* root rot (J. Cutting, per. comm.). However production has not increased significantly since 2001. To increase profitability to growers and other industry stakeholders in New Zealand, per hectare production must increase, without a reduction in fruit quality. To achieve a further increase in productivity in the future, the New Zealand avocado industry will require both a greater understanding of avocado physiology and the development of refined methods of avocado production.

1.1.2 Limits to avocado tree productivity

A wide range of orchard practices, pest pressure, environmental conditions and tree life history can affect avocado crop yield. Low fruit set and poor fruit retention has been recognised as of concern to the industry and imposes limits on the profitability of individual orchards (Cutting, per. com.). The maintenance of high photosynthetic capacity and overall plant carbon productivity is seen as being central to meeting any fruit production targets. Orchardists should aim to maintain robust, photosynthetically active leaves and trees with sufficient resources to sustain heavy fruit sets to maturity (Whiley *et al.*, 1988). The maintenance of good starch reserves going into flowering is important for fruit set and retention. The productivity of leaves in winter may have a major impact on starch accumulation in the wood, flowering, fruit set and fruit growth (Dixon, 2006). Problems such as irregular bearing, a pattern of high and low crop yields over subsequent years may be linked to either excessive demand for carbohydrate or to insufficient carbohydrate reserves that may be exacerbated by poor photosynthetic capacity during winter. Typically, an avocado tree in New Zealand will have two shoot flushes each year and one main flowering occurring in spring (Dixon, per.com.).

Surprisingly, considering the length of domestication of avocados, there appears to be very little information about the photosynthetic abilities of avocado leaves. This is particularly so for New Zealand where there have been no studies of leaf gas exchange in

orchard conditions. Problems with the photosynthetic processes might be anticipated because the plant is sub-tropical in origin and is thought to be close to its southern limit where it is grown in New Zealand. There has also been considerable interest in the occurrence of leaf-yellowing. Leaf yellowing has been observed to follow periods of cold temperature in winter and is viewed as an important problem because it may restrict leaf longevity. The winter yellowing of the leaves is considered to be an indication of a decline in leaf chlorophyll content and it is assumed that this results in a large reduction in net photosynthetic rate and consequential decline in carbon reserves.

A foliar application of urea and magnesium sulphate is currently used by avocado growers to mitigate leaf yellowing in winter. The treatment consists of a 1% low biuret urea and 0.5% magnesium sulphate solution applied in sufficient volume to achieve spray run off. The recommended time of spray application is at the first signs of leaf yellowing. Anecdotal evidence suggests that the spray treatment can be effective in returning leaf colour to green (H. Pak, per. comm.). However, it is not known if a return of leaf colour also indicates a return of photosynthetic performance. The foliar spray could potentially be restoring leaf colour while having no effect on leaf photosynthetic performance.

Due to the strong sink demand for plant nutrients during late winter, early spring with the development of flower inflorescence, a new spring shoot flush and existing fruit, any application of urea could potentially be translocated to the flower inflorescence and new shoot flush in preference to utilisation in the leaves. As there is a high demand for nitrogen during winter (Bar, Lahav & Kalmar, 1987), any urea application timed to coincide with this demand, is likely to be beneficial in restoring leaf nitrogen levels and promoting growth of flower inflorescence and new shoot flush.

With further understanding of avocado ecophysiology, the management of leaf yellowing could potentially be a tool to maintain optimal photosynthetic leaf function all year round.

1.1.3 Leaf yellowing – an hypothesis

Avocado is one of many species of tropical or sub-tropical origins that are grown outside their original range. Other examples include citrus, maize, cucumber and tomato. Typically, it appears that these plants show little ability to develop chilling or frost tolerance. Chilling is when a plant shows negative responses to low temperatures that are above freezing point. A common response to chilling is the occurrence of photoinhibition (indicating photosystem damage) that can be transitory or photo-oxidation that indicates longer term damage. A feature of this damage is that although the tissues of the leaf are chilled overnight it is only when high sunlight intensity occurs following the chilling that the photodamage manifests itself. In the Bay of Plenty it is normal that cool temperatures occur on very clear nights and are almost always followed by a clear day with high sun insolation from dawn onwards.

The focus of this research was to determination the underlying causes of the yellowing in 'Hass' avocado leaves during winter in New Zealand. It is suspected that it is a result of the creation of free-radical oxygen that causes photo-oxidation of leaf components under excess light during low temperature conditions, such as experienced on clear winter mornings in the Bay of Plenty (Halliwell & Gutteridge, 1989). As a framework for the research the following hypothesis for the occurrence of leaf yellowing was formulated on the basis of research conducted on other susceptible plant species.
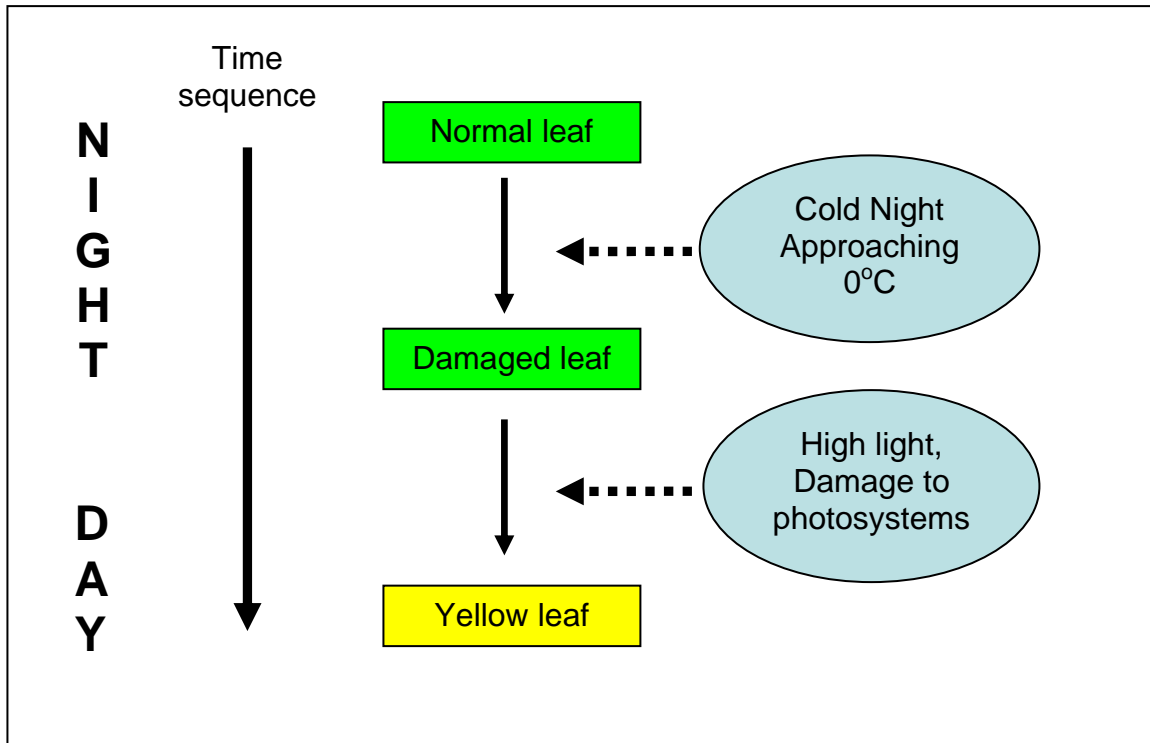
Figure 1.1   The premise: time sequence of overnight leaf chilling, leading to leaf-yellowing after exposure to high incident light levels the following day.

The premise that a time sequence of overnight chilling, followed by high light exposure leading to leaf-yellowing was used as a framework for this research (figure 1.1). The leaf is first chilled overnight at temperatures approaching freezing point, causing damage to part of the carbon fixation pathway or to the photosystems themselves. The following morning the high incident light cannot be utilised by the photosystems either because they, themselves are damaged, or there is no carbon fixation. The excess light then damages the photosystems and leads to photoinhibition that can be detected using chlorophyll *a* fluorescence techniques that measure photosystem II quantum efficiency. Continued or repeated damage will lead to photodestruction and a loss of photosynthetic activity and chlorophyll destruction leading to yellowing of the leaves.

Figure 1.2 Typical winter leaf yellowing, note flower buds forming on apex of stem.

1.1.4 Foliar application of urea as a restorative treatment for leaf function

Foliar application of 1% low biuret urea and 0.5% magnesium sulphate is currently used by avocado growers to restore leaf colour in leaves that have become yellow (Cutting, per. com). However, there is currently no knowledge or research finding to confirm that the return of leaf colour (i.e. chlorophyll) also indicates the return of photosynthetic performance. The foliar nitrogen spray could potentially be restoring leaf colour while having no effect of photosynthetic performance. A second aim of this research was to provide insight into this foliar treatment and provide an evaluation of its true effectiveness.

1.2   Summary of the research

This research aimed to:

1. Provide information about the photosynthetic performance of avocados in New Zealand,

2. Quantify the extent to which chilling reduces photosynthetic performance, and

3. Quantify the effectiveness of the current industry practice in returning photosynthetic function.

This research attempted to reach these aims by regular monitoring of plant physiological parameters and by conducting an experiment to evaluate the effectiveness of the foliar urea an magnesium treatment. The foliar application of urea as a restorative treatment for leaf colour experiment is designed to test two hypotheses:

- Avocado leaves with evidence of photo-oxidation will have reduced chlorophyll content, maximal net photosynthesis and maximal quantum efficiency compared with leaves without evidence of photo-oxidation.

- Treating photo-oxidised avocado leaves with a foliar application of 1% low biuret urea and 0.5% magnesium sulphate will return chlorophyll content, maximal net photosynthesis and maximal quantum efficiency of PSII to pre-chilling levels more rapidly than untreated leaves.

2 Literature review

2.1 Overview of *Persea americana*

Avocado (*Persea americana* Mill.) belongs to the aromatic *Lauraceae* family, of which only one other genus, *Cinnamomum* is cultivated. All *Persea* species studied have a chromosome number of $2n = 24$. The avocado tree is evergreen, forming a dome canopy up to 20m tall (figure 2.1). When grown in close proximity, trees will form a single closed canopy. Shoot growth occurs in flushes, alternating with root growth flushes.

Figure 2.1 Left: 'Hass' avocado tree in spring, with young replacement tree in foreground. Right: 'Hass' avocado fruit.

Leaves are arranged spirally along stems and are variable in both size and shape. The leaf blade is elliptic to lanceolate, ovate or obovate and has a simple shape and smooth, entire leaf edge. The veins and midrib are prominent on both the dark green waxy upper surface and the light green glaucous lower surface. There are no stomata on the upper surface. Petioles are smooth and light green between 3 and 15cm in length. The leaves are often red and soft to the touch when young (Whiley & Schaffer, 1994). Avocado trees extend anchorage roots down to 3 to 4 meters when soil conditions permit (Whiley & Schaffer, 1994). However, a shallow root system provides the primary source of nutrient and water uptake. These roots are relatively thick and have few root hairs to assist nutrient uptake.

The pollination and fruit-set of avocado is highly inefficient, setting vastly more flowers than resultant fruit. Estimates of 100 - 300 flowers per fruit set have been proposed with up to 1.6 million flowers per tree (Cameron, Mueller & Wallace, 1952). Flowering branches can be functionally determinate or indeterminate, with the new flush developing from the apical tip of the inflorescence and competing for plant resources.

2.1.1 The origins of *P. Americana*

Avocado varieties present today are the product of thousands of years of human cultivation and are considered to be a cultigen, the product of both evolution and artificial selection back to antiquity. The commercial avocado *P. americana*, is classified into three subspecies or botanical varieties (also known as horticultural races); *Persea americana americana* or West Indian, *P. americana gautemalensis* or Guatemalan and *P. americana drymifolia* or Mexican (Bergh, 1992). The latter two subspecies carry names which are consistent with their accepted original locations. *P. americana americana* or West Indian sub-species, however, is believed to have originated in the tropical lowlands along the pacific coast of Central America and was moved to the West Indies after Spanish conquest (figure 2.2) (Bergh, 1985, 1992; Storey, Bergh & Zentmyer, 1986). Williams (1976) provides evidence that the Mexican sub-species was a precursor to the West Indian. The precise origins of the avocado sub-species is unknown due to the long history of utilization (Whiley & Schaffer, 1994), with evidence that avocado was in semi-cultivation as early as 8000-7000 years B.C. (Williams, 1976). By the time of the Spanish conquests in the 1500s, avocados had been spread throughout Central America and the Caribbean (Zentmyer, 1991).

Figure 2.2 Proposed centres of origin for Mexican, Guatemalan and West Indian ecological races of avocado. Modified from Storey *et al.* (1986).

2.1.2 The 'Hass' cultivar

A chance seedling of unknown parentage, selected by Rudolph Hass in California because of its high flesh quality, higher yield and later maturity than 'Fuerte' was patented in 1935 as the 'Hass' avocado variety (Hass, 1935; Newett, Crane & Balerdi, 2002). 'Hass' fruit are medium in size, up to 400g, with thick pebbled skin (Whiley, 1991). The fruit remain green whilst on the tree, but turn purple-black when ripe, after removal from the tree. The tree has a broad, upright growth habit and is less sensitive to cold temperatures than 'Fuerte' but is still affected by temperatures below -1.1°C (Newett et al., 2002). The proportion of determinate to indeterminate inflorescence is higher in 'Hass' than all other studied cultivars. 'Hass has an "A" type flower pattern (figure 2.3), less cold sensitive than 'Fuerte' cultivar, but with little protection below 0°C (Whiley, 1991).

10
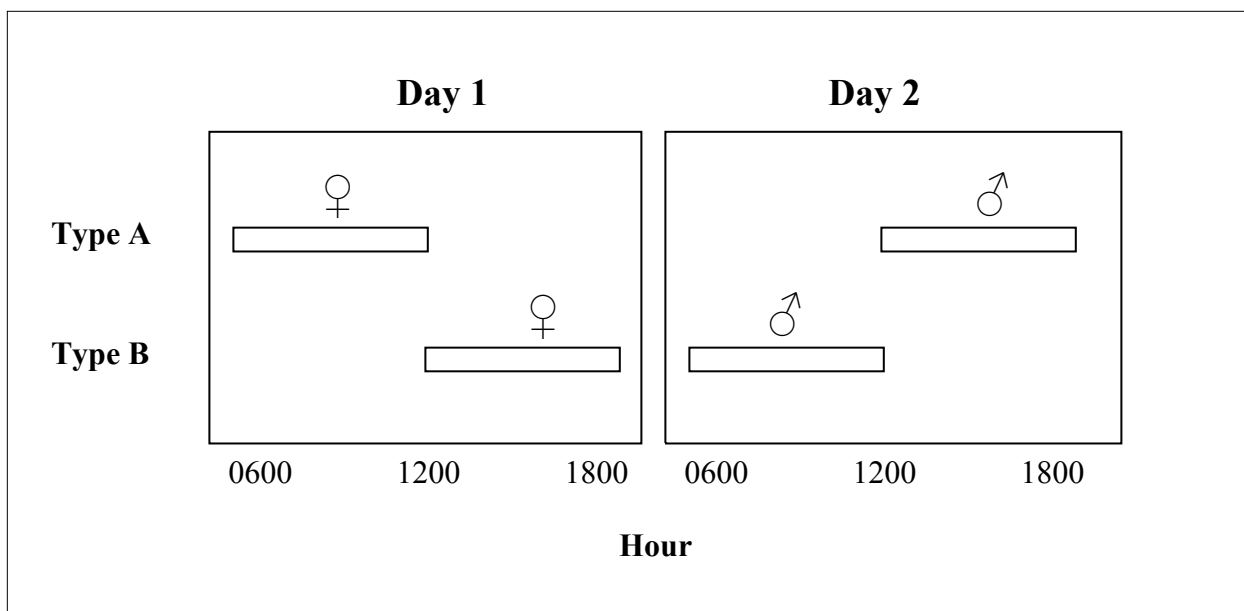
Figure 2.3 The sequence of flower opening in type "A" and type "B" avocado cultivars over a 48-hour period. Horizontal bars indicate the period that flowers are open. (Whiley & Schaffer, 1994)

2.2   Avocado production in New Zealand

The majority of New Zealand avocados orchards are located along the coastal Bay of Plenty, the Mid North/Whangarei and the Far North regions of the North Island. The principle concerns when identifying suitable orchard locations are climate, contour and avoidance of soils prone to water saturation.

The Avocado Growers' Association of New Zealand (2006) makes best practice recommendations for the temperature minimums for avocado orchard placement. Ideally the microclimate of the orchard will ensure only mild frosts, down to -4°C occur during winter. Avocado trees are most susceptible to frost during flowering, and any frost will damage developing flowers, resulting in non-viable flowers. Day time temperatures during flowering above 20°C and night time temperatures above 10°C are thought to be required for consistent fruit set (Avocado Industry Council, 2006). The current locations of New Zealand's avocado orchards reflect the temperature requirements as set out above.

11

The commercial production of avocado in New Zealand is almost exclusively limited to the 'Hass' cultivar and 'Hass' is currently the only cultivar being exported. Seedlings of 'Zutano' cultivar are widely used as rootstock. Small numbers of other rootstock cultivars are also grown including 'Reed' and 'Fuerte'. Inter-planting non-commercial cultivars as polleniser plants is common to help increase fruit-let retention and crop yield through cross pollination. Having type "B" cultivars, inter-planted with type "A" 'Hass' trees (such as 'Zutano' and 'Bacon') is popular. The effectiveness of inter-planting of polleniser plants, given the reduced number of producing trees per hectare, has not yet been conclusively shown under New Zealand conditions (Avocado Industry Council, 2006).

The majority of avocado orchards in the Bay of Plenty region of New Zealand are grown without irrigation. This places them at risk of drought due to the shallow rooting nature of avocado trees. Irrigation is frequently applied using a 'recipe' approach, applying a given volume across a given period of time. However the use of tensiometers, with a cyclic irrigation and drying cycles is recommended.

Over irrigation is as detrimental to production as under irrigation as water logging can lead to the development of Phytophthora root rot (*Phytophthora cinnamomi*) (Avocado Industry Council, 2006). Avocado fine roots have a low proportion of air space and are dependent on soil oxygen to avoid anoxia, especially during warm soil conditions. The air space is not so low as the around 3% found in kiwifruit but the sensitivity to anoxia is similar and flooding is to be avoided at all times in the summer (Smith et al. 1989).

2.3 Ecophysiology of avocado leaves

2.3.1 Original habitat

There appears to be little information about the environment of the avocado in its natural habitat. In a summary, Wolstenholme & Whiley (1999) emphasise that the tree is typical of medium altitude cloud forests in the tropics and sub-tropics with populations existing in highlands of Central America. The climate in the presumed native habitat of avocado is summarised in Praloran (1970) with additional information from Mackintosh (2000) (table 2.1). Annual mean temperature at Tauranga were warmer than the higher site in Mexico and the range between coldest and warmest month was greater (9.5 ^{o}C versus 5.9 ^{o}C) reflecting its temperate location. The mean temperature of the coldest month was the same for the Tauranga and higher Mexican site. These data suggest immediately that if there is a temperature limitation to the performance of avocado at the Bay of Plenty site then these would be expected to be in the winter.
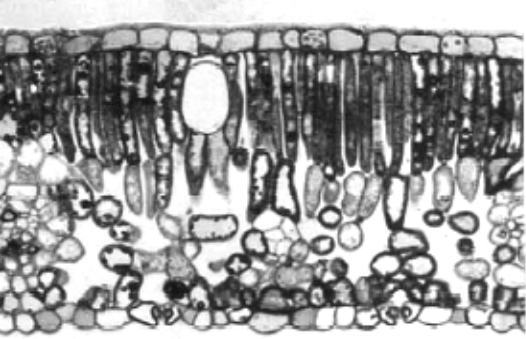
Table 2.1 Microclimate of selected natural avocado growing environments and Tauranga, New Zealand. Data from Praloran (1970) and Mackintosh (2000).

Location	Altitude (m)	Rainfall (mm)	Mean temperature (^{o}C)		
			Annual	**Warmest month**	**Coldest month**
Mexico	1399	1562	17.5	19.8	14.2
	2675	665	12.8	15.6	9.7
Guatemala	1502	1394	19.6		
	2350	671	14.9		
Tauranga	10	1799	14.5	19.2	9.7

2.3.2 Leaf adaptation

Wolstenhome and Whiley (1999) have characterised the leaves of avocado as being low sun/low stress according to the classification of (Smith *et al.*, 1989). Such leaves are large, laminar broadleaf, relatively thin (less than 400 µm, figure 2.2), hypostomatous, showing bicolouration, with single palisade layer held horizontal and with medium to low maximal photosynthetic potential. This description indicates that the tree is best considered as a small gap coloniser or under story tree within forests. The environment of a gap coloniser or under story plant is not stress-free, with the fluctuation of light intensity being a particularly important and potentially damaging to leaf function. A rapid change from the low light when cloudy, to the high light when the sky clears or sun fleck fall on the leaf, has the potential to cause damage to the photosystems of the chloroplasts. In such a situation the avocado tree cannot be completely adapted to either shade or full sunshine and must be able to handle large and rapid changes in its environment.

Table 2.2 Thickness of the layers in a 'Hass' leaf (from Chartzoulakis et al. 2002).

Layer	Dimensions (µm)	
Upper cortex	14.9	
Palisade layer 1	72.8	
Palisade layer 2	34.0	
Spongy mesophyll	65.3	
Lower cortex	14.0	
Total	203.1	

2.3.3 Leaf gas exchange

Somewhat surprisingly for a plant that has been so long in domestication and has wide commercial importance, there seems to have been only a small number of detailed studies into the gas exchange of the avocado leaf. The most important are those of Heath and associates (Heath, Arpaia & Mickelbart, 2005; Mickelbart *et al.*, 2000)and Whiley and Schaffer (Schaffer & Whiley, 2002, 2003; Schaffer, Whiley & Kohli, 1991; Whiley, 1994).

Table 2.3 Some examples of maximal CO_2 exchange rates (A_{max}) and stomatal conductance (from various authors).

Authors	A_{max} ($\mu mol\ m^{-2}\ s^{-1}$)	Stomatal conductance ($mmol\ m^{-2}\ s^{-1}$)	Comments
(Mickelbart & Arpaia, 2002)	7 - 8		Hass, California Container grown
(Heath *et al.*, 2005)	Up to 20	300	California Orchard grown
(Schaffer, 2006)	10 - 12		Queensland
(Whiley *et al.*, 1999)	19		Queensland
(Schaffer *et al.*, 1991)	9		Queensland
(Kimelmann, 1979)	6		Israel
(Heath *et al.*, 2005)	20		New Zealand
(Heath *et al.*, 2005)	9	150	

It is accepted (Heath *et al.*, 2005) that CO_2 exchange rates are lower for avocado trees in California. This is thought to be a result of the higher vapour pressure deficient (VPD) in that environment. It is also known that many of the early measurements of CO_2 exchange

rates were made on plants grown in containers. These appear to have suffered from some form of limitation, possibly root restriction and had substantially lower rates than similar trees in the normal orchard (Whiley *et al.*, 1999). It seems that, under optimal conditions that CO_2 exchange rates can reach between 15 – 20 $\mu mol\ m^{-2}\ s^{-1}$ and the single data point available from New Zealand is 20 $\mu mol\ m^{-2}\ s^{-1}$, estimated from a response curve of CO_2 exchange rates to CO_2 concentration (table 2.3). It is often suggested that CO_2 exchange rates will be reduced by low water availability, cold temperatures and low VPD.

Avocado leaves seem to have a very large photosynthetic capacity, up to 50 $\mu mol\ m^{-2}\ s^{-1}$, but are limited by CO_2 concentration to less than half this rate under normal orchard conditions (Heath *et al.*, 2005). This is a relatively unusual situation as leaves normally saturate at less than 1000 ppm CO_2 and not at the much higher levels of over 1500 ppm CO_2 found for avocado (Körner, 2000; Lawlor, 2002). There seems to be no simple explanation for this situation which may indicate some complex interaction between leaf structure, physiology and environment.

Avocado leaves have often been referred to as shade leaves because of their low light saturation level for photosynthesis of around 20 – 33% of full sunlight (Whiley, 1994). These studies, however, were on container grown plants and studies of orchard trees suggest that saturation can be at much higher PFD of around 1100 $\mu mol\ m^{-2}\ s^{-1}$, or over 50% of full sunlight (Wolstenholme & Whiley, 1999). This suggests that avocados are closer to being sun plants than originally thought. It is generally accepted that there is a strong link between stomatal conductance (gs) and net photosynthetic rate. Several examples of the response are available and all are linear or near linear over the stomatal conductance range found in orchard pants (Heath *et al.*, 2005). It is not clear whether stomatal conductance is the controller of net photosynthesis or vice versa.

2.3.4 Leaf age and photosynthetic capacity

Avocado is an evergreen tree with a leaf longevity of 10 to 12 months (Wolstenholme & Whiley, 1999). This is a relatively short leaf life span compared to other evergreen fruit trees such as citrus and mango (Whiley & Schaffer, 1994). Leaf growth occurs during two distinct flushes (figure 2.4), one in spring and the other in summer/autumn with most leaves abscising during the subsequent year's growth. (Lui *et al.*, 2002). As leaves grow and age, physiological changes alter the photosynthetic performance as the leaf passes from a sink to a source of photoassimilates.

Figure 2.4 Vegetative flush on 'Hass' avocado tree

Schaffer *et al*. (1991) (1991) monitored changes in leaf area, dry weight, specific area, chlorophyll concentration and gas exchange on field grown 'Booth-8' and 'Peterson' cultivars over two years. In both cultivars net CO_2 assimilating increased until about 42 days after bud-break and then levelled off. Maximal CO_2 assimilation was approximately 5 $\mu mol \ m^{-2} \ s^{-1}$ and 8 $\mu mol \ m^{-2} \ s^{-1}$ for 'Booth-8' and 'Peterson' cultivars respectively. For 'Peterson' cultivar, net CO_2 assimilation began to decrease after 70 days until 133 days, when frost caused leaf abscision. The increase in CO_2 assimilation as leaves age is not due to stomatal conductance as this remains relatively constant with leaf age (Schaffer et al., 1991). Heath *et al.* (2005) linked plastochron index of leaf age to

carbohydrate productivity by monitoring changes in chlorophyll content as a proxy for carbohydrate productivity. Total chlorophyll content increased by 11 mg m^{-2} per day to a maximum of about 550 to 650 mg.m^{-2} by plastochron day 30 to 40. Chlorophyll content reached 50% of total content 8 days after leaf size achieved 50% leaf area growth.

In 'Hass' trees, field grown in California, maximum CO_2 assimilation occurred 50 days after bud-break. This corresponds to the time when leaf colour has developed to dark green leaf colour (Lui, Hofshi & Arpaia, 1999).   For individual leaves, net CO_2 assimilation became positive after 17 days, at a time when the previous season's leaves are performing at 50% of their previous maximum. Whole tree net CO_2 gain was achieved 20 days after new leaves fully expanded. (Lui et al., 1999).   Whole leaves continue to be sink for photoassimilates until about 40 days after bud break. (Schaffer & Whiley, 2003).   Although older leaves continue to play an important role in carbon supply (Lui et al., 1999), during periods of flush the younger leaves, still sinks rather than sources of photoassimilates, shade the older leaves, reducing overall carbon gain (Schaffer & Whiley, 2003).

2.3.5 Water relations and photosynthetic performance

During drought conditions and in un-irrigated orchards, soil water potential can become significantly reduced as to limit photosynthetic performance by reducing stomatal conductance. Chartzoulakis *et al.* (2002) treated container grown 'Fuerte' and 'Hass' plants with two irrigation regimes for 6 months. The wet treatment having irrigation applied when soil water potential reached -0.03 MPa and a dry treatment irrigated at -0.5MPa. In both cultivars stomatal conductance and photosynthetic performance was significantly reduced in the water stressed trees 5 days after withholding water. By day 12, photosynthesis had reduced by 27% and 35% for 'Fuerte' and 'Hass' respectively. "The relationship between photosynthetic rate and stomatal conductance was linear during the stress period" (Chartzoulakis et al., 2002). 'Fuerte' recovered pre-water stress

photosynthetic rate and stomatal conductance 2 days after re-watering, while in 'Hass' plants retained 20% lower values than that of controls (Chartzoulakis et al., 2002).

Responses appear to be very rapid on occasions and five hours after discontinuing irrigation of two year old potted 'Fuerte' plants, Ramadasan (1980) found a reduction in maximum net photosynthesis from 3.6 μmol m^{-2} s^{-1} to 1.3 μmol m^{-2} s^{-1}. This corresponded with an almost 3 fold decrease in stomatal conductance. Leaf water potential remained steady during this time. Stomatal conductance increased by 50% one hour after irrigation was restored and net photosynthesis had returned to pre-drying levels after 4 hours. Bower, Wolstenholme, & de Jager (1977) found very little decrease in stomatal conductance for soil moisture potentials between zero and -40kPa. Stomatal conductance was steadily reduced thereafter, being completely closed by -80kPa soil moisture potential. Bower (1978a) found that avocado plants are close to the stress threshold at moderately dry soil conditions.

It should be noted that these studies used potted plants and would have had a low volume of exploitable soil. This should be contrasted with the results obtained from South Africa where orchard grown 'Hass' avocado trees showed an excellent ability to tolerate water restrictions and maintained high stomatal conductance through high root hydraulic conductivity and extremely elastic leaf mesophyll cells (Sharon, Bravdo & Bar, 2001).

2.3.5.1 Root necrosis due to *Phytophthora cinnamomi* infection reduces photosynthetic performance

Schaffer & Ploetz (1989) examined potted 'Simmonds' trees inoculated with varying levels of *P. cinnamomi*, left for 4 weeks before applying a flooding treatment. In plants with root rot necrosis of $\leq$ 20%, net CO_2 assimilation and stomatal conductance decreased dramatically when flooded. In plants that were not flooded, net CO_2 assimilation and stomatal conductance was significantly reduced only in plants with $\leq$65% root rot necrosis (Schaffer & Ploetz, 1989). *Phytophthora cinnamomi* may reduce

net CO_2 assimilation by limitation of stomatal conductance, caused by reduced hydraulic conductivity of roots or reduced water uptake ability (Schaffer & Ploetz, 1989). The implication is that root health is important for maintaining productivity and a consideration of root health must be made when examining photosynthetic performance of avocado.

2.3.6 Optimum temperature range and upper and lower temperature limits for photosynthesis

There is a difference in temperature responses among the 3 ecological races (Mexican, Guatemalan and Lowland) of avocado (Krezdorn, 1970; Whiley & Schaffer, 1994). Studies and observations on growth and anatomical damage indicated that Mexican race cultivars are the most cold-tolerant, whereas Guatemalan race cultivars are intermediate in cold tolerance and Lowland (or West Indian) race cultivars are the least cold-tolerant. No comparisons of photosynthetic responses to temperature among races have been reported but it is probable that the photosynthetic responses would most likely parallel anatomical damage and growth responses to temperature (Schaffer & Whiley, 2002).

Photosynthetic rates of avocado may be significantly affected by slight fluctuations in temperature. For the 'Edranol', a Guatemalan hybrid cultivar, in containers, the optimal temperature range for photosynthesis was 20-24°C (Bower, 1978b). Within ± 5°C of this temperature range, net photosynthesis declined by about 20%. For container-grown 'Fuerte' trees maximal net photosynthetic rates were at temperatures of 28-31°C and that rate decline by about 33% at temperatures below 15°C or above 40°C (Scholefield *et al.*, 1980). It was observed (Whiley, 1994) that temperatures lower than 10°C during winter significantly reduced apparent quantum yield of leaves of field-grown 'Hass' avocado trees from 0.055 µmol CO_2 µmol^{-1} quanta to 0.034 µmol CO_2 µmol^{-1} quanta.

In warm growing areas such as Florida and California, peak summer temperatures limit photosynthesis performance. Net photosynthesis was reduced to near zero in Californian

20

grown 'Hass' trees when leaf temperature was between 35°C and 40°C, correlating strongly with a reduction in g_s (Lui et al., 2002). "The photosynthetic characteristics of container grown 'Fuerte' tress indicated that the optimum temperature for assimilation was between 28-31°C" (Whiley & Schaffer, 1994). Assimilation was found to be maintained at 33% of maximal levels for temperatures above 40°C (Scholefield *et al.*, 1980; Whiley & Schaffer, 1994). Upper temperature limits are unlikely to be of concern for 'Hass' trees growing in New Zealand.

Avocados are affected by cold temperatures in two ways. First, there is the more dramatic and visually obvious damage caused by frosts and subzero temperatures. Second, there is the less obvious and not well researched effect of chilling, damage caused by cold temperatures above freezing point.

Avocados are very sensitive to frosts and the response is what might be expected for plants with subtropical origins. Frost damaged leaves become brown, darkening quickly and branches become defoliated (Scorza & Wiltbank, 1975) followed by damage to stems and branches and whole plant death during more severe frost events (Witney & Arpaia, 1991). During the December 1990 freeze in California, the minimum temperature in Tulare County was below -2°C for 14 consecutive days, reaching a low of -11°C. This freeze severely damaged or killed avocado trees, primarily 'Zutano' (Witney & Arpaia, 1991). In the Riverside/Corona area the minimum temperature fell to below -3°C for 14 consecutive days, reaching a low of -8°C, severely damaging 'Hass' trees. Scorza and Wiltbank (1975) evaluated 9 to 24 month old potted plants of 'Topa Topa', 'Mexicola', 'Waldin', Itzamma' and 'Gainesville' and reported 50% leave damage between -4.4°C and -7.2°C for unhardened plants.

The impacts of chilling on warm-climate plants has been recently reviewed (D. J. Allen & Ort, 2001). Chilling refers to non-freezing temperatures ($0 - 12^oC$) that can be relatively common in temperate regions, even in the growing season, and can substantially compromise plant productivity. Many crops cultivated in temperate climates (e.g.: maize, tomato, mango, cucumber and avocado) originate from tropical and

sub-tropical backgrounds and these species apparently lack the ability to become freeze or even chill tolerant.   It appears that chilling can disrupt all major components of photosynthesis including thylakoid electron transport, the carbon reduction cycle and control of stomatal conductance.   Unfortunately, with so many possible effects it is difficult to identify what the primary cause of chilling damage is in any particular species.

Photosynthesis following a dark chill is primarily compromised by interference with carbohydrate metabolism, inhibition of Rubisco activity and stomatal closure.   In particular, the role of the stromal bisphosphatases, SBPase and FBPase can be important. For tomato, the primary restriction imposed by a light chill is a decrease in the activity of these two enzymes cause by an impairment in their reductive activation (Hutchinson et al. 2000).   The reduction or absence of carbon reduction, and possibly associated stomatal closure, leads to an increase in energy dissipation as heat in the thylakoid antennae and possible temporary (photoinhibition) or more permanent (photo-oxidation) damage to the photosystems.   One consequence is that a collapse in photosystem activity and net photosynthesis can occur in sunlight following a chilling event.   A typical example is the collapse in photosynthetic ability of coffee species following chilling at $4^{o}C$ overnight (Guo & Cao, 2004).   A more complex situation is found in mango, where a night chill at $5^{o}C$ and $7^{o}C$ produced no immediate reaction but inhibition of photosynthesis followed in the middle of the following day, due to early stomatal closure, following disruption of circadian rhythms (J. A. Allen *et al.*, 2000).   The important points appear to be that chilling can occur at relatively high temperatures, up to $10^{o}C$, and that it is not at all easy to predict how a particular plant might respond.   Although little work on this problem exists for avocado it does appear that cold nights at around $8 - 10^{o}C$ can cause substantial declines in net photosynthesis, lowered from 19 to 10 μmol m^{-2} s^{-1}, apparent CO_2 quantum efficiency, 0.055 to 0.034 μmol CO_2 μmol^{-1} quanta, and optimal quantum efficiency of photosystem II (F_v/F_m) from 0.81 to 0.41 (Whiley *et al.*, 1999).   It is reasonable to expect that avocados in the New Zealand growing areas may be negatively impacted by winter temperatures when one considers that monthly mean daily temperatures are below $10^{o}C$ for two months of the year.

The sub-tropical origin of avocado and the cold temperatures in New Zealand growing areas in winter provide the basis for the hypothesis put forward for the occurrence of yellow leaves observed in New Zealand avocado tress. Essentially, the breakdown of the photosynthetic system (photooxidation) is expected to lead to a loss in chlorophyll providing the visible signal of damage.

Actual impacts of freezing and chilling may be altered slightly by the condition and pre-treatment of the plants. Cultivar, time of year, location, ice nucleating temperature, orchard conditions, tree age, leaf age and drought all influence the cold hardiness of avocado leaves (Krezdorn, 1973; McKellar, Buchanan & Campbell, 1983; McKellar *et al.*, 1992; Witney & Arpaia, 1991). During the 1990 California freeze (Witney & Arpaia, 1991) stressors such a nitrogen deficiency, *Phytophthora cinnamomi* infection and reduced canopy size due to pruning, increased an orchards susceptibility to frost damage. Exposure to low, non-damaging temperatures prior to exposure to freezing temperature may result in greater cold tolerance (Scorza & Wiltbank, 1975) by up to 0.6°C.

2.4   Leaf nitrogen content and fertilisation

Wolstenholme (2004) declared nitrogen to be the most important element in avocado nutrition. With careful management, inputs of nitrogen to an orchard have the capacity to increase yield, increase leaf longevity, modify growth towards vegetative or reproductive sinks, increase fruit quality and minimise leaching into ground water (Arpaia et al., 1996; Lovatt, 2001; Wolstenholme, 2004).

Leaf nitrogen content for spring flush leaves from fertilised trees in Israel was 1.9% dry weight during the first phase of growth (mid. June, northern hemisphere). Leaf nitrogen continued to increase as the leaves matured, till reaching a peak of 2.1% in the summer (late August). By autumn and winter leaf nitrogen content had settled at about 1.7%. As

the winter ended and the spring began leaf nitrogen content fell and by spring (mid. June) the one year old leaves had a leaf nitrogen content of 1.3% (Bar, Lahav & Kalmar, 1987).

Lovatt (2001) investigated the optimal timing of nitrogen fertilisation soil application to increase fruit yield and found a 70% increase in yield when fertilizer was applied "during anthesis to early fruit set and initiation of vegetative shoot flush at the apex of indeterminate floral shoots (mid-April)" compared with other times of the year. This is supported by Wolstenholme (2004) who reported that the greatest demand for nitrogen was during flowering and that nitrogen fertiliser applications could "improve the efficiency and longevity of photoinhibited over-wintered leaves."

In conjunction with flowering and shoot growth, trees may also be hanging the mature crop. 'Hass' avocado fruit are a strong sink for nitrogen (Lovatt, 1996), having 2.4% nitrogen by fresh weight at harvest, much higher than most tree fruits. In trees with insufficient leaf nitrogen, Zilkah, et al (1987) found that shoot growth from indeterminate inflorescences competed for nitrogen resources more strongly with existing, older leaves than with flowers.

2.4.1 Foliar fertilisation

For a foliar urea treatment to be effective in ameliorating the effects of photoinhibition, first the nutrients must penetrate the leaf surface and become available for utilisation by the leaf. Debate exists as to whether foliar applications of urea are able to enter via leaves and be avaiable to increase leaf nitrogen in leaves adapted to full sunlight, field conditions.

Generally plant leaf structures and functions have evolved to capture sunlight and exchange gases, therefore any absorption of nutrients by leaves is therefore likely to be more fortuitous than by design (Alexander, 1985; Newett, 2005). A thick cuticle layer, on both the upper and lower surfaces of avocado leaves limit translocation of nutrients

into the leaf. Investigations into foliar nitrogen application on avocado have proved conflicting. Early studies by *Aziz et al.* (1975) found that foliar sprays of urea increased fruit set, yield, and fruit size. However, Nevin & Lovatt (1990) and Newett (2005) suggest that the volume of spray applied was so great that significant amount of nutrient entered the plant via the soil and root uptake pathway. Lovatt (1994) found mixed results in an initial glasshouse trial using 'Hass' on 'Duke 7' rootstock produced a 50% increase in yield with a foliar application of Urea. A field trail the following year was unable to replicate the results.

Increases in leaf N of up to 50% were found by Li *et al.* (1997) when 50 year old 'Booth' and 'Lula' trees were sprayed with low-biuret urea. The increase was not sustained however, due to translocation of nitrogen from leaves to other plant structures but did lead to an increase in yield. Zilkah *et al.* (1996), working with 'Hass' trees in Israel found a 26% increase in leaf N when applying foliar low-biuret urea, which was maintained for one year. Additionally, the spray application was found to increase freezing tolerance by 2.5 times and reduced leaf senescence.

Low-biuret ^{14}C-urea was painted onto 'Hass' leaves to determine measure the ability of field grown plants to absorb N, using radioactivity tracking. Maximum uptake was achieved after 2 days of application, but as only 2.1% of applied urea entered the leaf it was assumed to be physiologically insignificant (Nevin & Lovatt, 1990). A further study by the same authors failed to increase leaf N significantly after applying low-biuret urea to young 'Hass' trees.

3 Materials & Methods

3.1 Study site

Field measurements were performed at a single avocado orchard southeast of Katikati, in the Western Bay of Plenty, New Zealand (S 37° 35' 23.4", E 175° 56' 0.50"). The Bay of Plenty is the largest avocado growing region in New Zealand, producing 62% of New Zealand's export crop in 2005. The orchard is approximately 5 meters above mean sea level and within one kilometre of the coastline of the Tauranga harbour.

Two neighbouring blocks were used. Block 'A' comprised of 176 'Hass' avocado trees on 'Zutano' rootstock planted in 1998 and reaching a height of approximately 6 meters by the winter of 2006. Block 'B' comprised of 180 'Hass' trees on 'Zutano' rootstock, planted in 2001 and reaching a height of approximately 3 to 4 meters by winter of 2006. Both blocks were inter-planted with 'Zutano' polleniser plants.

The orchard is actively managed, receiving a regular 'Cuttings mix' fertilizer regime, up to 8 Copper fungicide sprays per year and routine phosphorus acid injections to prevent *Phytophthora cinnamomi* root rot infection. An integrated pest management scheme, AvoGreen®, forms the basis of pest control decisions. The orchard is irrigated with micro sprinklers, with irrigation decisions made with the assistance of soil tensiometers. The orchard is equipped with automatic frost protection, in the form of over head sprinklers, triggered when the air temperature falls below 0°C, although the latter were disconnected in the area utilised for the research.

The orchard was selected because it has a history of leaf yellowing, the trees are of a suitable size for measurement and for practical reasons, having flat contours and an available electricity supply.

3.1.1 Climate

The long term mean annual precipitation in the Western Bay of Plenty, measured at the Tauranga climate station, amounts to 1198mm.   Tauranga receives 2260 hours of sunshine per year and 111 days of 1mm rainfall or greater. The mean annual temperature is 14.5°C, with the warmest month being January which has a mean temperature of 19.2 °C and a mean daily maximum of 23.9°C. The coolest month is July with a mean temperature of 9.7°C (figure 3.1). There are on average 42 days of ground frosts per year, the majority occurring between April and November (Mackintosh, 2000).
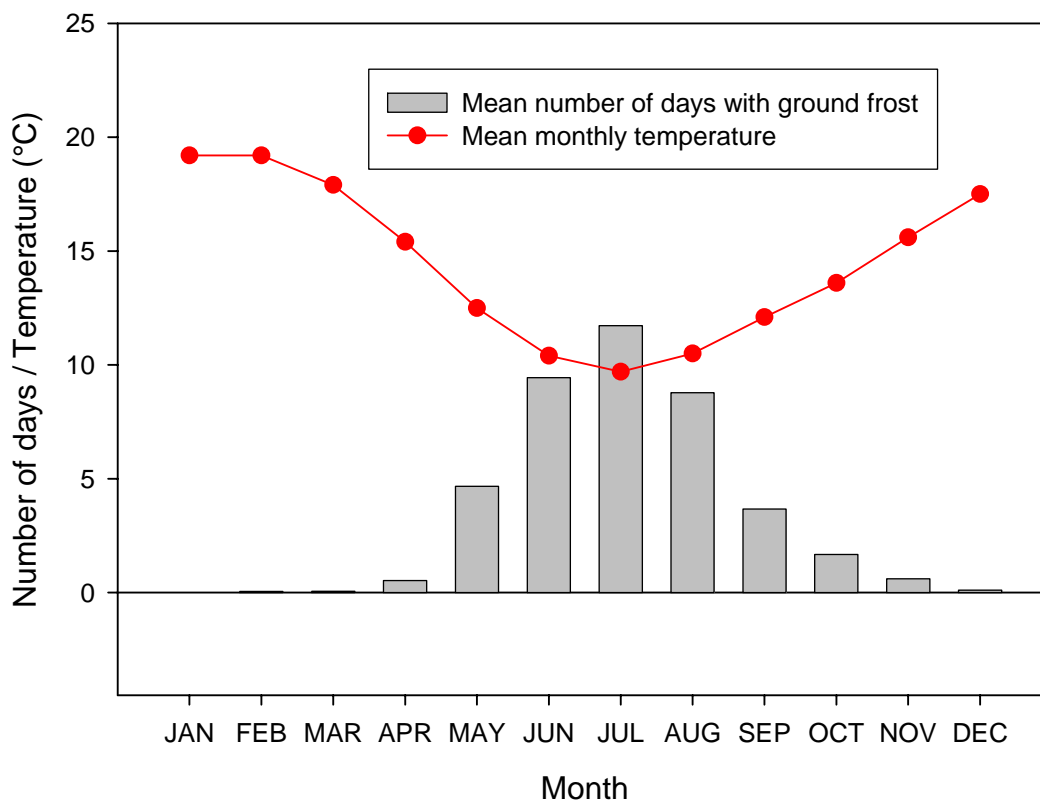
Figure 3.1 Climate of Tauranga, mean monthly temperature and number of days with ground frost. From dataset by Mackintosh (2000).

3.1.2 Soil

The orchard is situated on free draining, fluvial terrace deposits. These deposits post-date the Waiteariki Ignimbrite and have been washed down from the dark brown Waiteariki Ignimbrite on the foothills of the Kaimai ranges (Briggs *et al.*, 1996). Top soil is Katikati sandy loam (Rijkse & Cotching, 1995) approximately 200mm deep, classified using the New Zealand soils classification as Typic Orthic Allophanic soil (Hewitt, 1998). The soil taxonomy is Typic, Hapludands, medial, thermic (Soil Survey Staff, 1999). The soil is regularly augmented with a woodchip and compost mulch as a ring at the drip line of each tree.

3.2   Ecophysiological measurements

The theory used at the start of the research to explain the occurrence of leaf yellowing is fully described in Chapter 2. The key features are a decline in net photosynthesis of leaves following cold temperatures, damage to the chloroplast photosystems by excess light, especially on bright sunny days that typically follow cold winter nights, and recovery following spraying. The key parameters that were measured in order to prove this theory are those relevant to leaf gas exchange i.e. CO_2 exchange and water loss of leaves, stomatal conductance, chlorophyll content, leaf colour and chlorophyll fluorescence parameters as indicators of the state of the photosystems. These needed to be combined with recordings of ambient conditions, in particular air temperature, PFD and humidity.

3.2.1 Chlorophyll content measurement using SPAD meter.

Leaf chlorophyll content was measured non-destructively using a handheld Minolta SPAD-502 chlorophyll meter (Minolta, Tokyo, Japan). The SPAD-502 (figure 3.2) measures the transmittance of red (650 nm) and infrared (940 nm) light through the leaf, produced in sequence by two LEDs. Chlorophyll has a high absorbance at 650nm (but is

unaffected by carotene) and extremely low absorbance at 940 nm. The transmission through the leaf is measured by a silicon photodiode. The ratio of transmission values at the two wavelengths is used to calculate SPAD values, a relative measure of chlorophyll content defined by Minolta (Minolta, 1989). The machine is simple to operate and needs only to have the "jaws" clamped onto the leaf to take a reading.

Figure 3.2 The SPAD-502 chlorophyll meter. (Photo: Minolta, Tokyo, Japan)

3.2.1.1 Calibration of SPAD values

A calibration between the SPAD values produced by the Minolta SPAD-502 and chlorophyll *a* and *b* concentration in avocado leaves was completed on 5th of May 2005. Twenty leaf disks, 10mm in diameter and avoiding main veins, were taken from block "A" of the orchard. Leaves were selected on appearance to represent as full a range as possible of leaf chlorophyll content, from yellow through to dark green. Each disk was measured with the SPAD-502 meter and then placed in a tube containing a small volume of 80% acetone and 20% 0.05M aqueous Tris buffer and kept at 0°C in the dark. Upon return to the laboratory, the leaves were ground with a mortar and pestle and allowed to

extract in darkness for 12 hours at 4°C. The extract was centrifuged for 10 minutes at 3900 rpm. The supernatant was decanted and made up to 10ml with extraction fluid. A Shimadzu UV-VIS spectrophotometer (Shimadzu Corporation, Tokyo, Japan) was used to measure the absorption of each sample at 663.6 nm and 646.6 nm (the absorption peaks of chlorophyll *a* and *b* respectively) and 750 nm (to correct for any reduced clarity of the extract), against a blank of extraction solvent. The absorption at 750 nm was subtracted from the absorbencies at 663.6 nm and 646.6 nm and Chlorophyll *a* (Chl *a*) and *b* concentrations (Chl *b*) were calculated following the equations of Porra, Thompson, & Kriedemann (1989):

$$[Chl\ a] = 12.15\ A^{663.6} - 2.55\ A^{646.6}$$

$$[Chl\ b] = 20.31\ A^{646.6} - 4.91\ A^{663.6}$$

$$[Chl\ a + b] = 17.76\ A^{646.6} - 7.34\ A^{663.6}$$

where $A^{663.6}$ and $A^{646.6}$ are the absorbance values at the corresponding wavelengths, less the absorbance at 750nm. Chlorophyll concentration of the abstract was in $\mu g\ ml^{-1}$ from which total chlorophyll extracted could be calculated and, from that, leaf concentrations obtained as $\mu mol\ m^{-2}$. Regressions were fitted to the data and used to change SPAD values to chlorophyll content using SigmaPlot 8.0 (Systat Software Inc., San Jose, CA, USA) software.
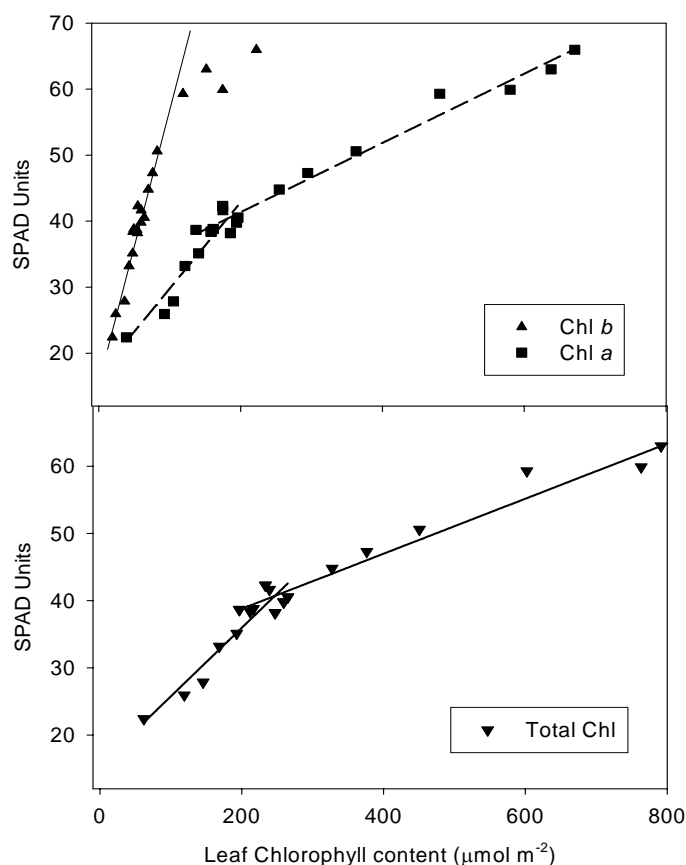
Figure 3.3 Calibration of SPAD units against chlorophyll concentration (μmol m^{-2}). Upper panel: Chlorophyll *b* – triangles, Chlorophyll *a* – squares. Lower panel: total Chlorophyll – inverted triangles. The fitted lines are all significant at P < 0.0001 and R^2 > 0.96

The calibration graphs (figure 3.3) show a sharp inflection at about 180 μmol m^{-2} for Chl *a* and Chl *b*, and slightly higher for total chlorophyll. There seems to be no explanation for this but it means that Chl *b* is linear over almost all its content range because it is always much lower than Chl *a*, whilst Chl *a* and total chlorophyll show the inflection. A similar inflection was found for mangrove plants (Catherine Beard, personal communication) so it appears not to be a feature of the avocado plants. The fit of the graphs is very good (R^2 > 0.96) indicating that the chlorophyll levels can be relatively accurately determined without damaging the leaf by using the SPAD. Whilst the inflection must clearly be taken into account for accurate determinations of chlorophyll

31

content it is not so important when declines in content are being followed qualitatively when SPAD units alone will give a good indication of chlorophyll levels.

3.2.2 Photosynthetic gas exchange measurements

3.2.2.1 Infrared Gas Analysers

There are several ways to assess the gas-exchange involved with photosynthetic activity from the classic manometric methods introduced by Otto Warburg in the early 20th century to modern techniques such as photoacoustic spectrometry. However, at present the non-dispersive infrared gas analysis is the most widespread procedure to assess photosynthetic CO_2 uptake and water vapour loss (Hall & Rao, 1999; Hunt, 2003; Long, Farage & Garcia, 1996; von Willert, Matyssek & Herppich, 1995).
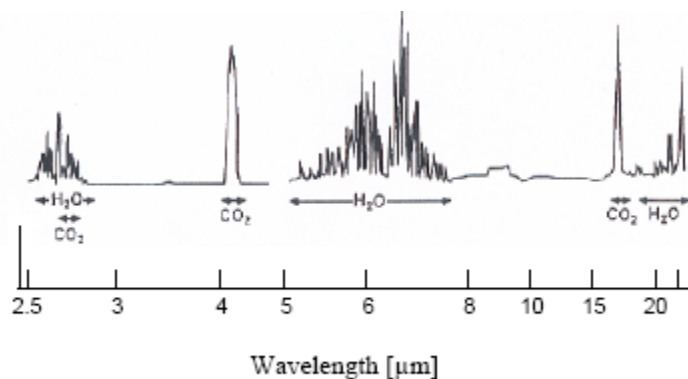
Figure 3.4 Infra red absorption bands for CO_2 and H_2O (from Sestak *et al*. 1971, in von Willert *et al*. 1995)

Both systems used for measuring leaf gas exchange (H_2O and CO_2) during the study, the CIRAS-1 and the CMS-400, utilised infrared gas analysers (IRGAs). IRGAs measure CO_2 and H_2O vapour concentrations in air. Hetero-atomic gas molecules, including CO_2, H_2O, NH_3, CO, N_2O and NO absorb radiation at specific sub-millimetre infrared

wavebands. Gas molecules consisting of two identical atoms, including major air components O_2 and N_2, do not absorb this radiation. The major absorption band for CO_2 is at 4.25 μm, with secondary bands at 2.66, 2.77 and 14.99 μm (figure 3.4). Both CO_2 and H_2O vapour absorb infrared wavelength radiation at known coefficients. The Beer-Lambert law describes the absorption at any wavelength and provides a method of determining gas concentrations given a fixed distance between radiation source and detector.

$$E = \epsilon \times c \times d$$

where E is the extinction in radiation, ϵ is the absorption coefficient of the regarded gas, c equals the concentration of the regarded gas and d is the distance between the radiation source and detector. The IRGA has to be calibrated with air streams containing zero and a known CO_2 concentration after which it is possible to continuously measure the CO_2 concentration of an air stream passing through the measurement cell of the IRGA.

IRGAs are used in two modes, differential and absolute. An absolute IRGA consists of a single gas cell through which the air flow passes; the extinction of infrared radiation in the cell is compared with stored values obtained when zeroed with CO_2-free air and calibrated with a known CO_2 concentration. Differential (or dual beam) IRGAs have two gas cells, the analysis and reference cells and the difference in CO_2 in these cells is measured. The infrared radiation is pulsed (mechanically using a 'Chopper blade' in the CMS-400, electronically in the CIRAS-1) through both gas cells and the detector compares the amount of radiation passing through each cell (Long *et al.*, 1996).

33

Motor

Photoelectric gate

← IR Source **(a)**

← Chopper blade

← Duplex filter

Gas Inlet (with filter)

← Gas cell **(b)**

Gas Outlet

← Filter Cell **(c)**

← IR Detector **(d)**

Signal processing electronics
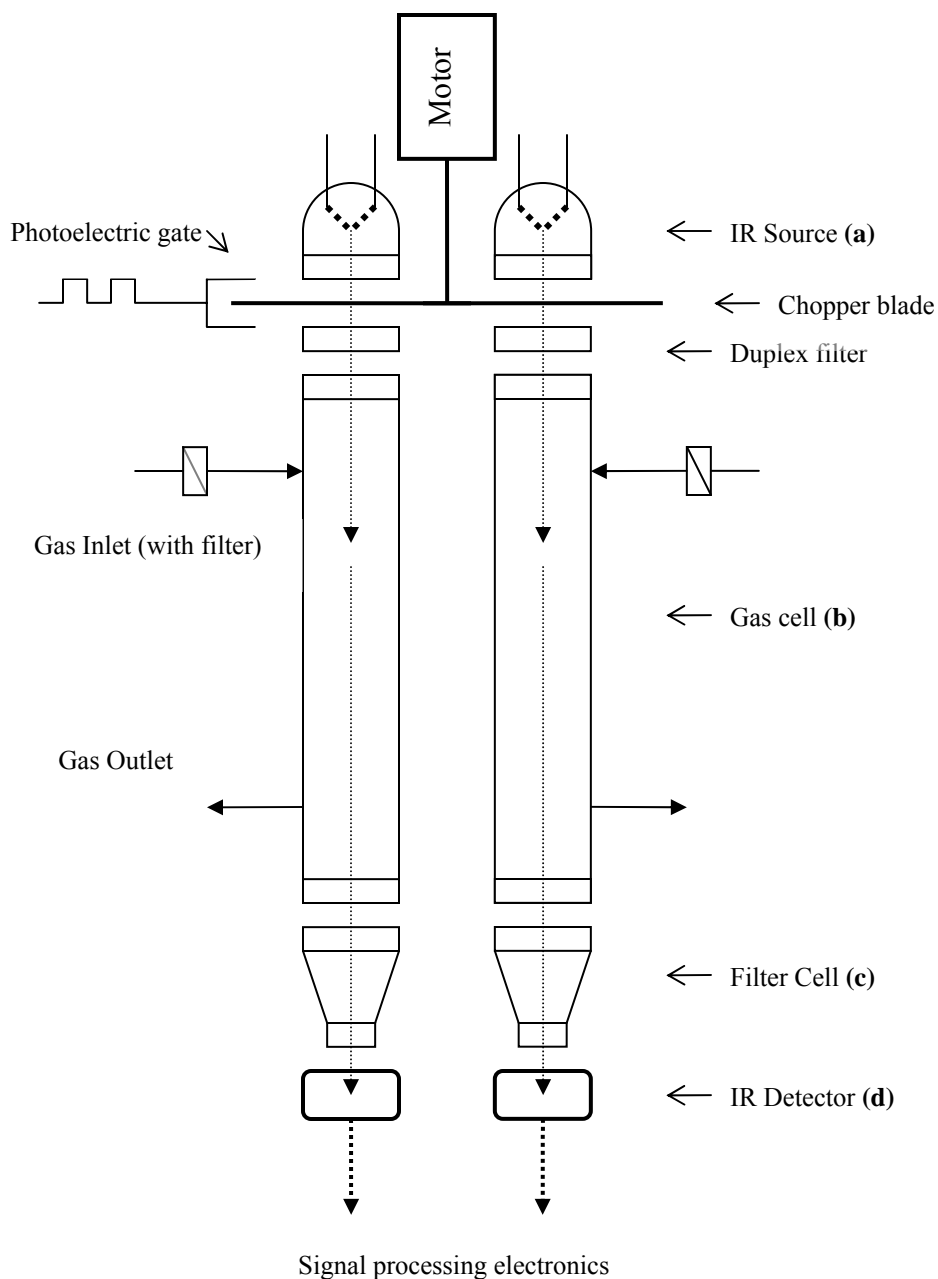
Figure 3.5 Schematic representation of the photometer assembly of the BINOS-100 infrared gas analyser, as used in the CMS-400 photosynthesis system. See text for explanation of identifying letters. Modified from BINOS-100 operation manual.

The schematic representation of the photometer assembly within the CMS-400 IRGA in figure 3.5 highlights the four basic parts of any IRGA. A broad-band infrared radiation source **(a)**, a gas cell with inlet and outlet for gas flow **(b)**, an optical filter to limit the

radiation reaching the detector to the wavelengths absorbed by the specific gas **(c)** and an infrared radiation detector **(d)** (Long *et al.*, 1996). Gas exchange systems can be open or closed. An open system, as used by all the equipment in this investigation, passes part of the air flow over the leaf or plant part being measured and then allows it to flow to waste after being measured by the appropriate IRGAs. Typically, a conditioned air supply is produced which has a defined or smoothed CO_2 concentration. This air supply is then divided into two streams one passing over the leaf, the measurement or analysis stream, and the other is passed unaffected or through a dummy cuvette to the IRGAs, the reference stream.

3.2.3 The CIRAS-1

The CIRAS-1 (Combined infra-red gas analysis system) is a battery powered, portable, open, differential gas exchange measurement system (PP Systems, Massachusetts, USA) that measures the uptake or loss of CO_2 and the loss of water by the leaf (figure 3.8). The CIRAS-1 utilises four absolute infra-red gas analysers (IRGAs), two measuring H_2O and two measuring CO_2, with one of each type on the analysis and reference air streams in an open flow system. The supply air stream is conditioned for CO_2 concentration using an internal supply of CO_2 provided by small soda charge cylinders (Kayser, Berndorf, Austria). Figure 3.6 below shows a simplified model of the gas flow and operation of the CIRAS-1 while figure 3.7 shows the details provided by PP Systems. Ambient air is drawn from the environment before being scrubbed of CO_2 by soda lime, and, if required, dried with Drierite® in a series of columns **(a)**. An automatic control system **(b)** regulates the addition of pure CO_2 from the canister **(c)** to achieve a selected CO_2 concentration (ideally around 360ppm). A solenoid valve separates the air flow, with the reference stream flowing directly to the reference IRGAs **(d)** and the analysis stream flowing to the leaf cuvette **(e)**. The air flow returning from the cuvette is passed through the analysis IRGAs **(f)**. The CIRAS-1 measures the CO_2 and H_2O differentials (ppm), absolute CO_2 (ppm), leaf and air temperature, relative humidity and flow rates. It is capable of calculating net carbon assimilation rate (*A*), transpiration rate (*E*), stomatal conductance to water vapour (g_s) and sub-stomatal cavity (internal) CO_2 concentration (C_i), based on

the equations by von Caemmerer and Farquhar (1981). The CIRAS-1 used PP Systems firmware v.4.8 and data was downloaded to a computer using PP Systems Transfer Software v1.03 (PP Systems, Massachusetts, USA).
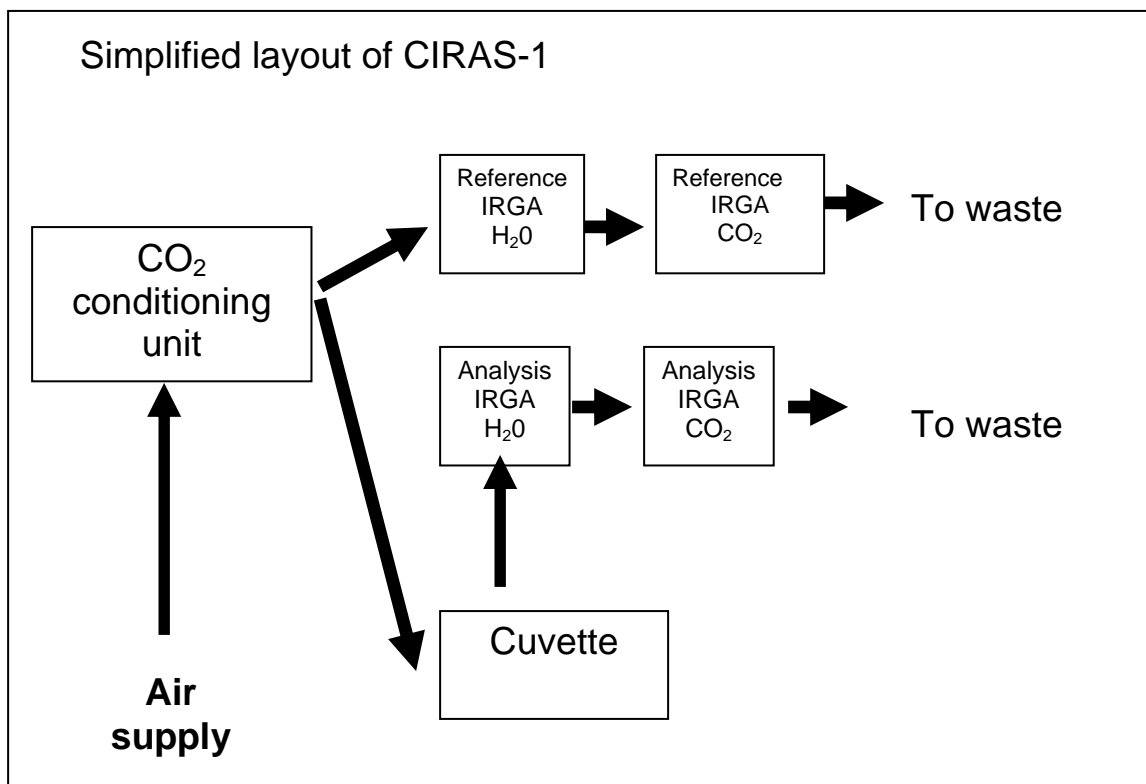
Figure 3.6 Simplified Flow diagram of the CIRAS-1 analyser gas circuit. Modified from CIRAS-1 Portable Photosynthesis System Operator's Manual Version 1.30 (PP Systems, Massachusetts, USA).
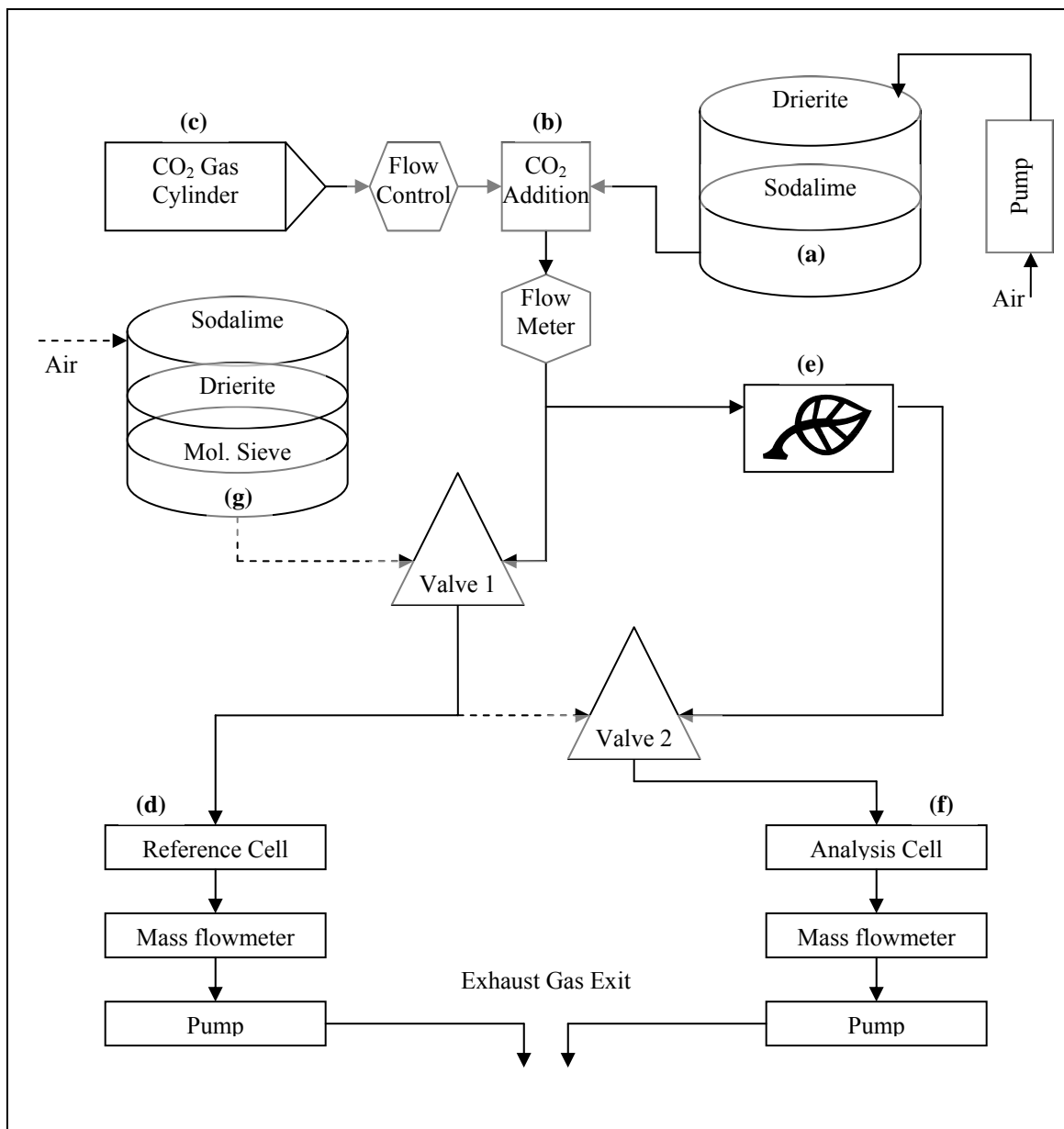
Figure 3.7 Flow diagram of the CIRAS-1 analyser gas circuit in measure mode. Dashed line indicates flow during zero and diff-balance modes. Refer to text for explanation of identifying letters. Modified from CIRAS-1 Portable Photosynthesis System Operator's Manual Version 1.30 (PP Systems, Massachusetts, USA).

3.2.3.1 Zero and diff-balance modes

The CIRAS-1 has an unusual configuration with four absolute IRGAs, two measuring CO_2 concentration and two measuring water vapour concentration. The systems are so arranged that there is one of each IRGA type on the analysis and reference air streams. The difference between the two airstreams is then calculated as the difference between the two paired IRGAs i.e. for the CO_2 differential, it is the difference between the CO_2 IRGAs on the measurement and reference air streams. To achieve the required accuracy the system has two modes that allow the outputs of the paired IRGAs to be fully aligned, the zero made and the diff-balance mode. During zero mode ambient air is drawn through Sodalime, Drierite and molecular sieve (**g**) to create CO_2-free air, which is passed through both analysis and reference IRGAs and a zero CO_2 setting is made. The diff-balance mode passes air from the reference stream (therefore containing CO_2) through both the analysis and reference IRGAs and a differential factor is calculated to correct for any offset differences in the IRGAs. A similar routine is carried out at the same time for the H_2O IRGAs.

Figure 3.8 The CIRAS-1 (Combined infra-red gas analysis system) portable, open, differential gas exchange measurement system (Photo, PP Systems, Massachusetts, USA)

3.2.3.2 Handheld Parkinson leaf cuvette (PLC)

Measurements were made by enclosing part of a leaf in a hand-held Parkinson leaf cuvette (PLC). Two PLCs were used, firstly a manual cuvette with an external light source where saturating light was provided by a quartz halogen light unit with a heat filter and cooling fan. This unit provided a light intensity of 950 to 1000 μmol m^{-2} s^{-1} on a 12 volt external battery supply. Preliminary studies showed that this was about 20% above the light level required to saturate photosynthesis for an avocado leaf. On 22nd July 2006 the cuvette was replaced with a PLC(u) automatic leaf cuvette. Light for the PLC(u) was provided by an integrated, self-regulating LED light unit complete with cooling fan, controlled by the CIRAS-1 interface and set at 1000 μmol m^{-2} s^{-1}. Measurements of maximal net photosynthetic rate were made under ambient temperature conditions and saturating light intensities provided by the lamps. The cuvette was clipped onto the leaf and measurements taken once net CO_2 exchange had reached a steady state. The PLC could also be used without the attached lamps and then the gas exchange rates were measured under ambient light levels.

3.2.4 The CMS-400

Continuous, automatic gas exchange measurements were collected using a Compact Minicuvette System (CMS-400) and a climatised cuvette (GK-022) with a custom built leaf chamber (Heinz Walz GmbH, Effeltrich, Germany). The CMS-400 is a mains powered, open flow differential system based on a central control unit (figure 3.9). Two differential IRGAs, measuring differences in CO_2 and H_2O concentrations between the analysis and reference air streams were housed in the central control unit in addition to an absolute CO_2 IRGA housed externally.

Figure 3.9 The CMS-400 mains powered, open flow, differential system for making continuous, automatic gas exchange measurements.
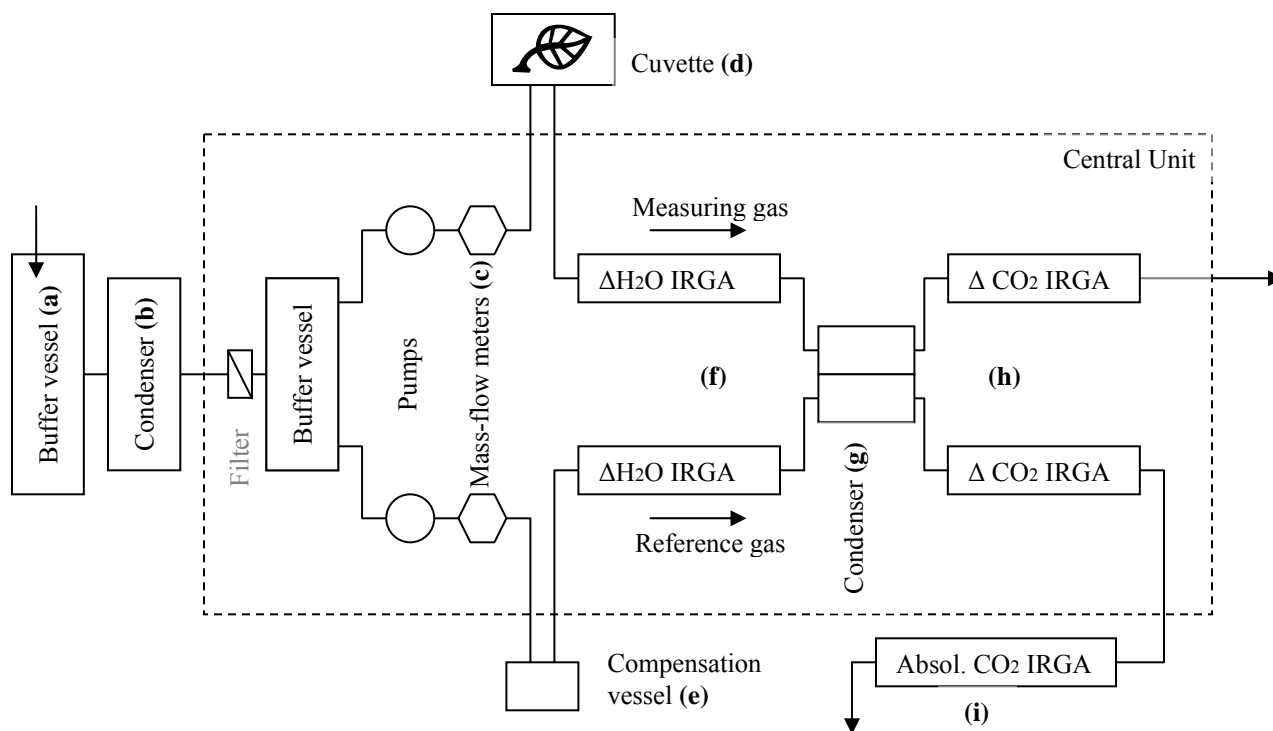
Figure 3.10 Air flow through the Walz CMS-400 photosynthesis system. Dashed line is the body of the central unit. Refer to text for explanation of identifying letters. (Modified from Central Unit CMS-400 manual, Heinz Walz GmbH, Effeltrich, Germany).

Figure 3.10 shows the flow of air through the CMS-400. Ambient air is drawn from nearby in the orchard by pumps within the CMS-400 central unit. The source was at approximately 1m above the ground and away from the movements of people. The air supply passed through a 200 litre, unstirred buffer vessel **(a) to** dampen short term fluctuation in air composition. The air stream then entered the main unit after passing through a MGK-4 condenser **(b)**, to adjust the air to a chosen dewpoint. The air flow was then divided into two streams, a measuring gas stream and a reference gas stream, with the flow within each stream controlled by mass-flow meters **(c)**. The measuring gas stream and a reference gas stream were operated at 2560ml min^{-1} and 1600 ml min^{-1} respectively. Unequal flow rates were used to compensate for differences between the residence times in the two gas streams and ensured simultaneous flow entry into the differential IRGAs. The flow rates were chosen after measuring residence times by

injection of CO_2 at the inlet point. The measurement stream passed via a 4.2m long PVC tube to the cuvette **(d)**. The reference stream passed through tubes of identical length and also an external compensation vessel **(e)** that partially imitated the cuvette. Both gas streams then flowed through an integrated differential H_2O IRGA (Rosemont Binos 100, Hanau, Germany) **(f)** to measure differences in H_2O concentration due to leaf transpiration, then a MGK-1 condenser **(g)** set at a dewpoint of 2^oC to lower the water vapour concentration. The two streams then flowed through a differential CO_2 IRGA (Rosemont Binos 100, Hanau, Germany) **(h)** to measure net CO_2 gain or loss in the analysis air stream (that includes the cuvette). The reference gas finally flowed to an external absolute CO_2 IRGA **(i)** to measure absolute CO_2 concentration (ppm). Both CO_2 and H_2O differential IRGAs were regularly zeroed by passing reference stream air through both sides of each IRGA until a stable value was reached. The absolute IRGA was zeroed with CO_2 free air, created by passing air through a soda lime column. A span calibration was completed with an alpha standard gas mixture (352 ± 3 ppm CO_2 in N_2).

3.2.4.1 The climatised cuvette

The cuvette consists of a climate unit (GK-022) with a plexiglass cuvette attached. The climate unit has a Peltier temperature controller with a stirred (fan) volume of about 500 ml (Figure 3.11). The temperature can be regulated over a range from -5^oC to $+45^oC$ and has the ability to track ambient temperature measured by a separate external thermistor probe. Parameters measured by the unit are RH, cuvette and leaf temperature, internal and external PFD. The climate unit had a specially designed plexiglass cuvette attached to it with one end open. The unit was arranged so that the lamina of a leaf closed the open end of the cuvette exposing 12 cm^2 of the underside of the leaf to the interior of the cuvette. In avocado leaves CO_2 exchange is entirely through stomata on the underside of the leaf (Blanke & Lovatt, 1993). Although the structure of the cuvette made temperature control less efficient this was not of major importance as the unit was always run in tracking mode so that the leaf was held at ambient air temperature.

Figure 3.11 The climatised cuvette attached to the CMS-400.

3.2.4.2 Ecophysiological parameters measured

The CMS-400 operated using firmware v 4.02 (Heinz Walz GmbH, Effeltrich, Germany) connected to a laptop computer, a Toshiba T2110/260 (Toshiba Corporation, Tokyo, Japan) operating DIAGAS software v 2.16 (Heinz Walz GmbH, Effeltrich, Germany). These programmes in combination controlled, monitored, calculated and stored gas exchange data from the CMS-400.

The following measured data were collected every minute:

- CO_2 differential δCO_2 ppm
- H_2O differential δH_2O ppm
- Leaf temperature T_{leaf} ^{o}C
- Cuvette temperature T_{cuv} ^{o}C

- External temperature T_{ext} ^{o}C
- Relative humidity   RH   %
- External light intensity Q_{ext} $\mu mol\ m^{-2}\ s^{-1}$
- Measuring flow rate   Flow   litres/min
- Vapour pressure deficit   VPD   hPa
- Absolute CO_2 concentration CO_2abs ppm
- Mol flow of CO_2 gCO_2 $mol\ s^{-1}$
- Mol flow of H_2O gH_2O $mol\ s^{-1}$

From which the following were calculated using the equations of von Caemmerer & Farquhar (1981):

- Photosynthetic rate   A $\mu mol\ m^{-2}\ s^{-1}$
- Transpiration rate   E $mmol\ m^{-2}\ s^{-1}$
- Stomatal conductance g_s $mmol\ m^{-2}\ s^{-1}$
- Sub-stomatal CO_2 concentration C_i ppm
- Leaf/atmosphere CO_2 gradient $(Ca – Ci)$ ppm

3.2.5 Calculation of gas exchange parameters in open gas exchange systems

Both the CIRAS-1 and the CMS-400 utilise open flow gas exchange systems to obtain differential values of CO_2 and H_2O of air at a given flow rate through a cuvette containing plant material. The equations of von Caemmerer & Farquhar (1981) provide the basis by which the CIRAS-1 and the CMS-400 calculate gas exchange parameter. The equations are outlined below:

Firstly, the transpiration rate (*E*) in mol $m^{-2}\ s^{-1}$ across a leaf area (*s*) in m^2 is calculated:

$$sE = u_ow_o\ \text{-}\ u_ew_e \tag{1}$$

where u_e and u_o are the molar flows of air entering and leaving the cuvette chamber and w_e and w_o are the mole fractions of water vapour in the gas streams entering and leaving the cuvette.

The rate of CO_2 assimilation (A) by the leaf, in mol m^{-2} s^{-1} per leaf area (s) in m^2 is calculated:

$$sA = u_e c_e - u_o c_o \tag{2}$$

where c_e and c_o are the mole fractions of CO_2 in the air going to and returning from the cuvette. However a further calculation is required to account for the increase in flow from the cuvette caused by the efflux of water vapour from the leaf:

$$u_o = u_e + (u_o w_o - u_e w_e) \tag{3}$$

CO_2 assimilation is calculated by combining equations (2) and (3):

$$A = (u_e/s)[c_e - c_o(1 - w_e/1 - w_o)] \tag{4}$$

Stomatal resistance (r_s) to water vapour loss from the leaf is calculated by:

$$r_s = [(e_{leaf} - e_{out}) / (E \times P)] - r_b \tag{5}$$

where e_{leaf} is the saturated vapour pressure at leaf temperature, e_{out} is the water vapour pressure of air leaving the cuvette, E is the transpiration rate from equation (1), P is the atmospheric pressure and r_b is the boundary layer resistance to water vapour.

Stomatal conductance (g_s) in mol m^{-2} s^{-1} is the inverse of stomatal resistance from equation (5):

$$g_s = 1/r_s \tag{6}$$

Stomatal conductance to CO_2 (g_c) in mol m^{-2} s^{-1} can be calculated with known ratios of diffusivities of CO_2 and water:

$$(g_c = 1/(1.6\ r_s + 1.37\ r_b) \tag{7}$$

where r_b is the boundary layer resistance and the ratio of diffusivities of CO_2 and water in air equals 1.6 and the ratio of diffusivities of CO_2 and water in the boundary equals 1.37.

Finally, the concentration of CO_2 in the sub-stomatal cavity (C_i) in μmol^{-1} is calculated using stomatal conductance to CO_2, assimilation rate and the transpiration rate:

$$C_i = [[(g_c - E/2)\ x\ u_o] - A]/ (g_c + E/2) \tag{8}$$

3.2.6 Principles of chlorophyll fluorescence

Since the discovery of the light/dark induction phenomenon in a dark adapted leaf following illumination, chlorophyll fluorescence has become ubiquitous in plant ecophysiology studies (Maxwell & Johnson, 2000). The development of highly user-friendly and portable chlorophyll fluorometers, instigated by the development of the modulated fluorometer and the saturation pulse method has lead to chlorophyll fluorescence becoming a standard method in plant physiology studies. Chlorophyll fluorescence measurements allow for non-destructive measurement of plant function and stress and can be used to track changes over extended periods of time.

Analysis of chlorophyll *a* fluorescence signals from Photosystem II (PSII) can provide information on the photosynthetic efficiency of plants and has been used extensively to examine the effects of stress, including chilling and freezing (Groom & Baker, 1992; Maxwell & Johnson, 2000). Changes in fluorescence values are indicative of the state of

46

PSII given that PSI is considered to be either non-fluorescent or only very weakly fluorescent. PSI fluorescence does not change significantly with changing proportions of photochemical and non-photochemical quenching of excitation energy at PSI.

The energy of light quanta is captured by the excitation of chlorophyll pigments in the antenna **(a)** (figure 3.12). The antenna consist of pigment protein complexes embedded in the thylakoid membrane (Schreiber, Bilger & Neubauer, 1994). There are three possibly fates for this excitation; 1) Photochemistry **(b)**, the energy drives photosynthetic processes and leads to carbon fixation or other processes such as the water-water cycle or 2) dissipation as heat **(c)** via non-photochemical quenching or 3) chlorophyll fluorescence **(d)**, re-emitted as longer wavelength light. Because the three possible fates compete for the absorbed quanta, fluorescence yield is highest when the yields of photochemical and non-photochemical quenching are lowest.
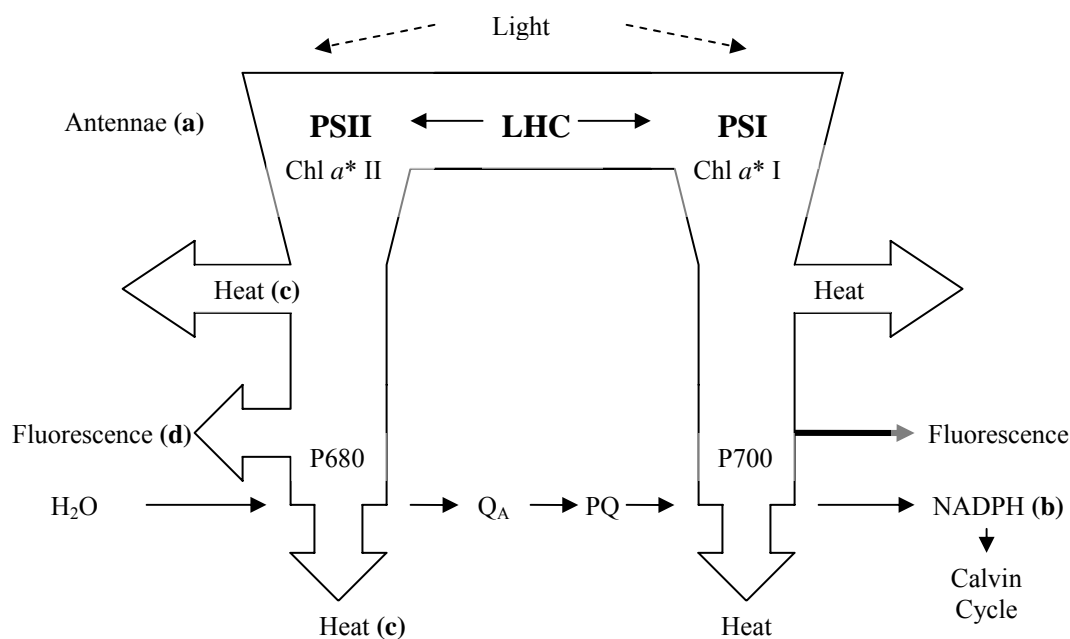
Figure 3.12 Schematic representation of the primary conversion in photosynthesis which governs *in vivo* chlorophyll fluorescence yield. See text for explanation of identifying letters. Modified from Schreiber *et al* (1994).

Because chlorophyll fluorescence is a longer wavelength (lower energy) than the original absorbed light, it is easily detected, despite only $1 - 2\%$ of the absorbed energy being re-emitted as chlorophyll fluorescence (Maxwell & Johnson, 2000).

A typical fluorescence trace is shown in figure 3.13, comparing relative fluorescence yield of a dark adapted leaf. Starting with the leaf in the dark, chlorophyll fluorescence yield is zero, until a measuring light is switched on. This low PPFD has no actinic effect, leaving all PSII reaction centres open and the first electron acceptor (Q_A) remains fully oxidised (Schreiber *et al.*, 1994; van Kooten & Snel, 1990). The fluorescence yield at this point is F_0, minimal fluorescence (dark adapted). A saturation pulse, a short duration of high intensity light, is then applied. All PSII reaction centres close and Q_A becomes fully reduced. This is recorded as F_m, maximal fluorescence (dark adapted). The difference between F_0 and F_m is the variable fluorescence (F_v), which in turn provides the intrinsic efficiency of PSII, F_v/ F_m, the quantum efficiency of PSII. Dark adapted values for F_v/ F_m reflect the potential (if all PSII reaction centres were open) efficiency of PSII and are used as a sensitive indicator of plant photosynthetic performance, with optimal values around 0.8 to 0.833 measured for most plant species. Values less than this are seen when plants are exposed to stress and there is an inhibition of photosynthesis (Maxwell & Johnson, 2000).
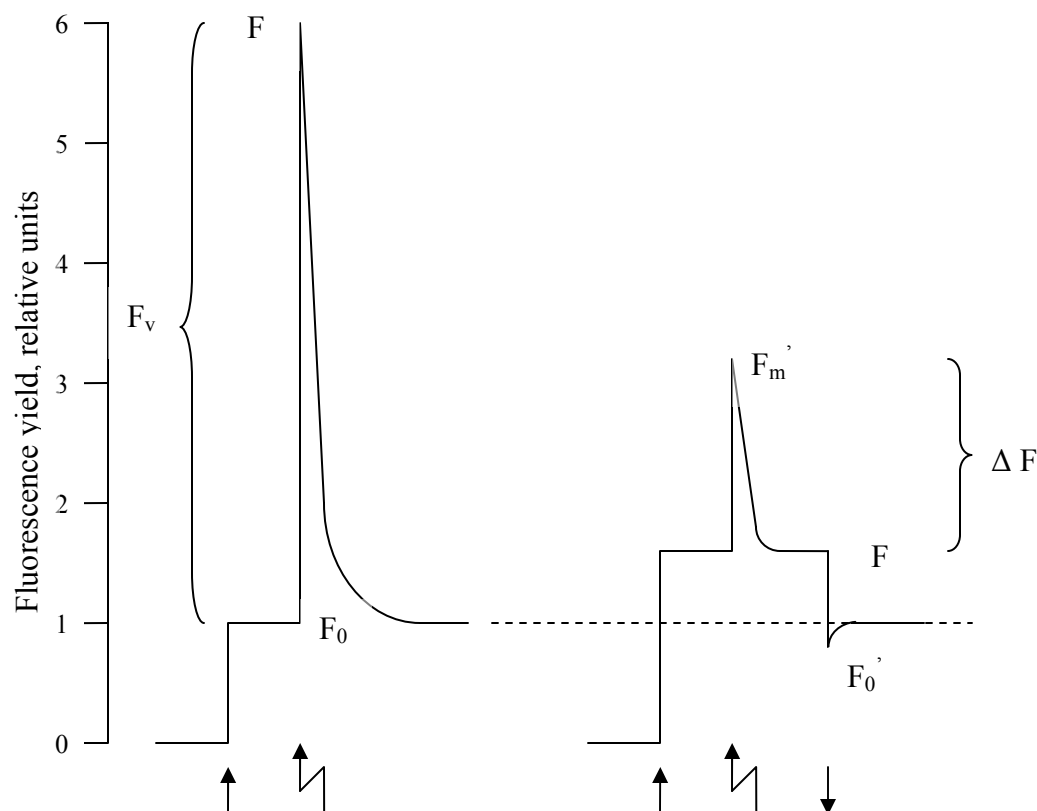
Figure 3.13 Fluorescence induction kinetics. Sequence of a typical fluorescence trace, in relative units, for dark adapted (left) and illuminated (right) leaves. Straight arrow represents measuring light (on or off) and the broken arrow represents a saturation light pulse. Modified from Schreiber *et al* (1994) and Maxwell & Johnson (2000).

After dark-adaptation, the fluorescence yield is defined as F_0 and the maximal fluorescence yield induced by a saturation pulse is Fm. During illumination the fluorescence yield is defined as F, with the maximal yield induced by a saturation pulse being Fm´ (see Fig. 3.13). The photochemical quantum yield after dark adaptation normally corresponds to the 'optimal quantum yield', which is lowered by illumination to an 'effective quantum yield'.

Optimal quantum yield:

$$(\Phi_{II})max = (F_m - F_0)/F_m = F_v/F_m \quad\quad\quad\quad\quad (9)$$

Effective quantum yield:

$$\Phi_{II} = (F_{m'} - F)/F_{m'} = \Delta F/F_{m'} \hspace{4cm} (10)$$

The fluorescence parameter $\Delta F/F_{m'}$ has been experimentally proven to be a reliable measure of PS II quantum yield for a variety of plants. Using PAM fluorometry and the saturation pulse method, $\Delta F/F_{m'}$ can be readily measured with a plant *in situ* under natural light conditions. Knowledge of the ambient quantum flux density (PFD) and of temperature is essential. If, for example, a sample shows a low $\Delta F/F_{m'}$, this could be due to an intrinsic deficiency (e.g. stress induced damage) or to high ambient light conditions or to low ambient temperature. For estimating the relative electron transport rate, ETR, the PFD apportioned to PS II is required. This information on energy distribution is normally not available and it is assumed that quanta are evenly distributed between the two photosystems. Also, only part of the incident light is absorbed. If no information on absorbance is available, it may be assumed that an average leaf absorbs about 84% of incident photosynthetically active radiation (Björkman & Demmig, 1987). Hence, the following expression may serve for an estimate of the relative electron transport rate in leaves:

Relative electron transport rate   =   ETR

                                           = $0.84 \cdot 0.5 \cdot PFD \cdot \Delta F/F_{m'}$

                                           = $0.42 \cdot PFD \cdot \Delta F/F_{m'}$

Normally, the absolute values of PS II absorbance and PS II quantum yield are uncertain and, as done in this investigation, the relative changes of ETR with environmental parameters are used and can be very informative. This is particularly true for the change of ETR with PFD. Plots of ETR versus PFD give light response curves that are analogous to corresponding curves obtained from gas exchange measurements. The slope at low PAR reflects maximal quantum yield (parameter α) and the plateau reached at light

50

saturation is a measure of photosynthetic capacity (ETR_{max} equivalent to the parameter P_{max}, defined as maximal gas exchange rate in P-I curves).

While healthy leaves are characterized by similar maximal quantum yields (0.80 – 0.85), they may display very different photosynthetic capacity, depending on their long-term light adaptation state during growth. In the case of leaves a quantitative comparison of absolute rates (e.g., as measured by gas exchange) and estimated rates based on PAM fluorometry is difficult due to the fact that the measured fluorescence primarily originates from the surface, whereas gas conventional P-I curves measured by gas exchange, at each PFD-value of a light response curve, require sufficient time for the sample to reach steady state during illumination. In practice, however, this is not done and such 'rapid light curves' depend strongly on the momentary state of light adaptation of a sample and, hence, vary considerably during the course of a day. The maximal relative electron transport rate, ETR_{max}, reached during rapid light curves generally increases during the morning, shows a dip at noon (mid-day depression) and increases again towards the evening. Diurnal changes in ETR_{max} reflect the photosynthetic performance of a plant in its natural environment.

3.2.6.1 The Mini-PAM and chlorophyll *a* fluorescence

The MINI-PAM (figure 3.14), like all PAM Fluorometers, applies pulse-modulated measuring light for selective detection of chlorophyll fluorescence yield. The actual measurement of the photosynthetic yield is carried out by application of just one saturating light pulse which briefly suppresses photochemical yield to zero and induces maximal fluorescence yield. The given photochemical yield then immediately is calculated, displayed and stored. Numerous studies with the previously introduced PAM Fluorometers have proven a close correlation between the thus determined YIELD-parameter ($\Delta F/F_{m'}$) and the effective quantum yield of photosynthesis in leaves, algae and isolated chloroplasts. With the help of the optional Leaf-Clip Holder 2030-B the photosynthetic active radiation (PFD) can also be determined at the site of fluorescence measurement, such that an apparent electron transport rate (ETR) is calculated. In

addition to this central information, the MINI-PAM also provides the possibility of measuring fluorescence quenching coefficients (qP, qN, NPQ), applying continuous actinic light for measurement of induction curves (Kautsky-effect) and automatic recordings of light-saturation. This quenching analysis was not used in this investigation where the emphasis was on monitoring changes in Photosystem II status and establishing the degree of photoinhibition or other light-induced damage.

Figure 3.14 The Walz Mini-PAM photosynthesis yield analyser (Photo T.G.A. Green).

3.2.7 The Minolta Chroma Meter CR-200b

The measurement of colour was conducted with a Minolta Chroma Meter CR-200b (Minolta, Osaka, Japan). The CR-200b is a lightweight and portable tristimulus colour analyser able to measure reflected light colour (figure 3.15). A pulsed xenon arc lamp in a mixing chamber provides even, diffuse light over the 8mm diameter sample area (figure 3.15) and measures the light reflected at a $0°$ viewing angle. Six high-sensitivity silicon photocells are used to measure both the reflected and incident light. By measuring

incident light, any variation in the spectral power distribution of the pulsed xenon arc lamp can be compensated for (Minolta, 2003). Prior to each use the CR-200b was calibrated against a standard white reflective plate. For each measurement the light unit was placed flat on the leaf surface, about midway along the leaf and clear of any vein or decolourisation, with a standard backing behind the leaf. Each leaf was measured three times, with each measurement within close proximity to each other. Values for each leaf were averaged.
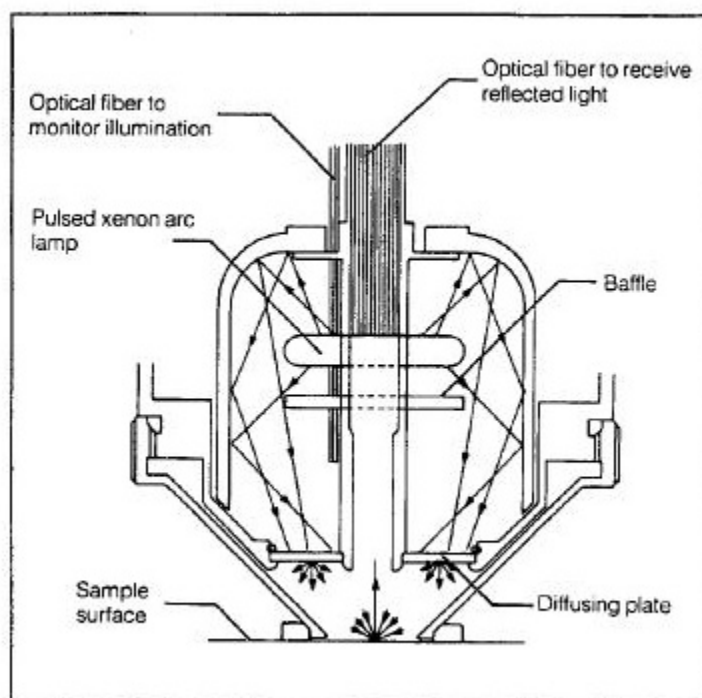
Figure 3.15 Diagrammatic representation of the head unit of the Minolta Chroma meter CR-200b. Note the xenon arc lamp, the diffusing plate and the 0° viewing angle. From the Chroma meter CR-200b manual (Minolta, 2003).

The CR-200b provides a digital output for chromaticity in a range of standards, however CIE (*Commission Internationale d'Eclairage*) 1976 L* a* b* colour coordinates were selected as this standard closely follows the sensitivity of the human eye. Each colour measurement is given as coordinates in 3 dimensional colour space. L* is the reflectance factor (Madeira *et al.*, 2003) or lightness variable where zero equals perfectly black and 100 equals perfectly white. This variable is represented as the vertical axis in figure 3.16.

53

The variables a* and b* are the chromaticity coordinates, with the a* variable representing green (- a*) to red (+ a*) and b* representing blue (- b*) to yellow (+ b*).
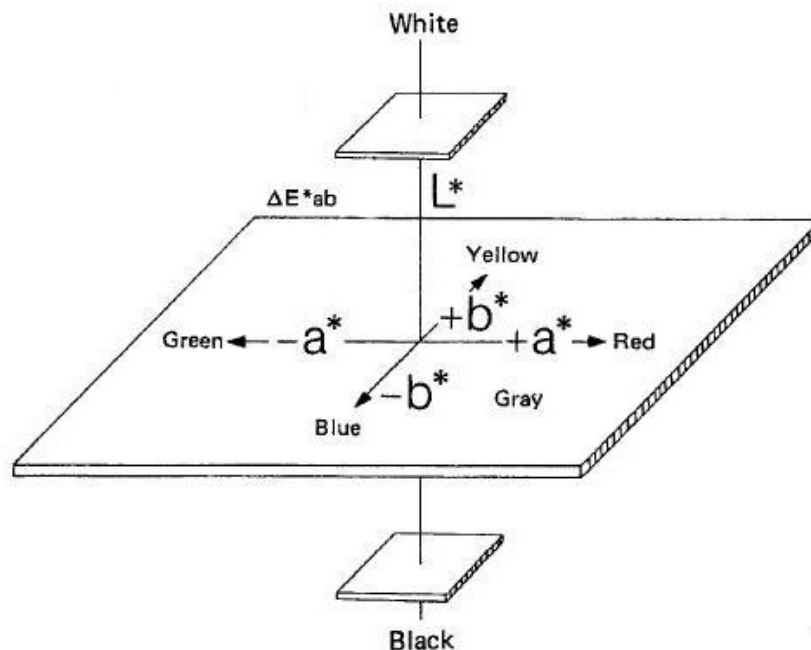
Figure 3.16 3D colour space for L*a*b* (CIE 1976) colour coordinates. Modified from Chroma meter CR-200b manual (Minolta, 2003).

3.2.8 Leaf water potential – Scholander Pressure Bomb

The technique is based on the Cohesion-Tension theory that water in the xylem ascents under negative pressure due the transpirational pull generated by evaporation into the atmosphere, as proposed by Dixon & Joly (1895). If this negative pressure were to be broken by the action of excising a leaf, the water within the xylem vessels will withdraw from the cut surface, being replaced with air from the atmosphere. Placing the leaf in a Scholander pressure chamber (Scholander *et al.*, 1965) with the petiole exposed and slowly increasing the external pressure on the leaf will force the water back to the cut surface (figure 3.17). The minimum pressure required is the balance pressure and is

assumed to be a direct measure of the tension that existed within the leaf prior to excision.

The following calculation was used to calculate water potential.

$$P = \Psi_w - \Psi_s$$

where P is the xylem pressure measured with the Scholander pressure bomb, Ψ_w is the water potential of the leaf cells and Ψ_s is the osmotic potential of the xylem fluid (which is considered to be negligible when compared to water potential of the leaf cells).

Controversy exists as to the reliability of the pressure bomb technique to accurately measure water status (Tyree, 1997; Wei, Steudle & Tyree, 1999); however the wide acceptance of the technique and its ease of use encouraged its use in monitoring diurnal fluctuations in plant water status.
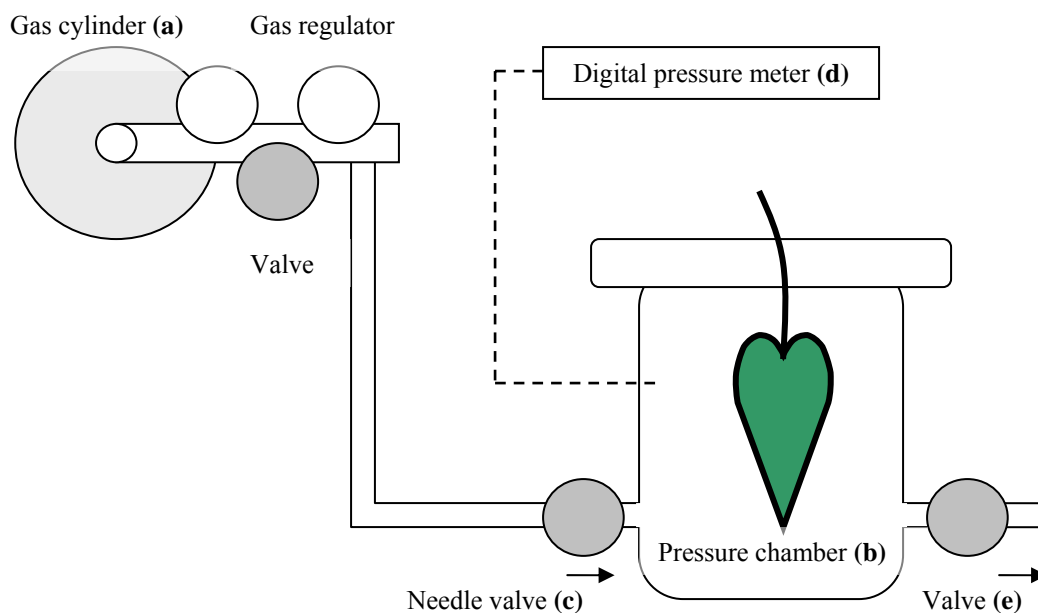
Figure 3.17 Schematic diagram of the Scholander pressure bomb for measuring leaf water potential. See text for explanation of identifying letters.

Fully expanded, fully exposed leaves, on the northern aspect, 1.5m above the ground were harvested. Each leaf is harvested using a single, clean cut across the petiole with a razor blade and placed immediately into a sealed plastic bag to reduce water loss. A rubber gasket was used to seal the leaf within the pressure chamber, with the cut petiole end exposed above the chamber allowing for close examination with a hand lens. Compressed dry air, from a gas cylinder **(a)** is slowly fed to the pressure chamber **(b)**, controlled by a needle valve **(c)**. As soon as water is seen to return to the cut surface of the petiole a measurement is taken of the pressure within the chamber using a digital pressure meter **(d)**. The pressure is released by venting to the atmosphere **(e)**.

3.3   Experimental protocols and procedures

3.3.1   Ecophysiological monitoring

Regular monitoring of plant ecophysiological parameters throughout winter was performed to gain an understanding of plant performance before, during and after chilling of leaves with either a northern and southern aspect.
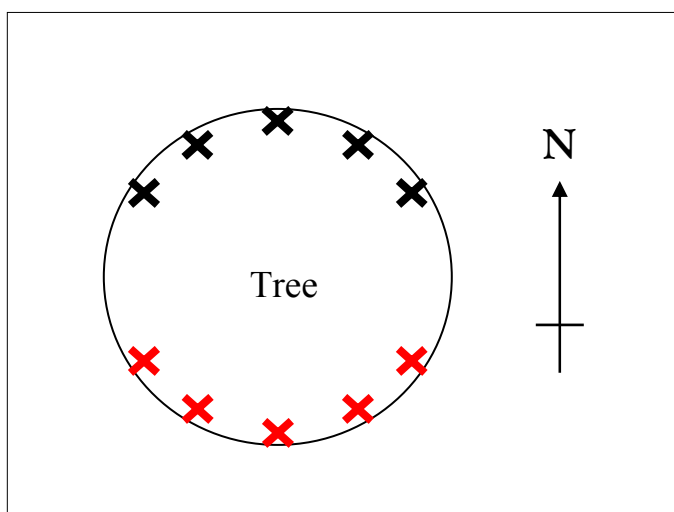
Figure 3.18 Sampling layout of a single tree for ecophysiological monitoring, with 5 leaves on the northern side (black crosses) and 5 leaves on the southern side (red crosses).

Ten leaves, on five tress in 'block A', were tagged on 25th March 2005, 5 leaves on the northern side of each tree and 5 leaves on the southern side, between 0.5 and 2.0 meters above the ground (figure 3.18). These were replaced on 1st December 2005 with fully expanded leaves as the original leaves began to senesce.

The CIRAS-1 (PP Systems, Massachusetts, USA) was used to monitor gas exchange parameters. Measurements were taken between 10am and 12am to minimise the possible effect of afternoon stomatal closure on gas exchange results. Each leaf was enclosed in a PLC cuvette chamber avoiding the central vein and sufficient time was allowed to pass (typically 1 to 2 minutes) until net CO_2 exchange had become stable. Maximal photosynthesis was measured with the leaves under saturating light intensities and

maintained at ambient temperature. These measurements were made in spring (15th and 29th November 2005) with the intention of investigating photosynthetic performance unaffected by winter chilling. Eight further monitoring days were successfully completed covering the winter of 2006 (from the 24th April to 12th September 2006).

Changes in chlorophyll fluorescence through the winter of 2006 were monitored with a Mini-PAM (Heinz Walz GmbH, Effeltrich, Germany). Dark adaptation clips were placed on the 20 leaves on trees 1 and 2 for 15 minutes, avoiding major leaf veins. Each of the 20 marked leaves was measured a total of 8 times between 18th May 2005 and 12th September 2006.

Chlorophyll content was monitored using the Minolta SPAD-502 chlorophyll meter (Minolta, Tokyo, Japan). Each leaf was measured 5 times on the same side of the main vein, within 10mm of the leaf edge. The first measurement of each leaf was taken from the petiole end, with subsequent measurements taken further along the leaf. Each of the 50 marked leaves was measured a total of 9 times between 18th May 2005 and 12th September 2006.

3.3.2 Foliar application of Urea as a restorative treatment for leaf colour

Block "B" was selected as the majority of leaves in this block had become yellow over the course of the previous winter, compared with block "A" used in the ecophysiological monitoring where only a few leaves on exposed uppermost braches had become yellow.

Two branches, on each of 5 trees were labelled to be sprayed or left unsprayed as a control. On each branch, 3 yellowed leaves were labelled and monitored for changes in gas exchange, chlorophyll fluorescence, chlorophyll content and leaf colour. Pre-spray measurements were taken on the morning of the 23rd August 2006. Subsequent measurements were taken 1 week later (the 30th August) and again 3 weeks after spraying (12th September)

The CIRAS-1 (PP Systems, Massachusetts, USA) was used to monitor gas exchange parameters. Each labelled leaf was measured once, between 10am and 12pm, under saturating light conditions to determine maximum photosynthesis. Chlorophyll content was measured non-destructively using the Minolta SPAD-502 chlorophyll meter (Minolta, Tokyo, Japan). Each leaf was measured 5 times on the same side of the main vein, within 10mm of the leaf edge. The first measurement of each leaf was taken from the petiole end, with subsequent measurements taken further along the leaf towards the tip. Chlorophyll fluorescence was determined using the Mini-PAM (Heinz Walz GmbH, Effeltrich, Germany) after dark adaptation of leaves for 15 minutes using leaf clips. Leaf colour was recorded using a Minolta Chroma Meter CR-200b (Minolta, Osaka, Japan). Three measurements were taken per leaf.

The spray treatment consisted of 1% Low-biuret urea and 0.5% magnesium sulphate (ABB Grain, Adelaide, Australia) made up to 10 litres in a hand pump pressurised backpack sprayer fitted with a wide angle fine droplet spray head (Solo, Virginia, USA).

The spray was applied till runoff to treatment branches on the 23rd August 2006, a clear day with a gentle southerly wind. Care was taken to ensure that no spray drift beyond the treated branches occurred.

Twenty days after spraying, 5 sprayed yellow leaves, 5 control yellow leaves and 5 untagged green leaves were destructively harvested for leaf nitrogen content analysis. Each leaf was carefully washed before being dried at 60°C for 45 minutes in a fan-forced drying oven. Nitrogen concentration in avocado leaf tissue was measured at the University of Waikato Stable Isotope Unit using a Dumas elemental analyser (Europa Scientific ANCA-SL) interfaced to a stable isotope mass spectrometer (Europa Scientific Tracermass, Scientific Ltd, Crewe, United Kingdom). The analysis procedure involved introducing individual samples (comprising 3 – 4 mg of dried ground tissue encapsulated in tinfoil) into an oxygen-enriched combustion reactor maintained at a temperature of around 1020°C. After combustion, the gases were swept with helium carrier-gas through

a reduction reactor and water filter onto a gas chromatograph column. CO_2, produced by combustion of carbon in the solid sample, was then separated from the other gases and a sub-sample was transferred into the mass spectrophotometer for the measurement of nitrogen content. Using this system, the precision of measurement for isotopic composition of duplicate samples was $\pm$ 0.14‰.

3.3.3 Diurnal gas exchange measurements

The CMS-400 was utilized to continuously measure environmental and gas exchange parameters for 42 diel courses between 25th July and 9th September, 2006. A single, north facing, fully expanded green leaf, 1.5m above the ground was selected and placed within the leaf chamber. The machine was checked and the IRGAs zeroed at regular intervals during the measurements. Recorded data was transferred to a laptop computer and analysed after data correction.

A major problem that occurred when air temperatures approached freezing point during the night was condensation on the measuring side of the system i.e. somewhere in the cuvette line. This resulted in high negative water differential readings in the night followed by a long burst of water vapour release during warming after dawn. On some occasions this long release was followed by a brief but high spike of both water and CO_2 release. This probably represents the drying out of water within the actual cuvette (Fig. 3.19). Measurements of water vapour differential in both the long and short spikes had to be removed from the database and also values for CO_2 exchange during the brief CO_2 spike.

Another problem was the small distance between the external PDF quantum sensor and the measured sample leaf surface. This lead to occasions when the leaf was shaded whilst the sensor was in the sunlight, and vice versa. These data points resulted in the relationship between net photosynthesis and PDF being much noisier than normal. These data were also removed when identified.

60
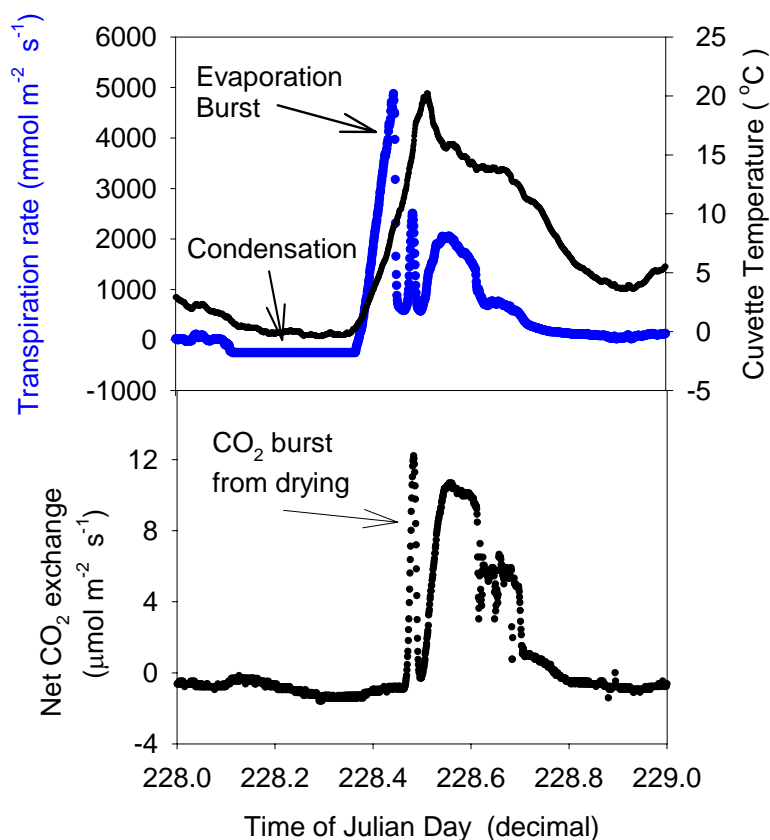
Figure 3.19 Upper Panel: transpiration rate (left-hand axis) and cuvette temperature (right-hand axis) versus time of day, and Lower Panel: net CO$_2$ exchange versus time of day. The periods of water condensation and release are indicated in the Upper Panel, and the burst of CO$_2$ associated with the second water release spike, in the Lower Panel. Data are for Julian Day 228, 16th August.

All results were analysed using Excel 2002 (Microsoft, Redmond, WA, USA), Minitab 13.32 (Minitab Inc., State College, PA, USA) and SigmaPlot 8.0 (Systat Software Inc., San Jose, CA, USA) software programs.

4 Results

4.1 Climate

4.1.1 Climate summary

Rainfall in the summer and autumn of 2005/06 was 150% higher than average for the Bay of Plenty with temperatures also up to 1°C higher than average. Winter 2006, by contrast was drier than normal where rainfall was less than 75% of the average winter rainfall, while temperatures were near average. By spring, a distinctive *El Nino* weather pattern had developed that led to an increase in blustery westerly winds and an increase in east/west weather contrasts. The Bay of Plenty received less than 75% of average spring rainfall, leading to a significant soil moisture deficient by the end of November (NIWA National Climate Centre, 2006a, 2006b, 2006c, 2006d).

4.1.2 Microclimate

Due to technical problems, no data was collected directly within the study orchard. Data collected at an alternative climate station, located on Prospect Drive, Katikati, approximately 3.0 km north of the study orchard is used to define the microclimate. Additional microclimate data for the month August are presented with the continuous gas exchange results.

Table 4.1 Climate summary for Prospect Drive, Katikati from January to November 2006. Mean daily temperature mean, minimum and maximum, number of chill nights (<4°C) and number of air frost nights (<0°C).

Month (2006)	Mean daily temperature minimum (°C)	Mean daily temperature mean (°C)	Mean daily temperature maximum (°C)	Number of chill nights, <4°C	Number of air frost nights, <0°C
Jan	13.24	18.74	24.33	0	0
Feb	12.78	18.56	24.65	1	0
Mar	10.94	16.26	22.25	1	0
Apr	10.89	15.41	21.16	0	0
May	7.64	12.06	17.30	6	1
Jun	2.39	8.12	15.16	17	10
Jul	3.70	9.62	15.83	14	7
Aug	4.90	10.38	15.80	12	5
Sep	7.27	13.03	18.55	5	0
Oct	7.46	13.32	18.94	8	0
Nov	10.18	15.68	21.42	1	0

Table 4.2 Climate summary for Prospect Drive, Katikati from January to November 2006. Mean relative humidity, maximum hourly mean radiation and total monthly rainfall.

Month (2006)	Mean relative humidity (%)	Maximum hourly mean radiation (W m^{-2})	Total monthly rainfall (mm)
Jan	77.07	1109	208
Feb	78.99	1018	99
Mar	79.90	1053	224
Apr	84.97	831	354
May	86.19	598	269
Jun	79.77	590	104
Jul	79.85	510	116
Aug	79.28	786	202
Sep	75.80	979	46
Oct	74.40	1032	81
Nov	74.45	1084	96

The warmest month was January, with a mean temperature of 18.7°C (minimum 13.2°C, maximum 24.3°C) and an absolute maximum of 28.6°C (Table 4.1). January was the only month with no nights below 4°C. The coldest month was June, with a mean temperature of 8.1°C (minimum 2.8°C, maximum 15.2°C) and a coldest temperature of -2.4°C (figure 4.1). There were 17 nights with an air temperature of less than 4°C in June, of which 10 were less than 0°C. There were total of 64 nights with a temperature of less than 4°C, of which 23 were less than 0°C over the period investigated. The greatest diurnal temperature range was 19.9°C on the 24th of February and the narrowest range was 2.2°C on 24th of January. Rainfall was unevenly spread between months with April having the greatest rainfall at 354mm and September the least with only 46mm (Table 4.2). Mean relative humidity peaked in May at 86.19% and reached a low of 74.4% in September. Maximum daily solar radiation showed a clear seasonal pattern with with a peak of 1109 W m^{-2} in January and a low of 510 W m^{-2} in July.
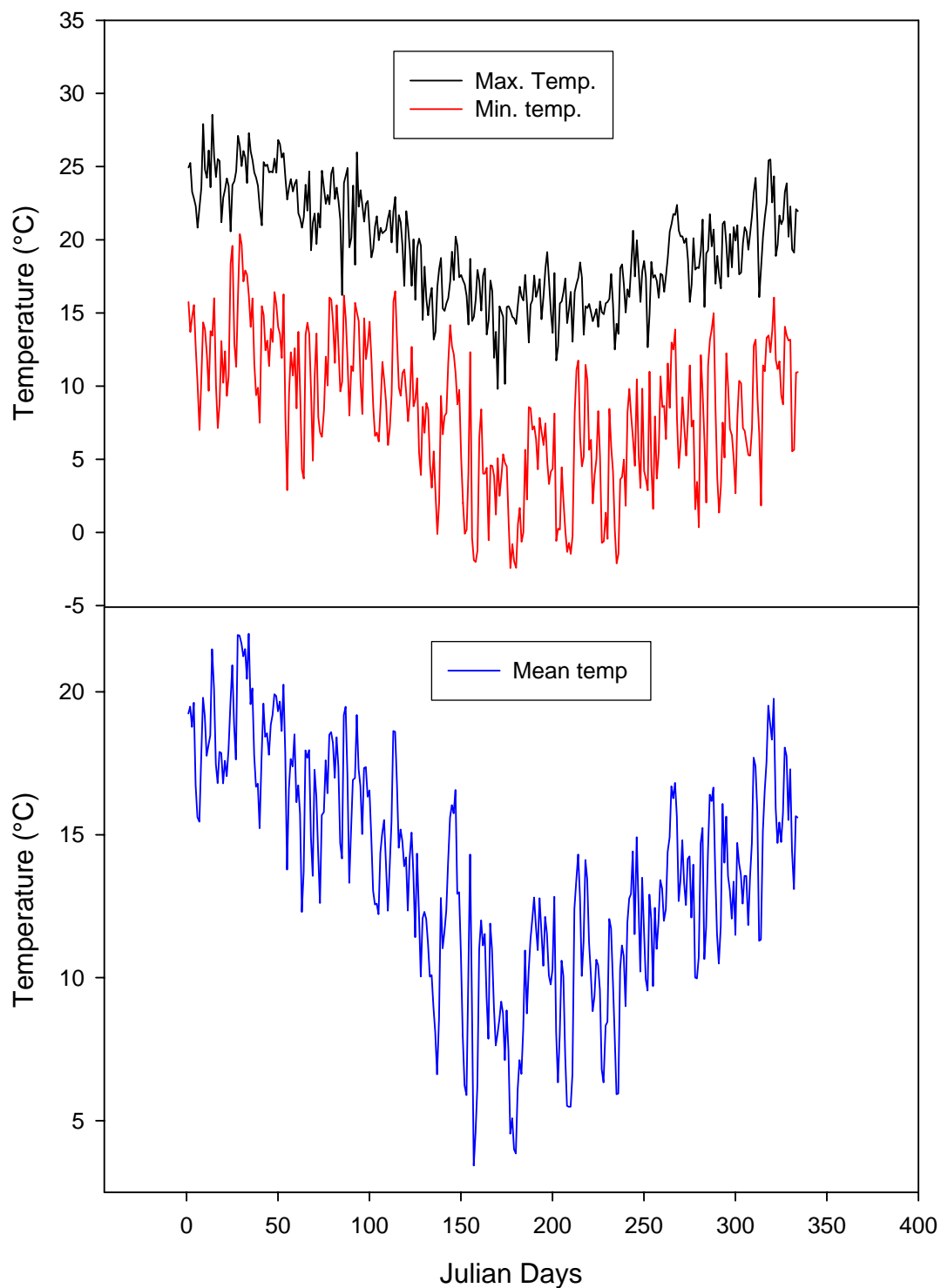
Figure 4.1 Microclimate conditions between January 1st to November 30th 2006. Upper panel, minimum (red line) and maximum (black line) temperatures, calculated from hourly means., lower panel, mean temperature.
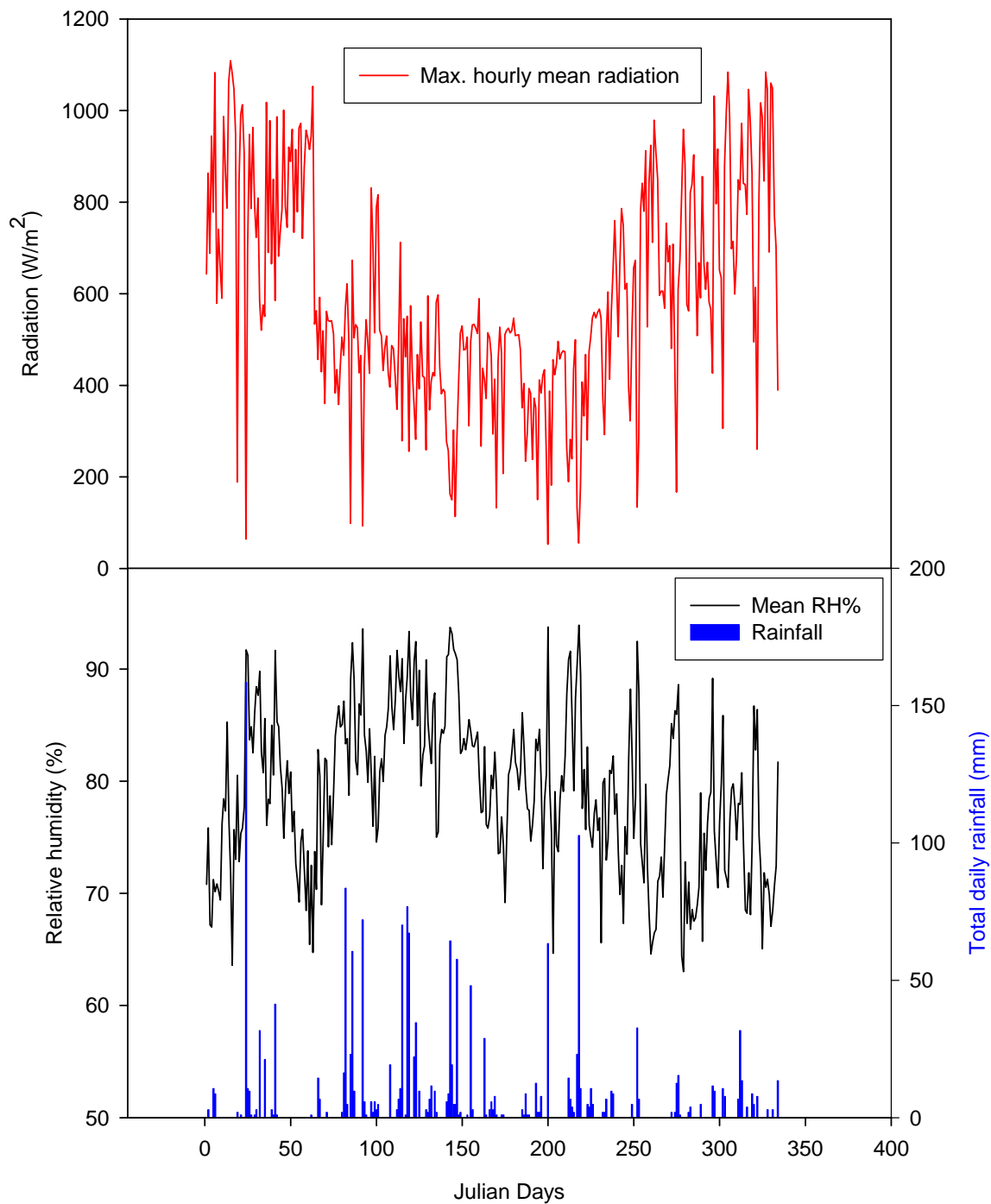
Figure 4.2 Microclimate conditions between January 1st to November 30th 2006. Upper panel, maximum hourly mean radiation. Lower panel, mean relative humidity (black line) and total daily rainfall (blue bars).

During the time in which microclimate were only the 24th of January and the 6th of August received more than 100mm of rainfall, reciving 158mm and 102mm of rainfall respectively (figure 4.2). In addition, there was a further 9 days with rainfall greater than 50mm, all occurring between March and July.

4.2 Monitoring of gas exchange and chlorophyll *a* fluorescence

Net photosynthesis, stomatal conductance and chlorophyll *a* fluorescence (F_v/F_m) were measured on 5 marked leaves on the north and south side of 5 trees at irregular intervals during the investigation (Table 4.3).

Table 4.3 Dates of gas exchange and chlorophyll fluorescence measurements during the investigation. Dates on the same line are identical or almost identical.

Year	Fluorescence	Gas exchange
2005	18th May	
		15th November
		30th November
2006	21st March	
		21st April
		11th June
	21st June	
	27th June	28th June
	6th July	7th July
	22nd July	21st July
		27th July
	19th August	19th August
	12th September	12th September

4.2.1 Gas exchange and chlorophyll *a* fluorescence

Net CO_2 exchange under saturating light intensities for leaves on both the northern and southern side of the tree were 7 to 12 μmol m^{-2} s^{-1} until the readings taken on 21st April when leaves on the south side had significantly lower net photosynthesis. Leaves on both north and south sides then declined in net CO_2 exchange to a lowest reading on 28th June followed by an almost complete recovery by the final reading on 12th September. At their lowest net CO_2 exchange rates were negative indicating a carbon loss from the leaves. This coincided with the cooler temperatures at that time of year. The low-point of net CO_2 exchange occurred at the same time for both sides of the tree, there was a difference between the north and south sides before and after the low-point had been reached. Leaves on the southern side of the tree showed a reduction in net CO_2 exchange earlier in the season and a later return to normal values afterwards compared to leaves on the northern side.   The leaves on the south and north sides were also very different in their chlorophyll *a* fluorescence (F_v/F_m) values (Fig. 4.3). Whilst these remained at about 0.83 on the south side, they were always lower for the north-facing leaves and these also showed a large decline in the colder winter reaching as low as 0.73 on the 19th August and 0.75 on 28th June. The latter low value coincided with the minima for the net CO_2 exchange of the leaves. The F_v/F_m values for the north leaves had fully recovered on the 12th September.
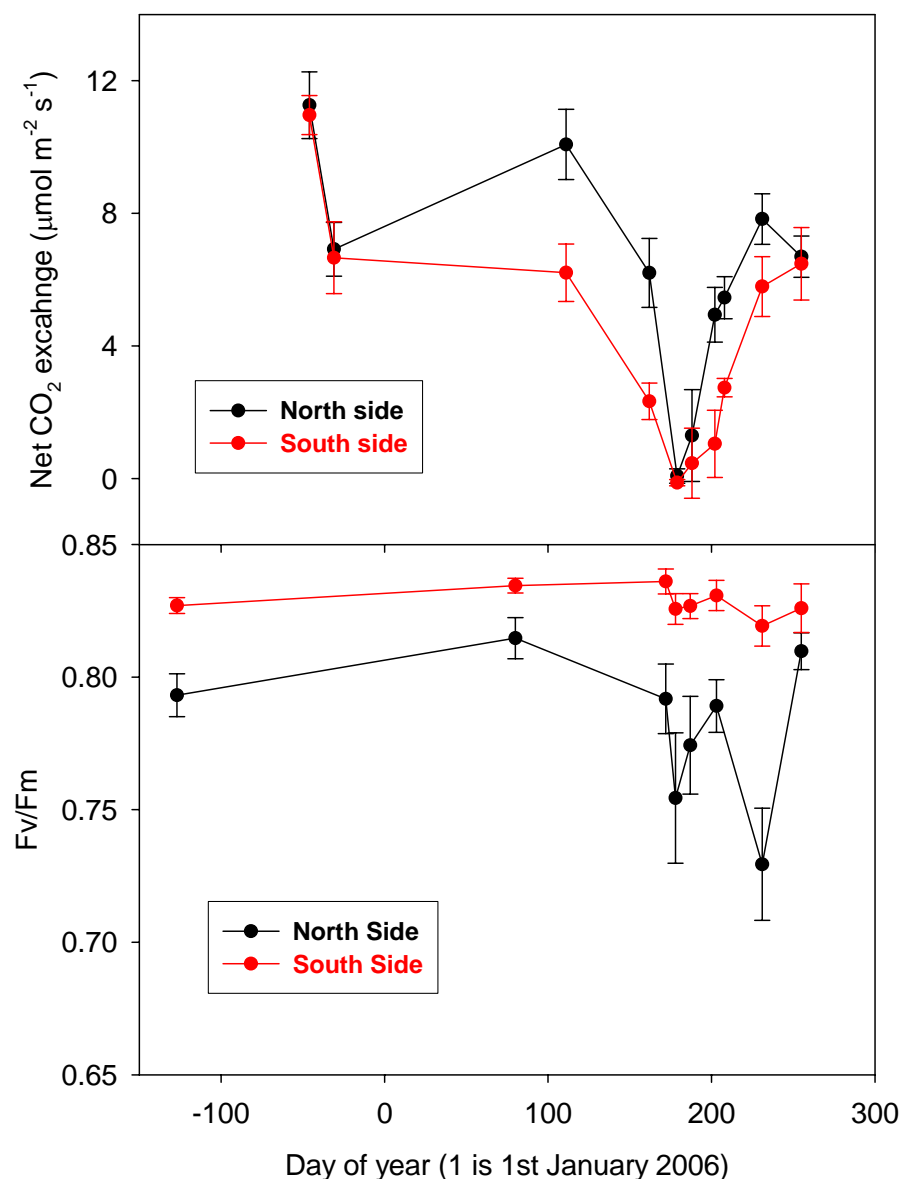
Figure 4.3 Comparison of leaves on north (black) and south (red) side of avocado trees through the investigation period. Upper panel: Net CO_2 exchange under saturating light conditions, Lower panel: F_v/F_m. Error bars are standard error of the mean, n=25.

A more detailed study over a single diurnal period was made on 27th March 2005 when the northern leaves were exposed to full sunlight during the day (Fig. 4.4). Leaves on the southern, shaded side showed high, near optimal values for F_v/F_m (around 0.83) for the entire day. Leaves on the northern side showed a significant decline during the morning to a lowest value of 0.79 at 13[30]. The F_v/F_m values then started to recover and reached

69

about 0.80 by 18^{00}. Although this indicates a level of transient photoinhibition in the leaves on the northern side that is certainly a result of the much higher light levels to which they are exposed, it is unlikely that this would affect net photosynthesis. The decline is not large and the decline in quantum efficiency would have no, or only minor, affect on maximal photosynthetic rates at the high light levels during the day.
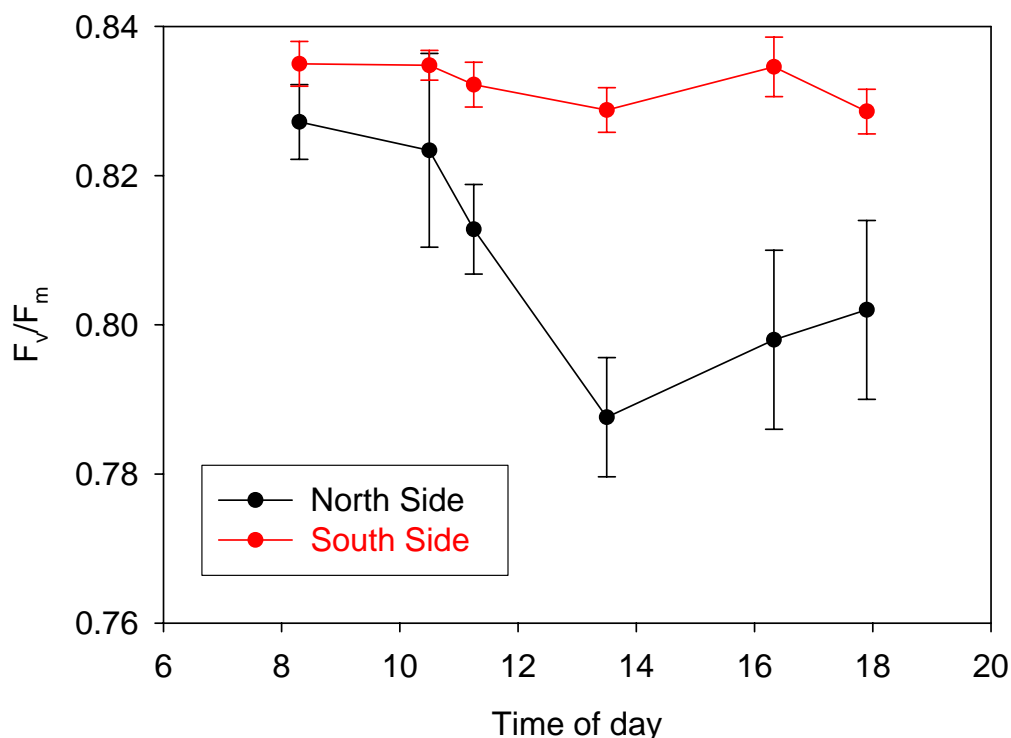
Figure 4.4   Diurnal pattern of F_v/F_m of leaves on the north (black) side and south (red) side of 5 avocado trees.   Error bars are standard error of the mean, n=25.

4.2.2 Stomatal conductance.

The pattern over the winter of 2006 for stomatal conductance was very similar to that found for net CO_2 exchange. Both north and south facing leaves had a decline in stomatal conductance values during the winter which coincided almost exactly with the decline and recovery in net CO_2 exchange (figure 4.5). At their lowest values on 28th June the stomata were effectively closed. Again, leaves on the southern side had an earlier decline

and later recovery than leaves on the northern side. Neither the north facing nor the south facing leaves recovered their stomatal conductance to the pre-winter values by the 12th of September.
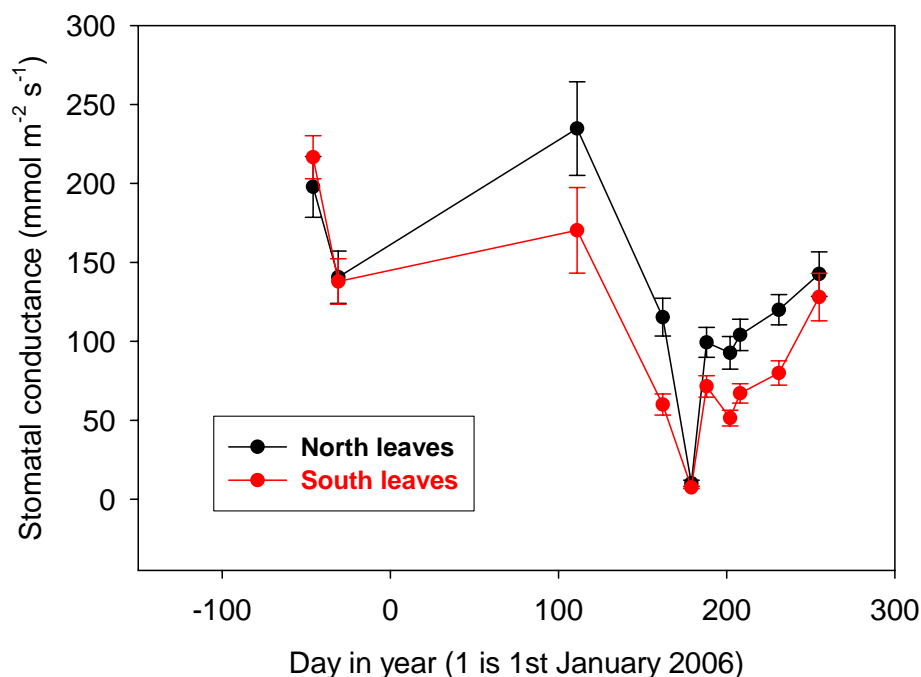
Figure 4.5 Pattern of stomatal conductance for leaves on the north (black) and south (red) side of the tree. Values represent 5 leaves on each side of 5 trees. Error bars are standard error of the mean, n=25.

Stomatal conductance measurements were taken at the same time each day (10^{00}-12^{00}), but this time would vary in numbers of hours after sunrise, being less during the winter months. The stomatal conductance results above may hay been effected by the water status of the tree at the time of measurement. Water status was measured over two days on two irrigated trees, from 07^{00} to 18^{00} on the 26th and 27th of March 2005 (figure 4.6). The trees were under no water stress at dawn, with near zero xylem tension. Peak xylem tension occurred at 12^{30} or 14^{30}, with approximately 1.2 – 1.7 MPa of negative pressure. Xylem tension returned to near zero values rapidly as dusk approached, with the trees having near zero values by 18^{00} and 16^{30} for days one and two respectively. This indicated that the trees were experiencing very little water stress on the 26th and 27th of March.
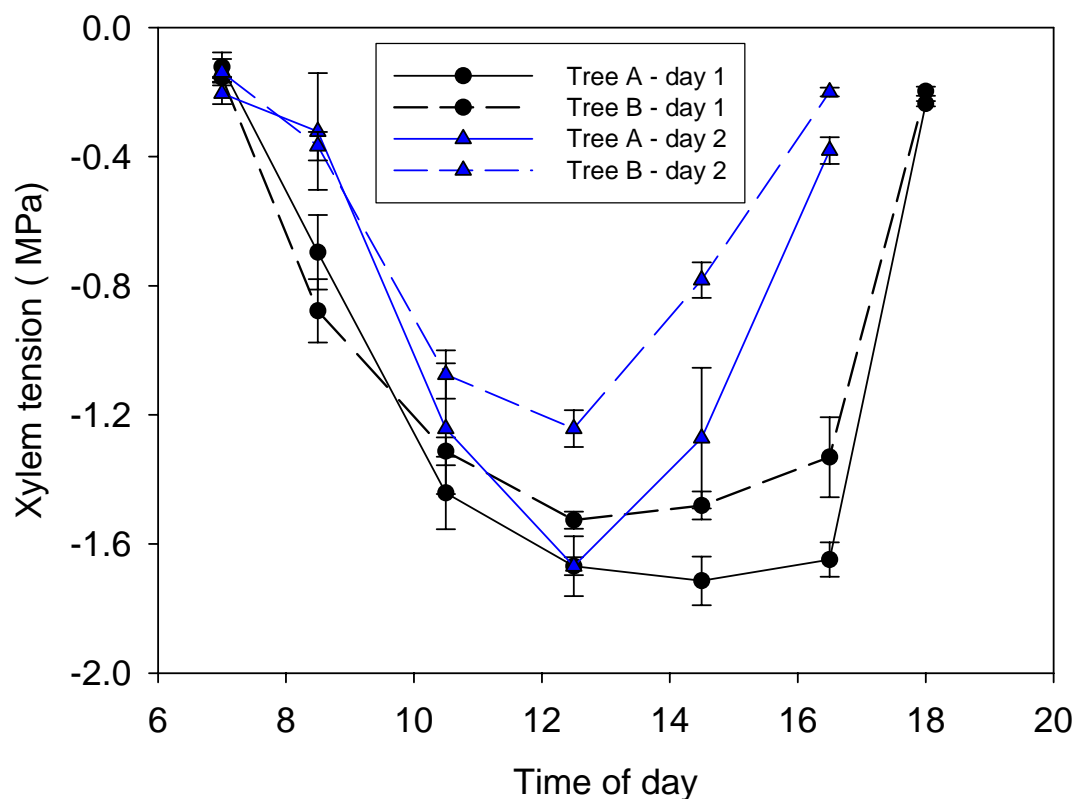
Figure 4.6 Xylem tension in excised leaves from the sun exposed north side of two trees (tree A = black, tree B = blue) over two days (day 1 = solid line, day 2 = dashed line), measured with a Scholander pressure bomb. Error bars are standard error of the mean, n=3.

4.2.3 Leaf internal CO_2 concentration and CO_2 gradient.

During the first readings over spring and summer both internal CO_2 concentration and CO_2 gradient from air to leaf remained constant (Fig. 4.7). Internal CO_2 was around 250 and 270 ppm for leaves on the north and south sides, respectively and CO_2 gradients between sub-stomatal cavity and environment of 110 and 90 ppm, respectively. The differences suggest higher photosynthetic rates on the northern side or stronger stomatal control. The decline in net photosynthetic rates during the winter (Fig. 4.3) led to a similar increase in internal CO_2 concentration and decline in gradient with a return to near normal values by the September sampling. At the sampling on 28th June 2006 the CO_2 gradient was actually negative indicating loss of carbon from the leaves.
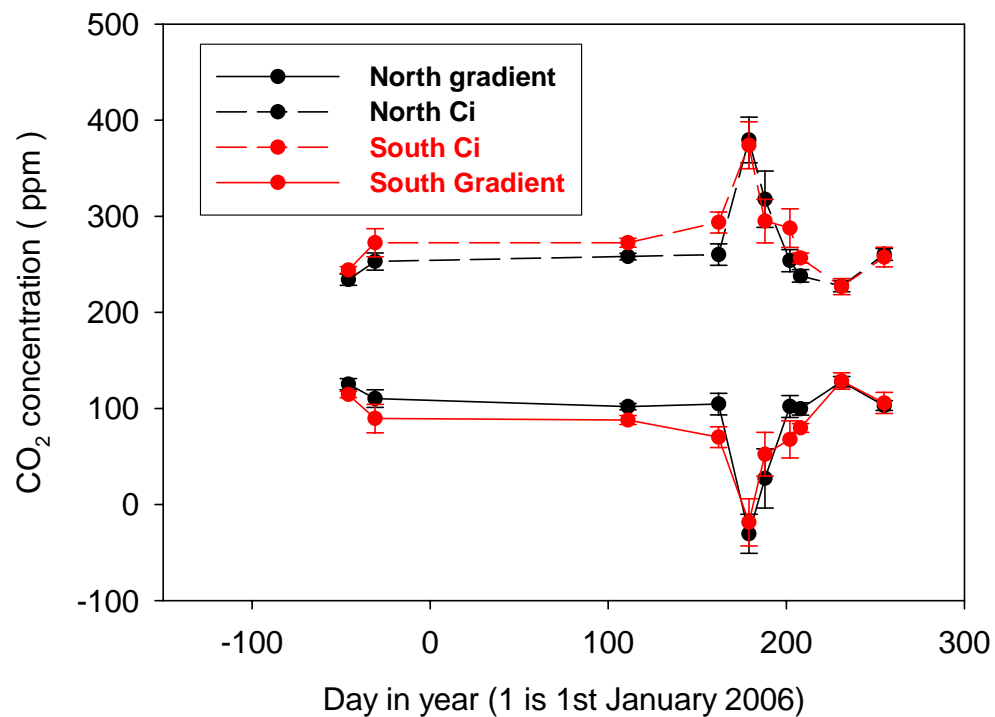
Figure 4.7 Pattern of internal CO_2 concentration (Ci, dashed lines) and CO_2 gradient between sub-stomatal cavity and environment (solid lines) for leaves on the north (black) and south (red) side. Values represent 5 leaves on each side of 5 trees. Error bars are standard error of the mean, n=25.

4.2.4 Leaf chlorophyll content
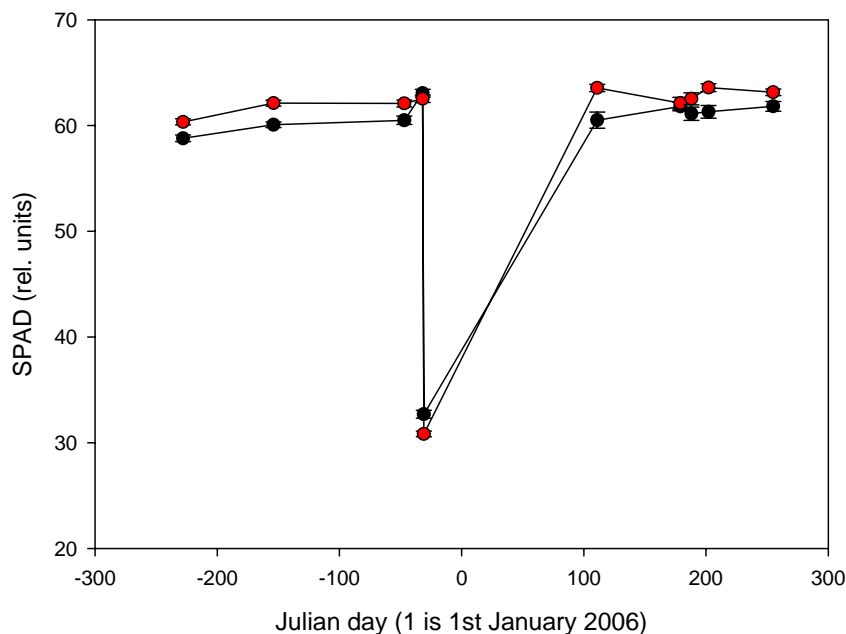
Figure 4.8 Chlorophyll content (SPAD units) measured with the SPAD chlorophyll meter for leaves on the north (black) and south side (red) of 5 trees. Error bars are standard error of the mean, n=108 to 250. New flush selected day -31 (1st December 2005).

Chlorophyll content of leaves on both the north and south sides remained almost constant through the whole measurement period with the exception of the measurement on 1st December, 2005, which was the first on leaves from the new flush (figure 4.8). It was necessary to move measurements to the new leaves because avocado leaves start to abscise once the new flush is established. Leaves in the new flush had low chlorophyll contents at their first measurement on 1st December 2005 but had reached typical values at the next measurement on 21st April 2006. Leaves from the southern, shadier side of the trees, almost always had a higher chlorophyll content than leaves on the northern side. Mean chlorophyll content for mature leaves was 61.7 SPAD units, or 763 μmol m^{-2} using the calibration in section 3.2.1.1. There was no decrease in chlorophyll content that might indicate the onset of leaf yellowing during the winter of 2006.

4.3   Diel patterns of leaf gas exchange.

4.3.1   Period of measurement

The Walz CMS400 climatised photosynthesis system was utilized to continuously measure leaf gas exchange and environmental parameters for 42 diel courses between 25th July and 9th September, 2006, as described in the Methods Section. A single, north facing, fully expanded green leaf, 1.5m above the ground was used and changed as necessary if damaged. After initial analysis and data correction only the period from Julian Day 206 to Julian Day 229 (25th July to 17th August) was used for the final comparisons.

4.3.2   Microclimate, temperature and light

The weather during the period when measurements were taken was not atypical with clear days and cold nights occurring together with days that were cloudy and warmer. Of the 23 days analysed in detail, 10 had mean temperatures <10.0 ^{o}C, 20 had minima <10.0 ^{o}C and 3 days had minima <0.0 ^{o}C. Temperature ranges were often large and 20 days had maxima >15.0 ^{o}C. The warmest day was Julian Day 214 (2nd August) with a mean of 14.2 ^{o}C and max/min of 17.1/11.9 ^{o}C. The coolest was Julian Day 210 (29th July) with a mean of 5.3 ^{o}C and max/min of 17.9/-0.8 ^{o}C (figure 4.9). That the coolest day had a higher maximal temperature than the warmest day showing the coincidence of cold nights with clear days. The light intensity showed a similarly high variability with 12 days reaching maximal PFD around $1100 - 1200$ μmol m^{-2} s^{-1}, indicating full sunlight on the horizontal sensor. These days typically also had a high total daily PFD, over 100 mmol m^{-2} with the highest reaching 358 mmol m^{-2} (Day 228, 16th August) with a high mean PFD of $238 - 539$ μmol m^{-2} s^{-1}. There were also some warm, very cloudy days Day 213 (1st August), with a mean temperature of 12.6 ^{o}C, mean PFD of 18 μmol m^{-2} s^{-1}, total daily PFD of 12 mmol m^{-2}, which can be compared to the bright, cloud-free but cold days

such as Day 228 with corresponding values of 6.2 ^{o}C, 1295 µmol m^{-2} s^{-1}, and 356 µmol m^{-2}.
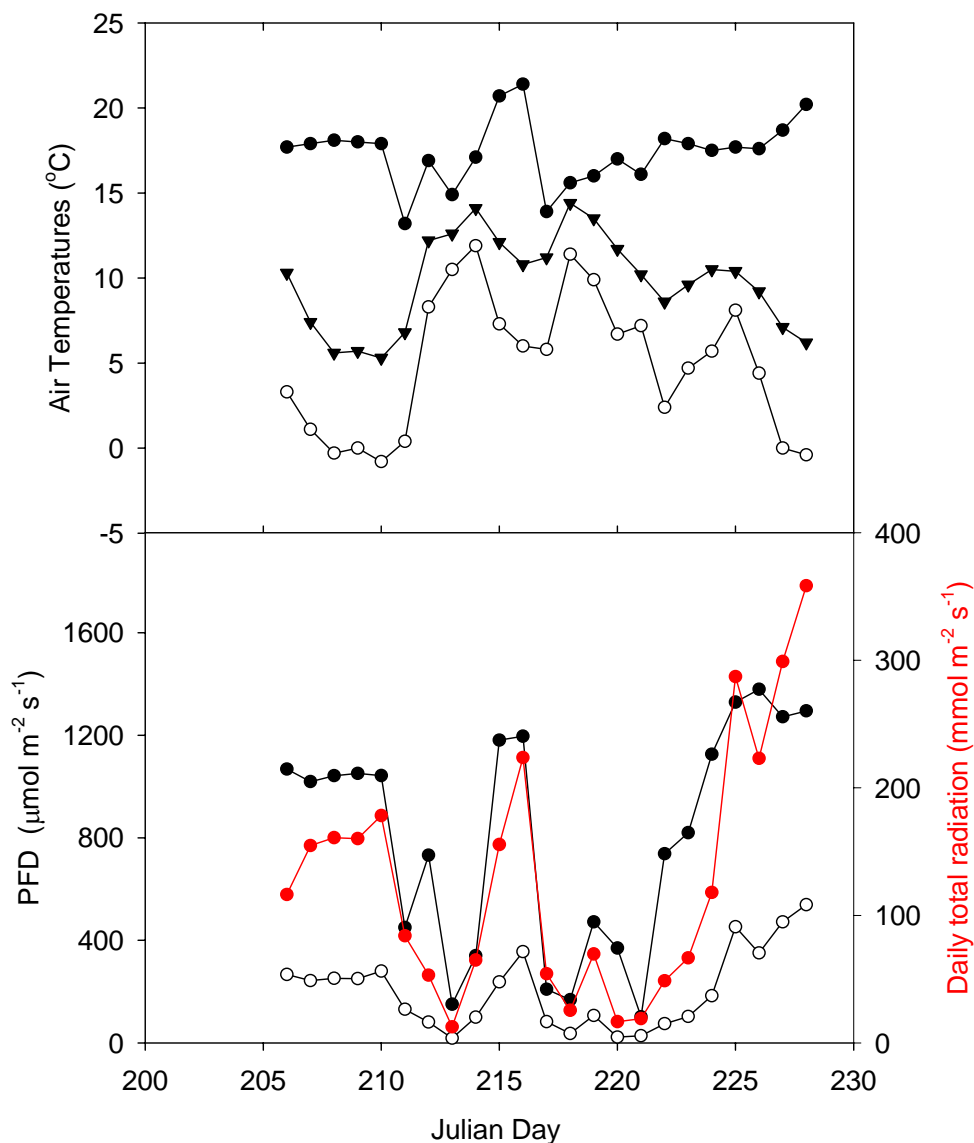
Figure 4.9 Upper panel; Daily values for air temperature maxima (closed round symbols), means (closed triangles) and minima (open symbols). Lower panel; daily values of PFD maxima (black), means (open symbols) and total daily radiation input (red). Values measured with CMS photosynthetic system between day 206 (25th July, 2006) and day 228 (16th August, 2006).

4.3.3 Diel gas exchange

For Julian Day 215 (3rd August), a typical warm winter day, net CO_2 exchange reached 17.5 μmol m^{-2} s^{-1} at the highest light level in the middle of the day. Both air temperature and stomatal conductance reached their maximum at about the same time (20.7 ^{o}C and 195 mmol m^{-2} s^{-1}, respectively). Net CO_2 exchange had the expected saturation response to increasing PFD with saturation reached at about the maximal PFD of 1181 μmol m^{-2} s^{-1} (figure 4.11). The good fit of the data shows that there was a tight linkage between net CO_2 exchange and PFD ($R^2 = 0.97$, P< 0.0001).

Net CO_2 exchange and stomatal conductance for another warm day, Day 225, 13th August, mean temperature was 10.4 ^{o}C and a minimum of 8.1 ^{o}C, are plotted in figure 4.10. The data are re-plotted to show the relationship between net CO_2 exchange and stomatal conductance in the lower Panel (figure 4.12).   Overall there was an approximately linear relationship between the two parameters up to an apparent saturation level of around 200 mmol m^{-2} s^{-1}, stomatal conductance. The colouring of the symbols shows clearly that the relationship differed in the morning and afternoon. At any particular stomatal conductance up to about 180 mmol m^{-2} s^{-1} net CO_2 exchange was higher in the morning than in the afternoon. This suggests that stomatal conductance was not directly controlling net CO_2 exchange.
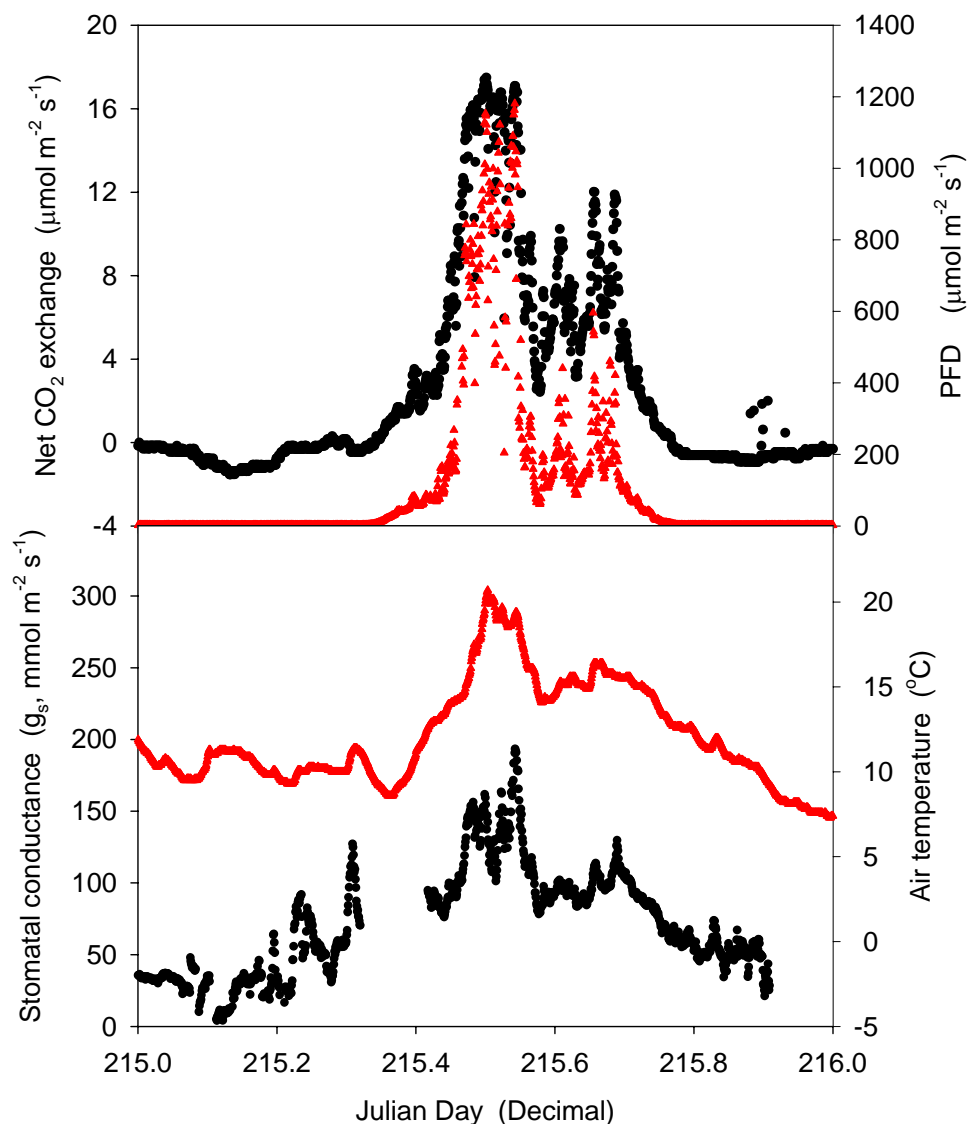
Figure 4.10 Diel patterns of gas exchange, air temperature and PFD for a warm, winter day, Day 215 (3rd August, 2006); mean temperature 12.1 ^oC, maximum 20.7 ^oC and minimum 7.3 ^oC. Upper Panel, Net CO_2 exchange (black symbols, left-hand axis), and PFD (red symbols, right-hand axis); Lower Panel, stomatal conductance to water vapour, g_s (black symbols, left-hand axis) and air temperature (red symbols, right-hand axis).
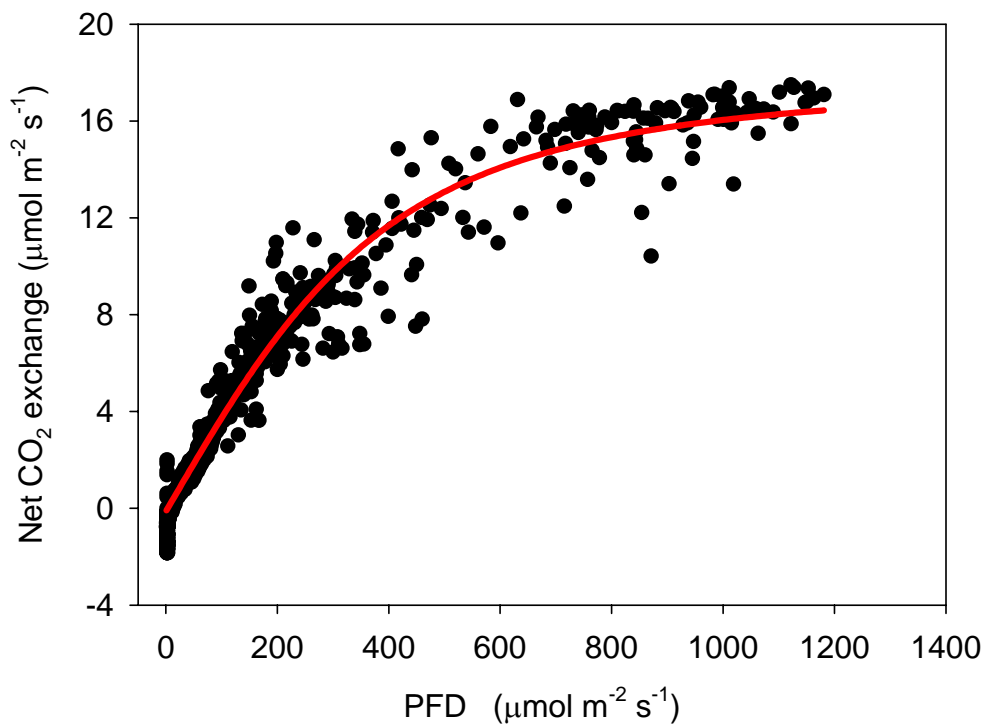
Figure 4.11 Response of net photosynthesis to PFD for Day 215 (3rd August, 2006), a warm, winter day; temperatures were, maximum, 20.7 ^{o}C, minimum, 7.3 ^{o}C and mean, 12.1 ^{o}C. The data set consists of all measurements made every one minute during daylight and are fitted fitted with a Smith curve with R^2 = 0.97, P<0.0001.
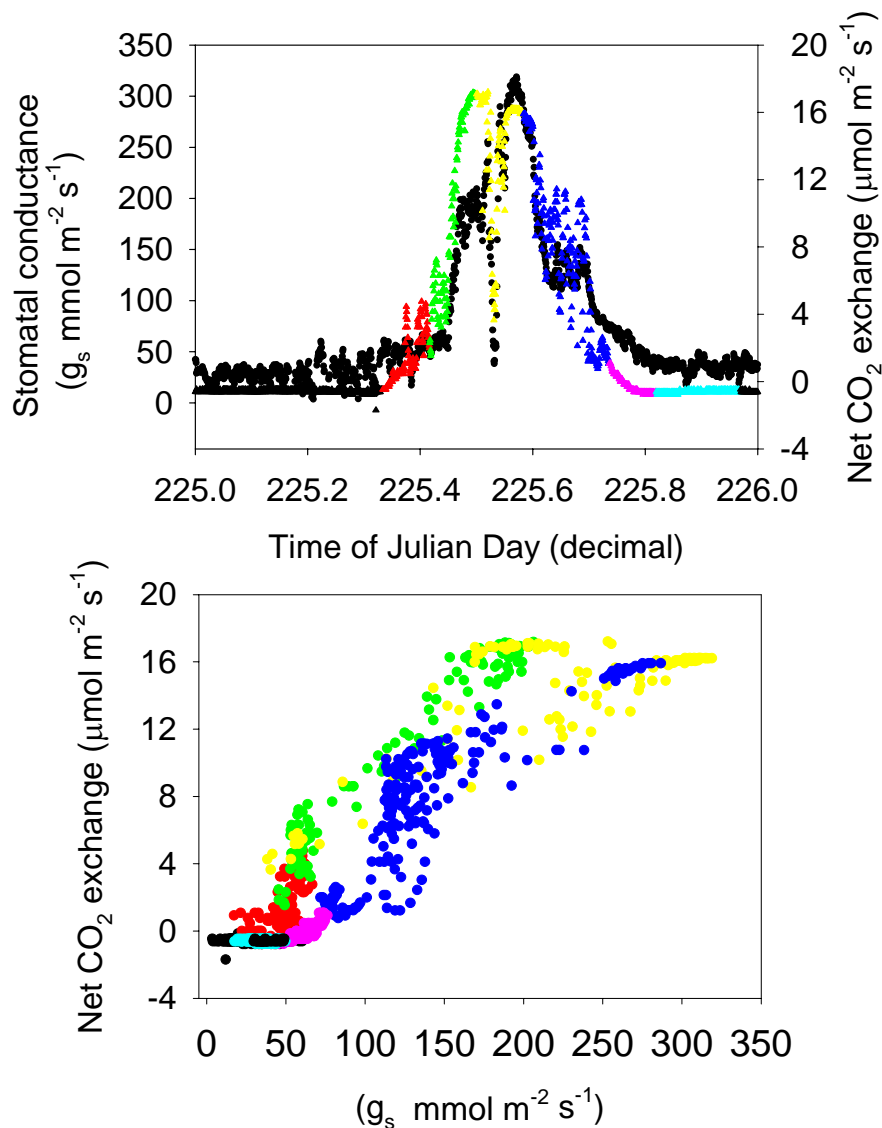
Figure 4.12 Upper panel: diel pattern of stomatal conductance to water vapour (g_s, black) and net CO₂ exchange (coloured line). Lower panel: net CO₂ exchange versus stomatal conductance to water vapour (g_s). A time sequence through the day is represented by colour code chart, explained below. Data is for Day 225 (13ᵗʰ August, 2006). Temperatures were, maximum 17.7 °C, minimum 8.1 °C and mean 10.4°C.

Time colour coding

●	-	0000 to 0800	●	-	0800 to 1000
●	-	1000 to 1200	●	-	1200 to 1400
●	-	1400 to 1600	●	-	1600 to 1800
●	-	1800 to 2400			

The good corolation between net CO_2 exchange and stomatal conductance is further demonstrated in figure 4.13 which shows the response of these parameters as well as Ci (internal CO_2 concentration) and WUE (water use efficiency, $\mu molCO_2/mmol\ H_20$) to two events of reduced incident PFD. The first event lasted about 25 minutes and PFD fell from around 1100 $\mu mol\ m^{-2}\ s^{-1}$ to 125 $\mu mol\ m^{-2}\ s^{-1}$ in 14 minutes and then returned to the original levels. A second, briefer event occurred 6 minutes later and lasted only 8 minutes, during which PFD fell to 473 $\mu mol\ m^{-2}\ s^{-1}$. Both net CO_2 exchange and stomatal conductance decreased and recovered almost. A plot of net CO_2 exchange and stomatal conductance against PFD (figure 1.14) shows how similar their responses were, and how tightly connected to PFD.

Internal CO_2 concentration and WUE were both stable before and after the PFD excursion but showed large transients during the period of changing PFD. Internal CO_2 first rose and then fell before settling to a new steady value of around 250 ppm CO_2. These transients suggest that changes in net CO_2 exchange preceded the changes in stomatal conductance. As net CO_2 exchange started to fall the gradient declined as stomatal conductance failed to change proportionately. As PFD returned to its original high values the stomatal conductance again lagged and, because net CO_2 exchange was then increasing the gradient also increased and Ci fell below original levels. WUE was almost identical before and after the PFD event and this suggests that WUE might be an important parameter for the water relations of the plant.
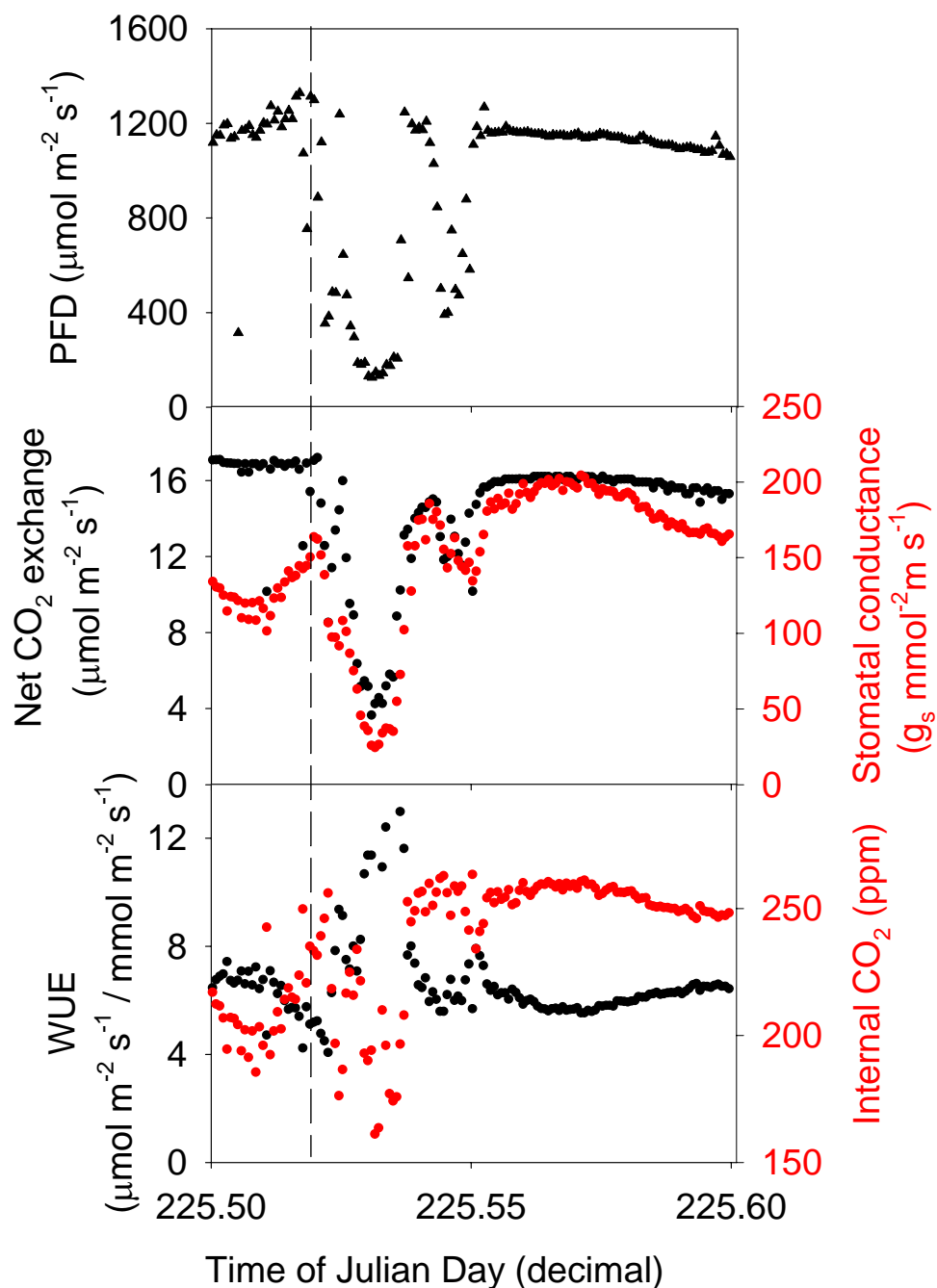
Figure 4.13 Upper Panel: Course of PFD for a short period after midday on Day 225 (13th August, 2006) showing a strong excursion to low PFD. Middle Panel: The response of net CO_2 exchange (black, left-hand axis) and stomatal conductance (red, right-hand axis) and Lower Panel: the responses of Water Use Efficiency (WUE, black, left-hand axis) and internal CO_2 concentration (red, right-hand axis). The vertical dotted line marks the start of the decline in PFD. Successive data points are one minute apart.
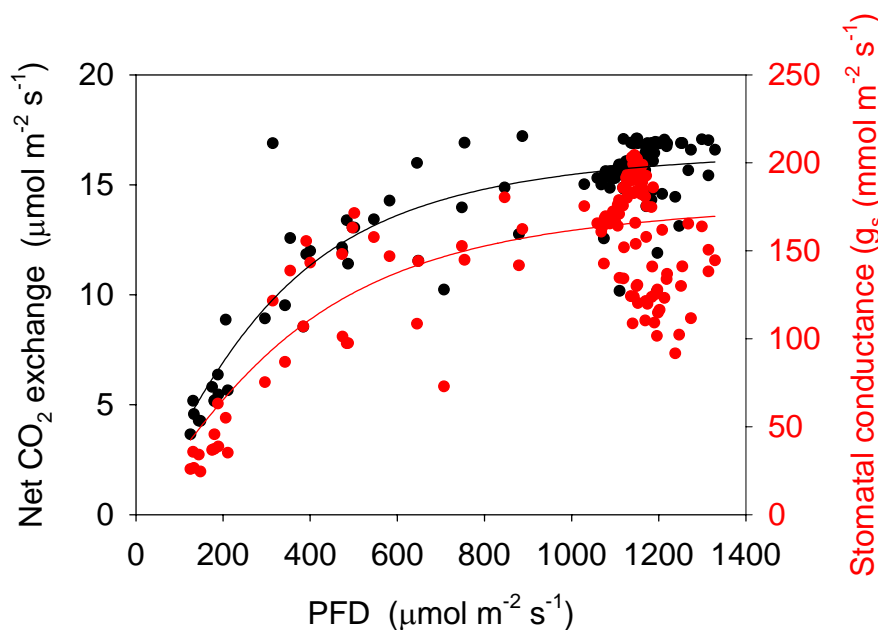
Figure 4.14   Response of mean net CO_2 exchange and stomatal conductance to PFD during the period described in figure 4.13 above.

4.3.4 Net CO_2 exchange rates and temperature

Maximum, mean and minimum net CO_2 exchange rates are shown in Figure 1.15 for the period Day 206 (25th July, 2006) to Day 228 (16th August, 2006). The mean net CO_2 exchange rate was calculated for all measurements during a 24 hour day and included the night-time dark respiration; a negative value would indicate a net loss of carbon during the day. Dark respiration rates were often around 1 µmol m^{-2} s^{-1} and this appears to be normal for the leaves and has been extensively reported from even warmer climates where respiration might be expected to be higher (Heath et al. 2005). This is possibly a result of the relative thinness of the leaves, only around 200 µm. Although there is some considerable variability in the maximal net CO_2 exchange rate, from 17.5 to 6.3 µmol m^{-2} s^{-1}, this did not correlate significantly with the minimum and mean temperatures for the day but did (P = 0.0003, R^2 = 0.44) with the maximum temperature (figure 4.16).

83
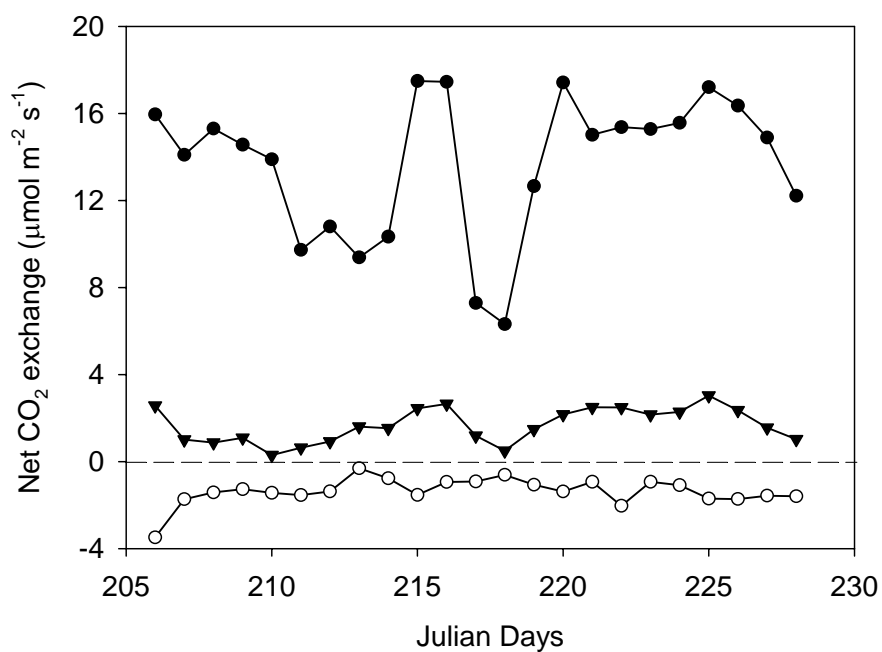
Figure 4.15   Maximum (closed circles), mean (closed triangles) and minimum (open circles) net photosynthetic rates over the period Day 206 (25th July, 2006) to Day 228 (16th August, 2006).
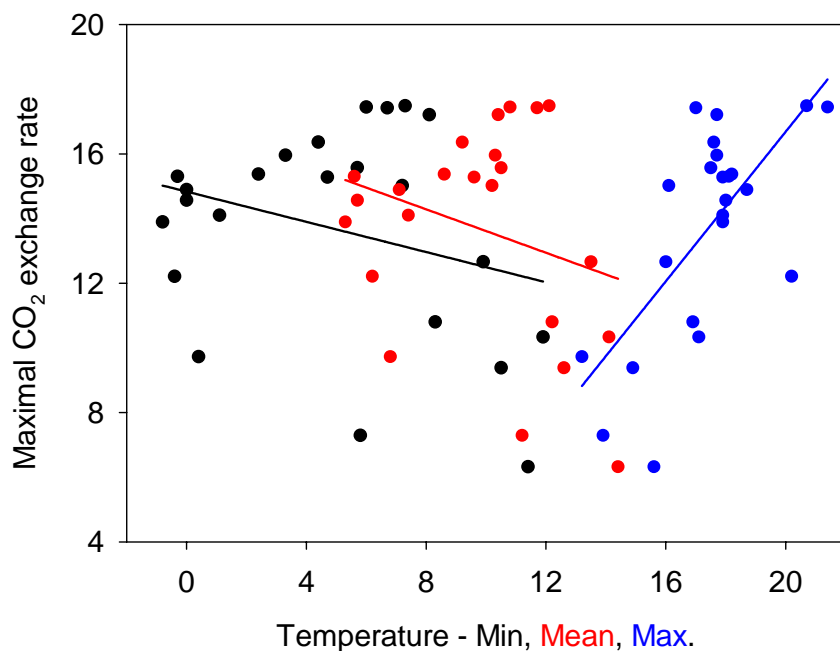
Figure 4.16   Relationship between maximal net CO_2 exchange rate and minimum (black symbols), mean (red symbols) and maximum (blue symbols) air temperature for the period Day 206 (25th July, 2006) to Day 228 (16th August, 2006). Only the linear regression with maximum temperature is significant (P=0.0003, R^2 = 0.44).

84

A possible disparity exists between the results obtained with the CIRAS porometer during the monthly sampling and those from the CMS400 diel studies. In the CMS400 results there are no days when the maximal net CO_2 exchange rate falls below 6.2 μmol m^{-2} s^{-1} and only on four days from the 23 analysed was it below 10 μmol m^{-2} s^{-1}. The CIRAS porometric studies, in contrast, report, albeit about a month earlier, negative net CO_2 exchange rates. This disparity is explored in the next section.

4.3.5 Diel net CO_2 exchange rates and low temperatures

The diel courses of net CO_2 exchange rate, stomatal conductance, PFD and leaf temperature are presented in figure 4.17 for Day 228 (16th August). This was a day that had low overnight temperatures that fell to a minimum of -0.4 ^{o}C. The day was sunny and clear and PFD followed an almost smooth course reaching 1295 μmol m^{-2} s^{-1} just after midday. Temperatures also rose rapidly and at about midday the leaf temperature reached 20.2 ^{o}C. Net CO_2 exchange and stomatal conductance followed almost identical courses reaching their maxima of 10.7 μmol m^{-2} s^{-1} and 257 mmol m^{-2} s^{-1}, respectively, at about 13^{30} (figure 4.17). There was an strong linear relationship between the two parameters (figure 4.18).
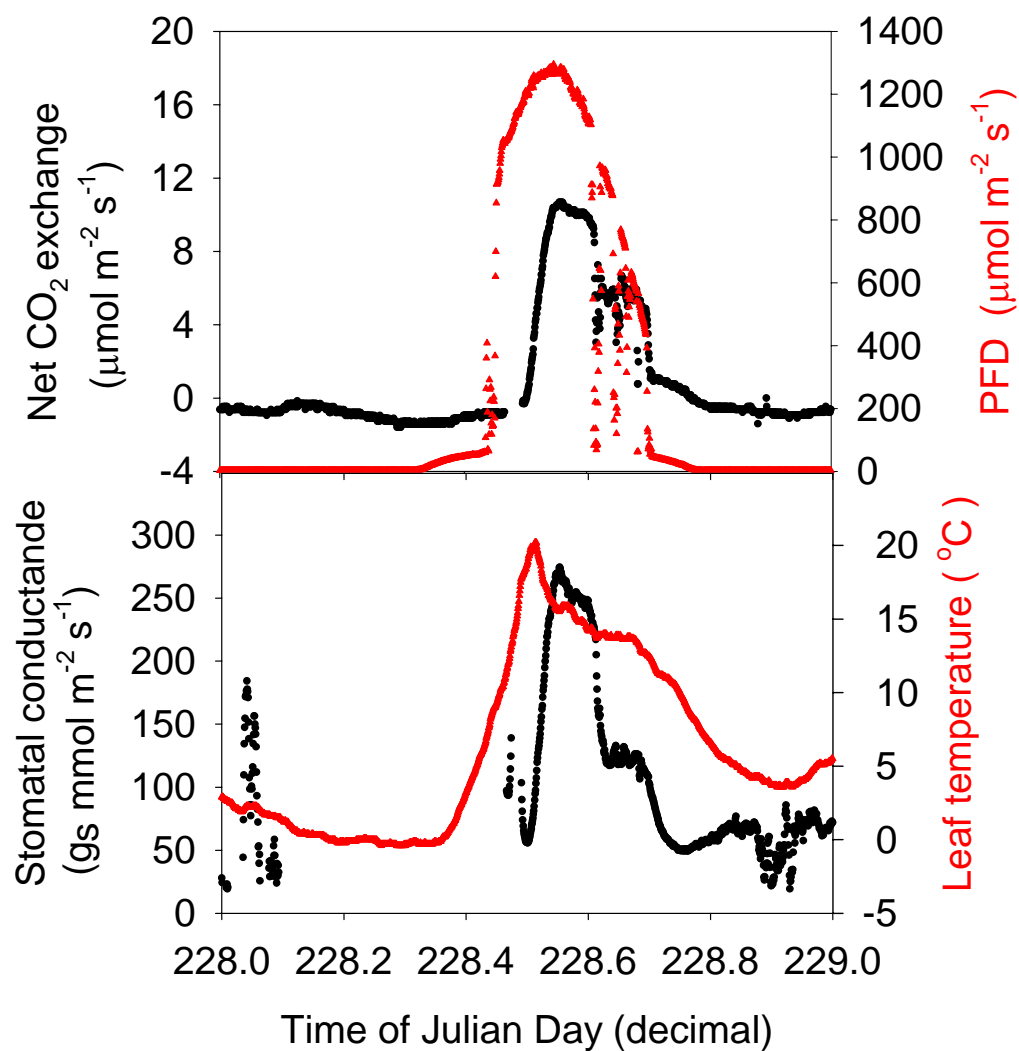
Figure 4.17 Diel patterns of gas exchange, leaf temperature and PFD for a cold, winter day, Day 228 (16th August, 2006); mean temperature 6.2 °C, maximum 20.2 °C and minimum -0.4 °C. Upper Panel: Net CO$_2$ exchange (black, left-hand axis) and PFD (red, right-hand axis). Lower Panel: Stomatal conductance to water vapour (g$_s$, black, left-hand axis) and leaf temperature (red, right-hand axis).
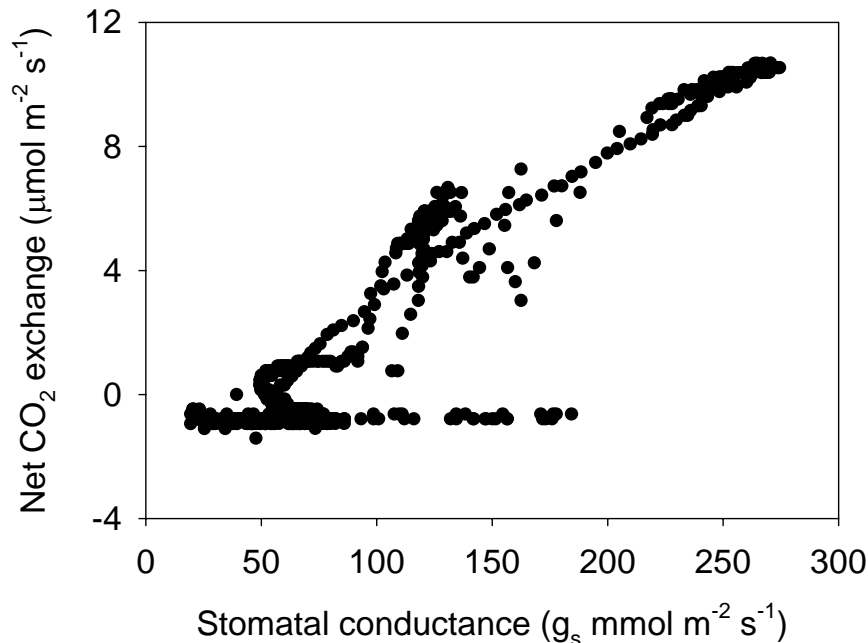
Figure 4.18   Net CO$_2$ exchange versus stomatal conductance, g$_s$. Data for Julian Day 228 (16th August, 2006) see Figure 4.17 for details.

This phenomenon is further examined in Figure 4.19 which presents the courses of PFD and net CO$_2$ exchange for three days with different temperature regimes. Day 210 (29th July) had a very low overnight temperature of -0.9 ^{o}C and had a long delay before net CO$_2$ exchange became activated despite high PFD. At the other extreme, Day 224 had an overnight minimum of 5.7 ^{o}C and relatively low PFD but there was no delay in net CO$_2$ exchange. The third day, Day 209, was intermediate in that the overnight temperature was 0.0 ^{o}C, PFD was high and the delay less than for Day 210. These results suggest that net CO$_2$ exchange and stomatal conductance were suppressed by low overnight temperatures. The length of time before the increase in net CO$_2$ exchange began each day may be related to the severity of the overnight chilling, the colder the temperatures the longer the delay.

Day 225 was a warm day with maximum/mean/minimum temperatures of 17.7/10.4/8.1 ^{o}C, and there was no delay in the activation of net CO$_2$ exchange or stomatal conductance (figure 4.14).   In contrast the temperatures for Day 228 were 20.2/6.2/-0.4 ^{o}C,

87

respectively, and there was a delay in activation of net CO_2 exchange and stomatal conductance until midday (figure 4.14). Day 225 shows a typical saturation response of net CO_2 exchange to PFD (figure 4.20, Upper Panel) whilst the period of minimal net CO_2 exchange can be clearly seen for the time period from 10^{00} to 12^{00} for Day 228,(Lower Panel).
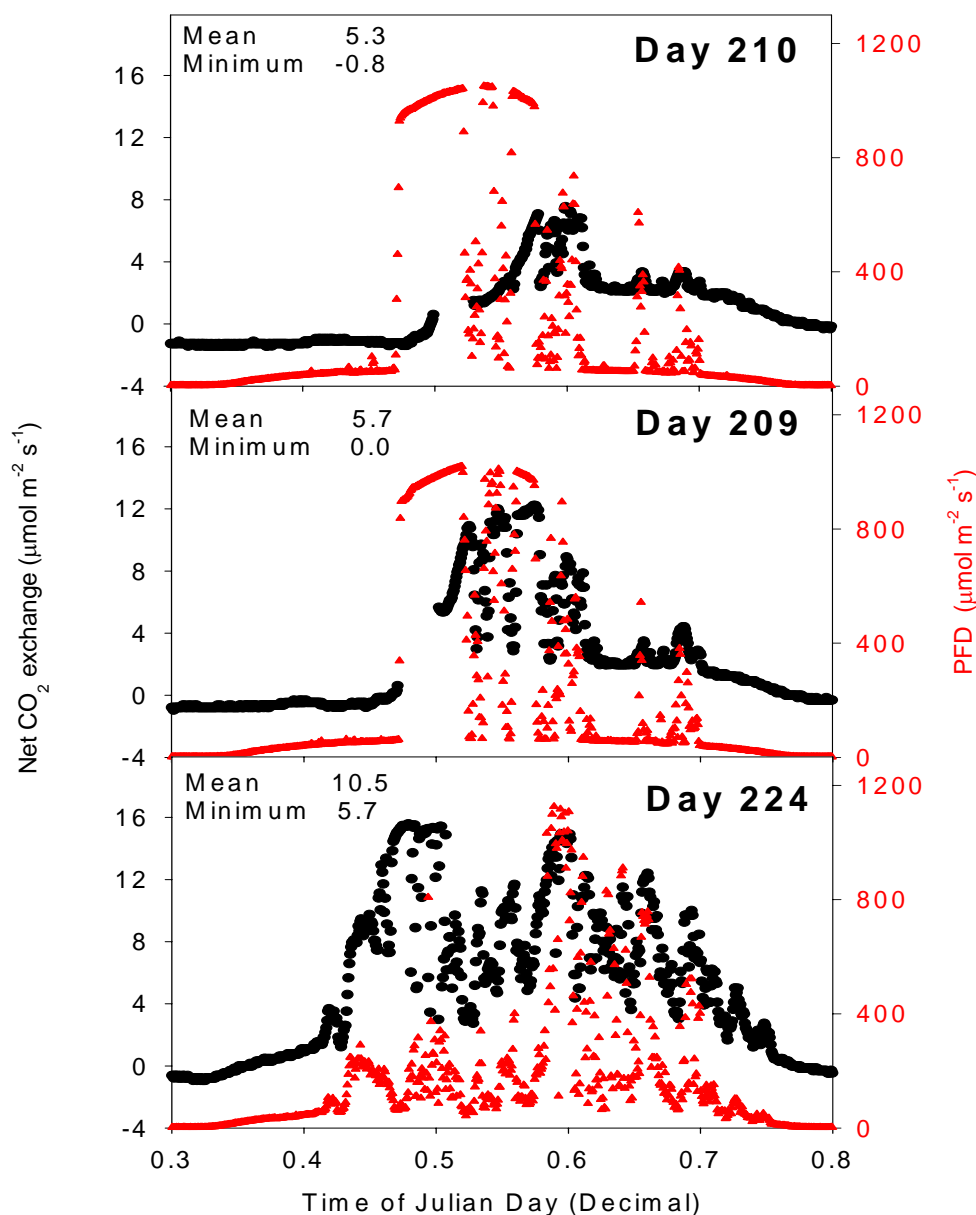
Figure 4.19 Diurnal patterns of net CO_2 exchange (black, left-hand axis) and PFD (red, right-hand axis) between approximately 7am and 7pm on three days with different temperature regimes. Upper Panel, Day 210 (29th July, 2006) with a mean temperature of 5.3 ºC and minimum of -0.8 ºC; Middle

Panel, Day 209 (28th July, 2006) with a mean temperature of 5.7 $^{\circ}$C and minimum of 0.0 $^{\circ}$C; and Lower Panel, Day 224 (12th August, 2006) with a mean temperature of 10.5 $^{\circ}$C and minimum of 5.7 $^{\circ}$C.
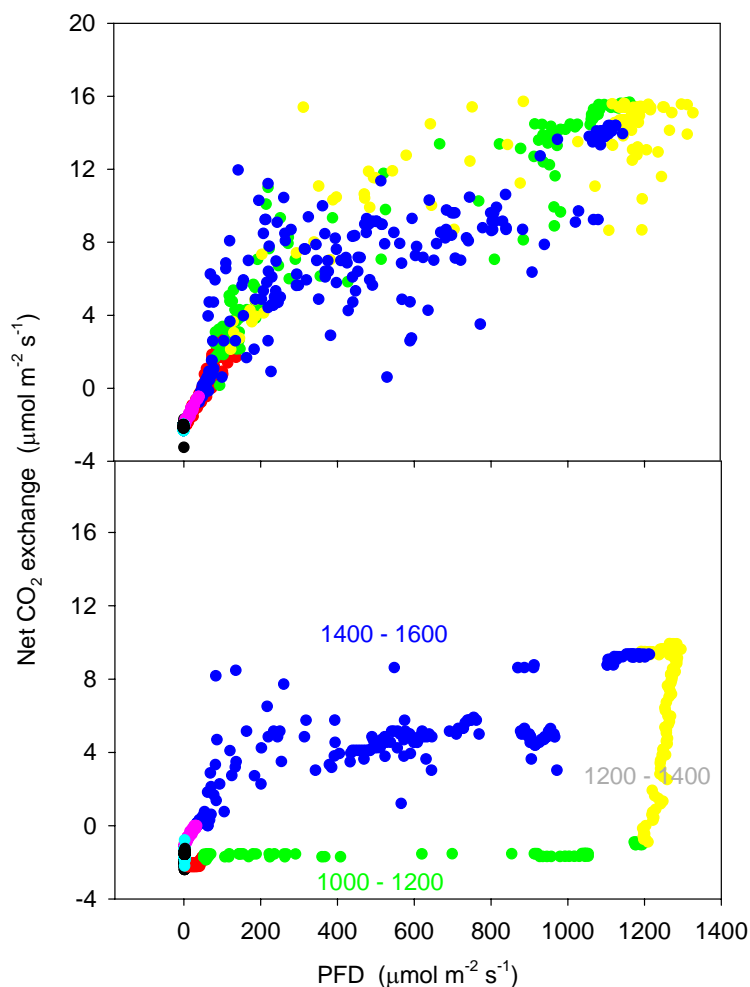
Figure 4.20 Relationship between net CO2 exchange and PFD for: Upper panel; Day 225 (13th August, 2006) and Lower panel; Day 228 (16th August, 2006). Mean and minimum temperatures were 10.4, 6.0 and 6.3, 0.4 for Days 225 and 228, respectively. A time sequence through the day is represented by colour code chart, explained below.

Time colour coding

●	-	0000 to 0800	●	-	0800 to 1000
●	-	1000 to 1200	●	-	1200 to 1400
●	-	1400 to 1600	●	-	1600 to 1800
●	-	1800 to 2400			

4.3.6 CO_2 exchange – temperature relations

The relationship between mean net CO_2 exchange and mean air temperature for the 23 days from Day 206 (25th July, 2006) to Day 228 (16th August, 2006) is presented in Figure 4.21. There is a highly significant (P < 0.0001, R^2 = 0.83) correlation between mean net CO_2 exchange and daily mean air temperature for days with optimal PFD. This suggests that, in winter, days at optimal PFD there will be lower productivity at a mean daily temperature below 10 ^{o}C.
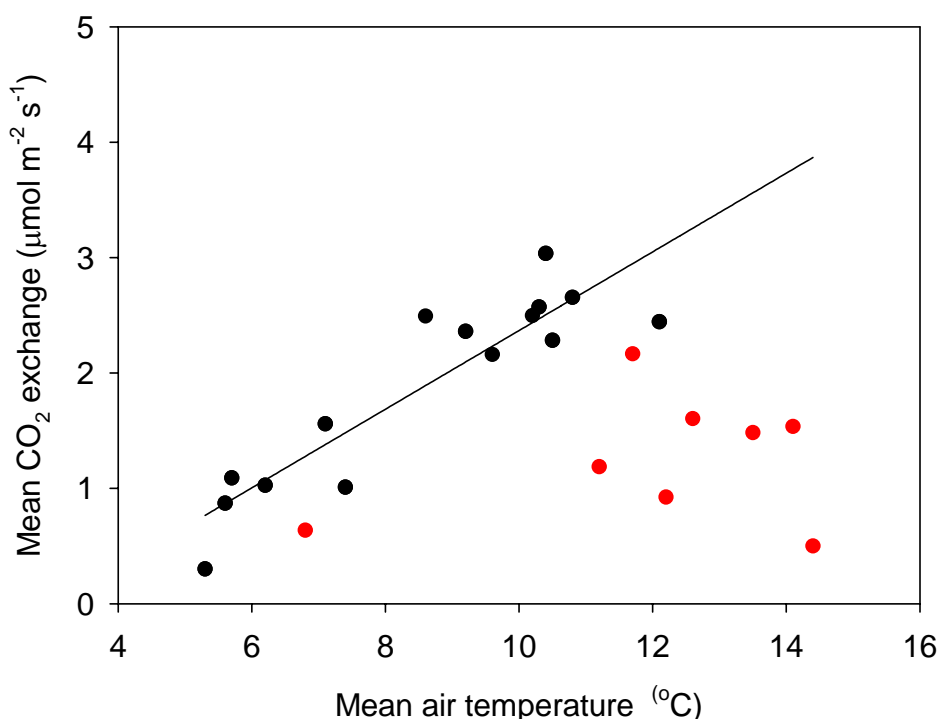
Figure 4.21 Mean CO_2 exchange rate versus mean air temperature for the period Day 206 (25th July, 2006) to Day 228 (16th August, 2006). The black symbols are for values obtained with high light days with maximal PFD over 1000 μmol m^{-2} s^{-1}, and the red symbols for values from cloudy days with maximal PFD below 1000 μmol m^{-2} s^{-1}. The regression line is fitted only to the black symbols (days with PFD exceeding saturating levels for net CO_2 exchange) and is significant, P< 0.0001, adjusted R^2 = 0.81.

4.4   Foliar nitrogen and magnesium application trial

The trial had two main parts, the first was to monitor and explain the occurrence of winter yellowing in leaves, and the second was to evaluate the apparent leaf function recovery of the yellowed leaves after a standard industry spray treatment.   In the absence of any strongly yellow leaves in the primary study area, block 'A', experimental samples were chosen from trees adjacent to the main study area that were showing signs of yellowing.   Two sets of 15 apparently similar leaves were selected by eye. One set was the control whilst the other received the standard industry spray regime.   In the event it turned out that the control leaves were significantly different from the treatment leaves from the start.   It is, therefore, important to look at trends in the results rather than comparing absolute values.   The trial was carried out on 23rd August 2006, under typical winter conditions.

4.4.1   Results: Chlorophyll content

The chlorophyll content of leaves for the control was 33.6 SPAD units, which was lower than the chlorophyll content of leaves to be sprayed with foliar nitrogen and magnesium. The difference in chlororphyll content between leaves at the start of the experiment was maintained for the duration of the trial.   Application of foliar nitrogen and magnesium had no significant effect on the chlorophyll content.   The SPAD values found were lower than for healthy green leaves which are typically around 60 SPAD units.
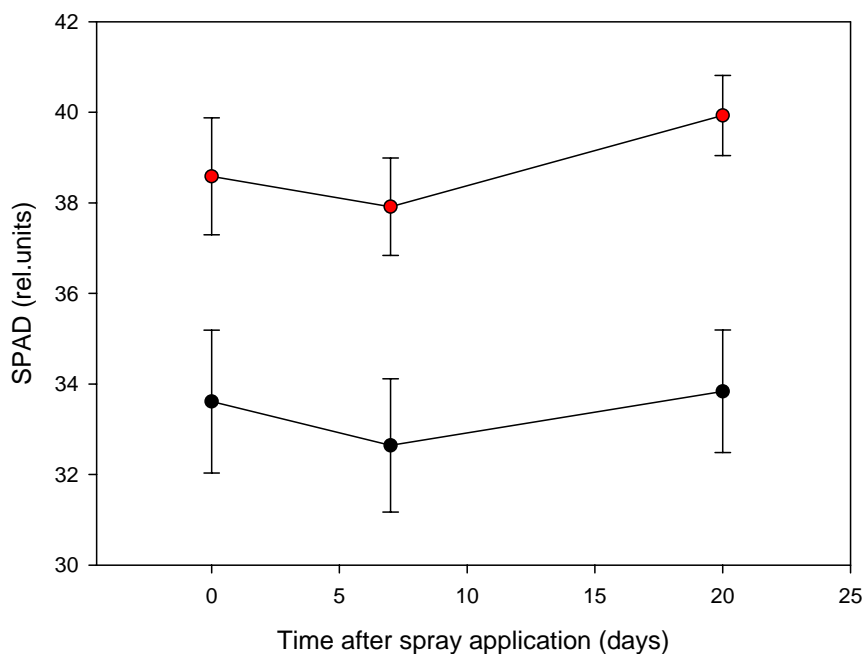
Figure 4.22 Chlorophyll content measured in SPAD units with (red) and without spray application (black). Error bars are standard error of the mean, n= 75. Day zero is initial values, prior to spray application.

4.4.2 Results: Leaf nitrogen

Twenty days after the spray application, 5 sprayed leaves, 5 control leaves and 5 unsprayed but green leaves from the same tree were analysed for leaf nitrogen content. Application of foliar low-biuret urea increased leaf nitrogen by 29% relative to control leaves, but was 26% below nitrogen levels found in green avocado leaves (table 4.4).

Table 4.4 Leaf nitrogen content for sprayed and control leaves, n = 5. Values with different letters are significantly different, p < 0.05.

Treatment	Leaf colour	Mean %N
Control	Yellow	1.53 a
Sprayed	Yellow	1.98 b
Control	Green	2.65 c

4.4.3 Results: Leaf colour

Leaf colour was measured using a Minolta Chroma Meter CR-200b (Minolta, Osaka, Japan) before spraying and then again 1 and 3 weeks after spraying. Three values were recorded. The lightness value (L*) measures reflectance, where zero equals perfectly black and 100 equals perfectly white, whilst the a* and b* colour values represent horizontal chromaticity coordinates, with the a* variable representing green (- a*) to red (+ a*) and b* representing blue (- b*) to yellow (+ b*).
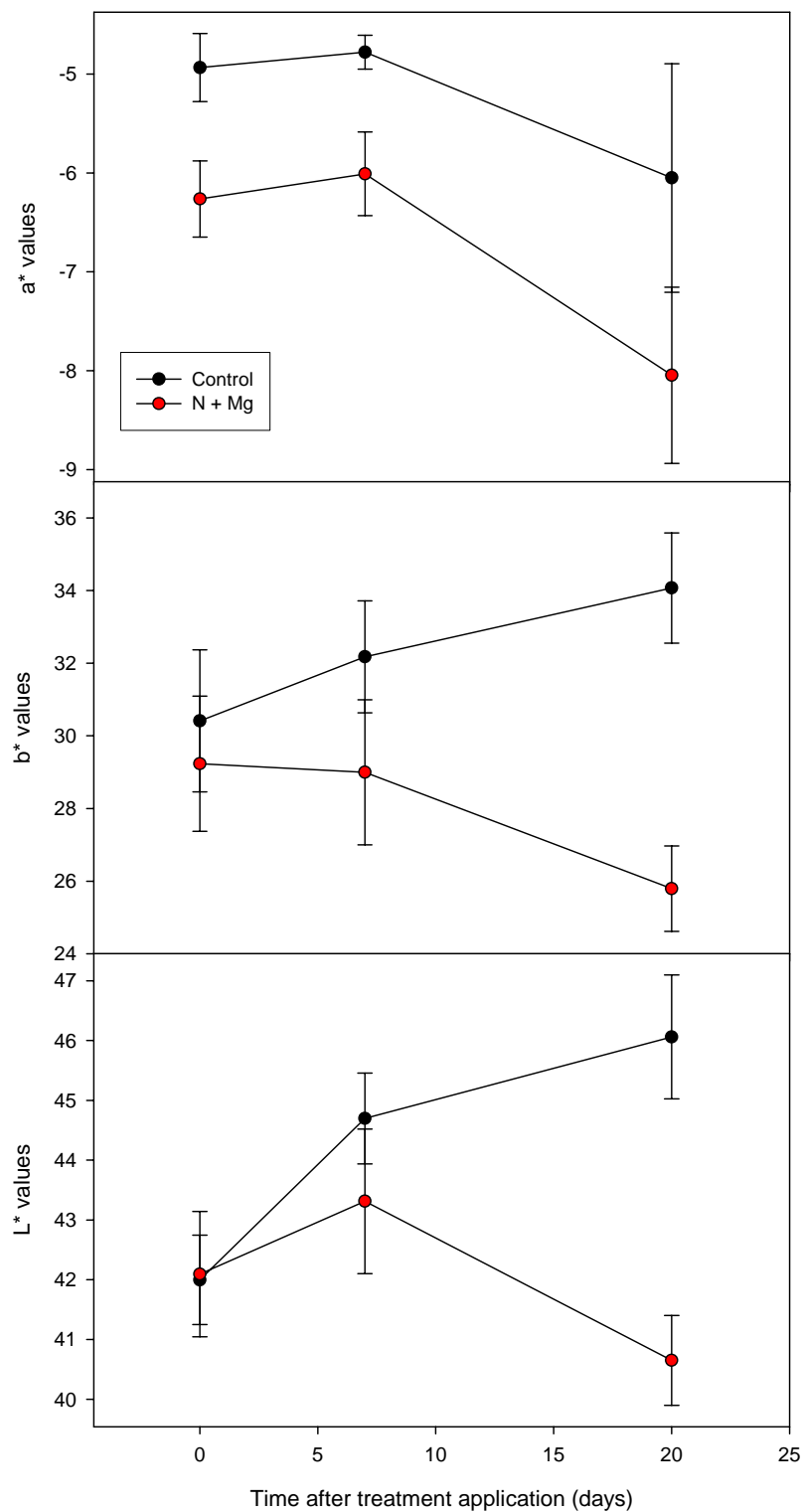
Figure 4.23 Colour change valves with (red) and without spray application (black), a*; upper panel, b*; middle panel and L*; lower panel. Error bars are standard error of the mean, n = 45. Day zero are initial values, prior to spray application.

Before treatment, both control and treatment leaves had a mean L* value of around 42.0 (figure 4.24). One week after spraying, both the treated and control leaves became lighter, with a mean L* values of 43.1 and 44.7, respectively. However, three weeks after spraying, control leaves had continued to become lighter, 46.0, whilst treated leaves had reversed their previous trend and, at 40.8, were darker than prior to spray application.

The b* value showed a similar pattern to the L* value, with control and treatment leaves diverging so that the controls became increasingly yellow with time and the sprayed leaves became less yellow. Results from the third axis in the three dimensional colour coordinate scheme, the a* value, were inconclusive. Control leaves were less green than treated leaves before the application of a spray treatment. Both control and sprayed leaves showed an increase in green colour by three weeks after spraying however this decrease was small and can be considered negligible in comparison to the L* and b* colour coordinate results. The treated leaves became visibly greener, with a lime green colour, starting at the petiole end, replacing the yellow colour of the leaves prior to spraying. The leaves investigated were selected because they were yellow at the onset of the experiments. Without the foliar nitrogen and magnesium treatment the leaves became increasingly yellow. The application on the foliar nitrogen and magnesium treatment was successful in preventing further yellowing of the leaves.

4.4.4 Gas exchange and Chlorophyll fluorescence
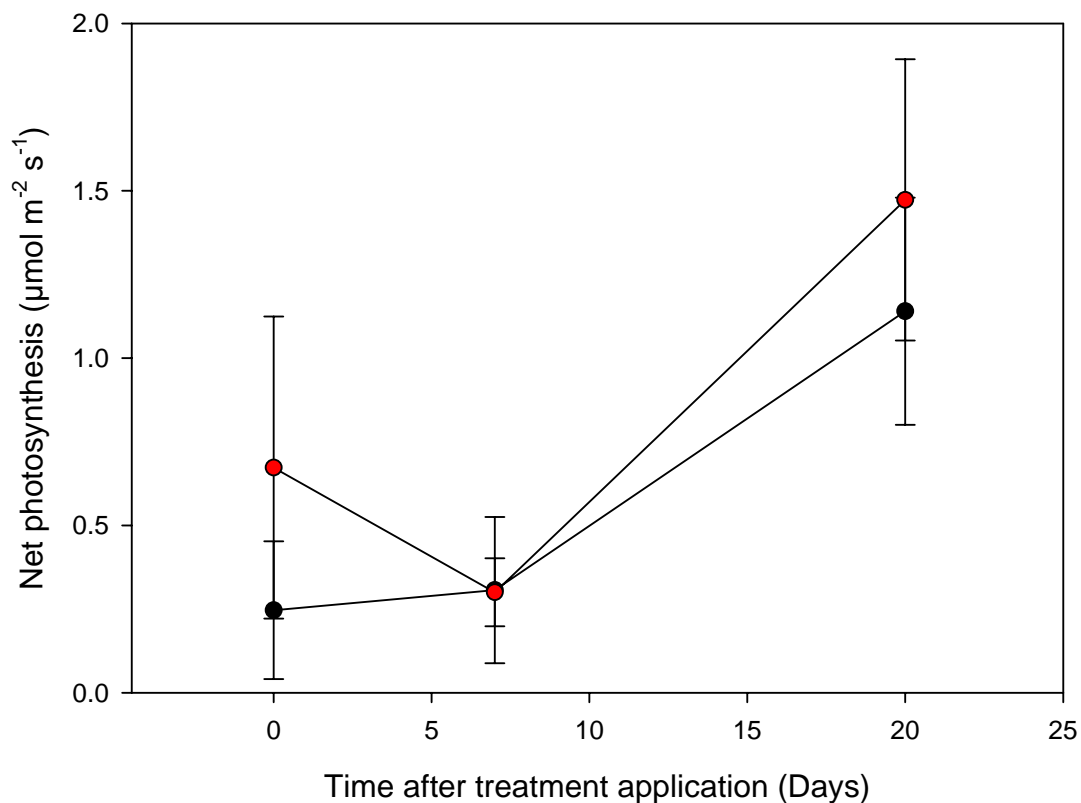
Figure 4.24   Net photosynthesis under saturating light conditions with (red) and without spray application (black). Error bars are standard error of the mean, n= 15. Initial values, prior to spray application, were made on Day Zero.

Gas exchange measurements were made with the CIRAS-1 differential gas exchange measurement system (PP Systems, Massachusetts, USA). The yellow leaves were relatively photosynthetically inactive in comparison to healthy, green leaves with a maximal net photosynthetic rates of less than 2 μmol m^{-2} s^{-1} compared to normal values of over 15 μmol m^{-2} s^{-1} (figure 4.24). Initial net photosynthesis was less than 1.0 μmol m^{-2} s^{-1} for both control and foliar nitrogen treated trees. There was no significant difference in net photosynthesis under saturating light conditions between treatments.
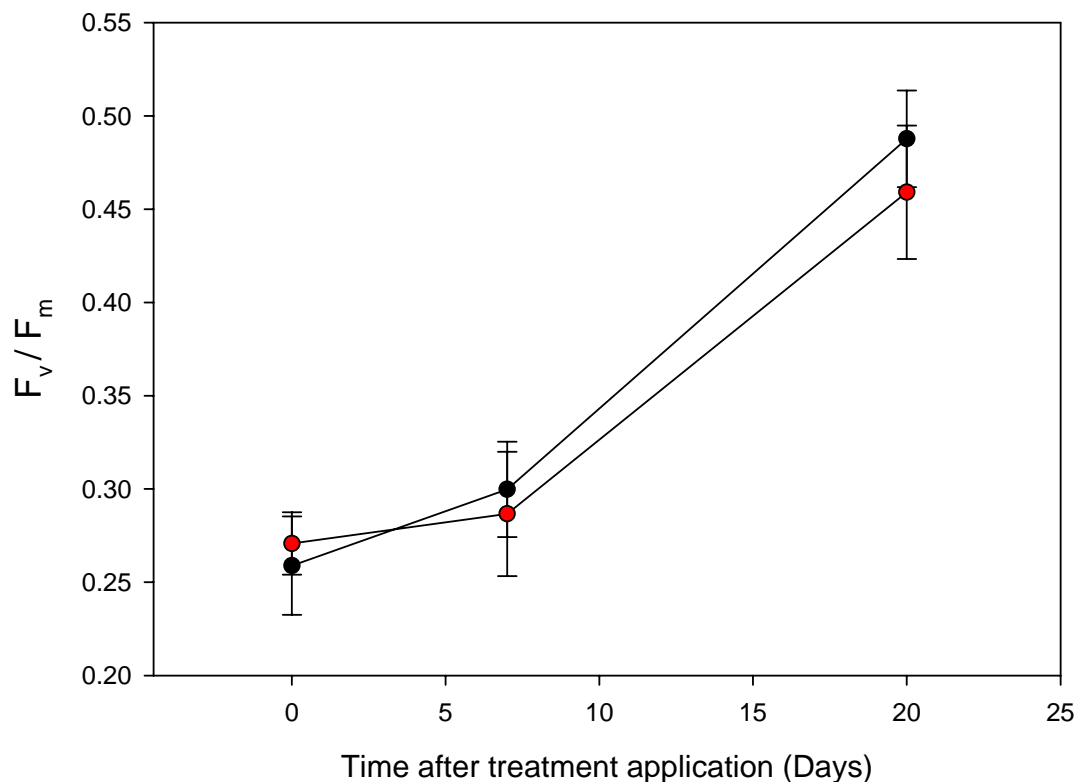
Figure 4.25 Chlorophyll fluorescence, F_v/F_m with (red) and without spray application (black). Error bars are standard error of the mean, n= 15. Day zero is initial values, prior to spray application.

Chlorophyll fluorescence measurements of maximal quantum efficiency of PSII (F_v/F_m) were made with the Mini-PAM using the standard procedures in Methods (Heinz Waltz GmbH, Effeltrich, Germany).   Quantum efficiency (F_v/F_m) ratios were very low, indicating significant damage to PSII (figure 4.25). The F_v/F_m ratio increased for both control and sprayed leaves rising from approximately 0.26 at the start to approximately 0.47 three weeks after spray application. However, there was no significant difference in F_v/F_m ratio between the treatments, suggesting that the foliar nitrogen and magnesium treatment has no effect on F_v/F_m ratio and the improvement in F_v/F_m ratio was a product of natural repair of PS II.

5 Discussion

5.1 The 'perception'

Production by the New Zealand avocado industry has not increased significantly since 2001 and has remained at 8.86 tonnes/ha despite having a target of 15 tonnes/ha. Potential causes for low production have been sought and there is considerable interest in the occurrence of so-called leaf-yellowing. Leaf yellowing appears to follow periods of cold temperature in winter and is perceived to be an indication of a decline in their chlorophyll content resulting in a large reduction in net photosynthetic rate and consequential decline in carbon reserves. This would be an important problem because it could restrict leaf longevity and reduce overall plant resources for the coming spring flowering. This thesis was planned to provide the information to test this perception. At the time the thesis started there was not only no real evidence as to what leaf yellowing was, let alone what caused it, but also there was an almost complete lack of information about the photosynthetic performance of avocado under New Zealand conditions. By New Zealand conditions is meant the growing of the species at what is generally accepted to be close to its southern limit for economic production.

5.2   The original premise
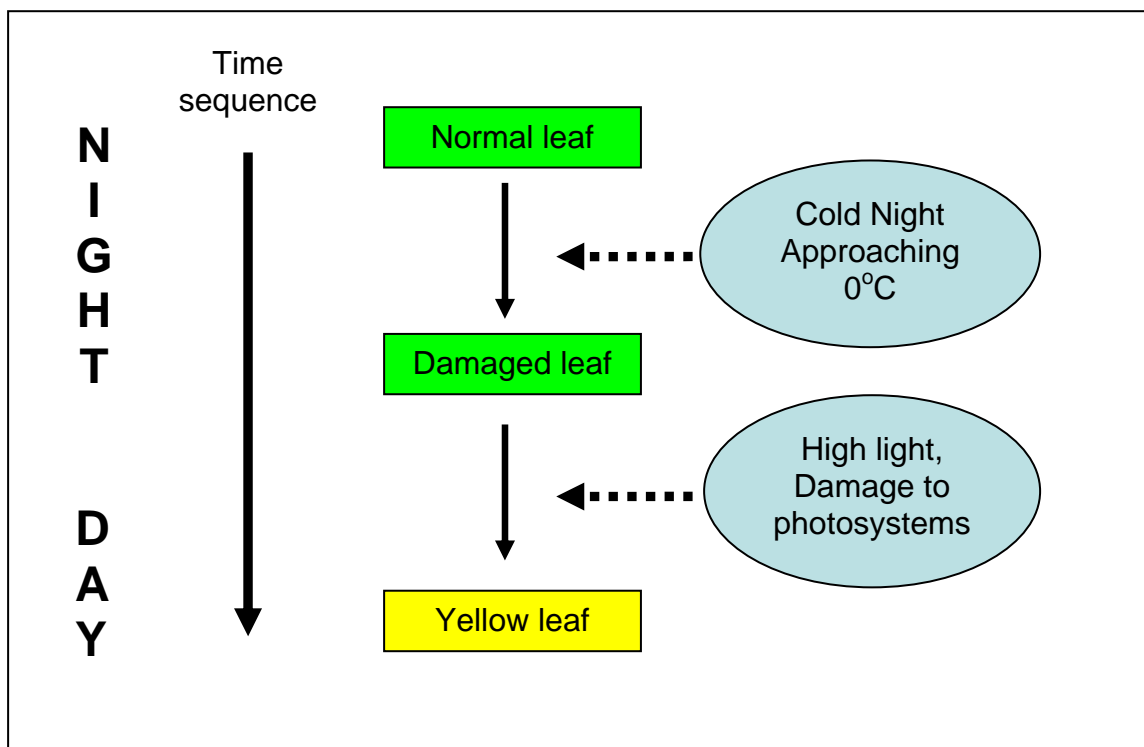
Figure 5.1   The premise: time sequence of overnight leaf chilling, leading to leaf-yellowing after exposure to high incident light levels the following day.

The premise presented in the Introduction (figure 5.1) proposes that there is time sequence that will lead to leaf yellowing. The main stages will be:

a.   Cold temperatures, at least chilling ($<4\ ^{o}C$) and possibly freezing (air below $0\ ^{o}C$).

b.   Reduction in leaf net photosynthesis due to the cold.

c.   Photosystem damage (photoinhibition and photo-oxidation) following exposure to high light (full sunlight) whilst net photosynthesis is reduced.

d.   Chronic photosystem damage that leads to chlorophyll breakdown and produces leaf yellowing.

The industry response is to spray with a urea/magnesium mixture that, anecdotally, will produce a rapid return to normal leaf colour and function.

5.3   The actual results

5.3.1 Cold and chilling

There is no doubt that suitable microclimate conditions occurred that would be expected to initiate the occurrence of leaf yellowing. Between January and September there were 56 chill nights (nights with temperature below 4°C) and 23 air frosts. Mean monthly temperatures were <10°C for June and July and mean day temperatures were <10°C for half of the days from 5th May to 7th September (4 months). Although these data were from a neighbouring site they were confirmed by the results from the diel measurements using the CMS400 which had 10 days of the 23 day period with a mean temperature of <10°C.

5.3.2 Reduced leaf net photosynthesis occurred

There was conclusive evidence that the cold nights resulted in decreased net photosynthesis. The results from the continuous monitoring with the CMS400 climatised photosynthesis system showed that a period of decreased, near zero or negative net photosynthesis occurred following nights with very low temperatures close to, or below, freezing. This period of negative net photosynthesis could last until midday, even when full sunlight was present. However, the surprising result was that there then followed a rapid recovery of photosynthetic capacity every day and the actual maximal net photosynthetic rate was loosely and positively correlated to the daily maximal temperature. This pattern of response of photosynthesis to chilling and freezing temperatures seems not to have been previously reported. That it was the carbon fixation pathway that was negatively affected by the cold temperature was clearly shown by the monthly monitoring with the CIRAS porometer. This study found depressed net photosynthesis over the winter with the depression starting in May and ending around the middle of August, dates that coincide closely with the period when days with mean

100

temperatures <10°C occurred. Moreover, the depressed photosynthesis started earlier and ended later on the southern, colder side of the trees.

5.3.3 Photosystem damage

Up until this point in the time sequence in the hypothesis for explaining leaf yellowing everything followed the proposed pattern. However, in strong contrast to the hypothesis and to expectation from studies on other subtropical plants like mango, coffee, tomato and maize (Allen & Ort, 2001), almost no evidence of photosystem damage was found for avocado. The most compelling evidence comes from the monthly porometric study. Although the decline in net photosynthesis occurred earlier, it fell to negative values and was reduced for longer on the south side of the tree than the north, there was no indication at all of any photosystem involvement. The optimal quantum efficiency of photosystem II (F_v/F_m) remained close to 0.83, the optimal values for normal higher plant leaves, right through the entire winter. On the northern side of the trees, where substantial declines in Fv/Fm might be expected because of the high PFD (full sunlight), there was evidence of a lowered quantum efficiency but values fell only to around 0.72, which is not regarded as serious photoinhibition. In a more complete daily study the decline was found but only to around 0.78 and it is important to note that recovery was already occurring in the afternoon.

Equally compelling were the data from the continuous measurements by the climatised cuvette. Although the photosynthesis was effectively non-existent for the whole morning while saturating PFD occurred there was obviously no damage to the photosystems because net photosynthesis recovered rapidly, in around an hour, to reach normal maximal values. This would not have been possible if there had been damage to Photosystem II. In studies on mango, for example, the decline in net photosynthesis does not occur until around midday and is then imposed by closing stomata, and is followed by rapid photoinhibition and photodamage (Allen et al. 2000). Chill-induced lowered net photosynthesis with low Fv/Fm (around 0.41) has been reported for avocado (Whiley et al. 1999) in Australia, but such low levels were never found in this study.

101

The results show that low temperatures did indeed cause lowered net photosynthesis in avocados and that this was some form of direct impact on the carbon reduction cycle and did not follow earlier damage to the photosystems. In fact, the absence of obvious photodamage of any form is surprising and indicates that the avocado has strong protection against light stress. This is perhaps an adaptation to its original, cloud forest, habitat where rapid and large changes in incident PFD are expected (Wolstenholme & Whiley, 1999).

5.3.4 Where to from here with the cause or causes of leaf yellowing?

The original hypothesis on which this thesis was planned was not supported. However, leaf yellowing obviously does occur and the following is a suggested route for further investigation. It was impressive that through the entire winter with many frosts and two months with mean temperatures below $10^{o}C$, there were no signs of any leaf yellowing. Leaf yellowing is, from anecdotal evidence, a late winter event. In the late winter, early spring, a flush with flowering occurs and this is known from studies in California to be a time of major nitrogen demand in the tree. Under such conditions it is possible that the trees seek a source of nitrogen within themselves. An obvious candidate would be under-performing leaves with lower than normal carbon reserves. Typically these would be older, shaded leaves but the situation would be mimicked by chilled leaves. Under these conditions the chilled leaves would rapidly lose nitrogen and go yellow as the chlorophyll and photosystem nitrogen was withdrawn.

It is suggested that, rather than being a coincidence of chilling and high PFD, the leaf yellowing follows a coincidence of chilling and flowering i.e. during cool spring temperatures.

5.3.5 Handling the leaf yellowing when it occurs; foliar application of urea as a restorative treatment for leaf colour

Leaves were treated with a foliar nitrogen and magnesium spray used by growers to return leaf colour to leaves that have become yellow. Fifteen leaves on 5 trees were sprayed with 1% Low-biuret urea and 0.5% magnesium sulphate till run off. Leaf colour, nitrogen content, SPAD chlorophyll content, maximum net CO_2 exchange and chlorophyll a fluorescence were monitored.

Colour was returned to the treated leaves, with a lime green colour replacing the yellow. Colour values showed a clear shift in colour 20 days after spraying with a decrease in leaf yellowing and a decrease in leaf lightness of colour for treated leaves. Untreated leaves by contrast continued to become increasingly yellow.

Leaf function was severely reduced at the time of the trial, with net photosynthesis at saturation light intensities less than 1.5 µmol m^{-2} s^{-1}, compared with 9 – 12 µmol m^{-2} s^{-1} for normal function. The application of foliar nitrogen and magnesium had no apparent effect on net photosynthesis. The F_v/F_m ratios obtain by investigating chlorophyll a fluorescence were also low at the beginning of the trial, less than 0.30, indicating that the yellow leaves selected had significant damage to PSII. These values improved to approximately 0.47 at the last measurement 20 days after spray application. This indicates that the leaves have may have been in a state of natural repair at the time of the spray trial. However, at no time was there a significant difference in F_v/F_m ratio between treatments, with the improvement in potential performance of control leaves being identical to sprayed leaves.

The foliar application of nitrogen and magnesium was able to increase leaf nitrogen by 29% and reverse leaf yellowing after 20 days, but had no discernable improvement on leaf function.

It is highly possible that there was no return of leaf function after 20 days simply because the leaves were too depleted of leaf nitrogen to be restored quickly and only a season length recovery period would be sufficient. However, this does not align with the anecdotal evidence of rapid return obtained from growers.

It is recommended that this trial be repeated, ensuring all leaves are similar prior to spray application, that more than one orchard is utilised and possibly earlier in the winter, at the very first signs of leaf yellowing.

5.3.6 The effect of chilling on productivity

The results suggest that the productivity of avocadoes in the major growing areas of New Zealand could be severely depressed by winter chilling. When, on a daily basis, mean net CO_2 exchange is related to mean day temperature productivity was seen to be decreased on days when mean temperature fell below 10°C. This is a temperature that is reasonable for a plant with subtropical origins (Allen & Ort, 2001). The depression was strong and, at a mean day temperature of 6°C which was reached on four days of the 23 day study, the mean CO_2 exchange would be only 44% of that at 10°C (figure 5.2). Zero net CO_2 exchange would be reached at a mean daily temperature of about 3°C, around 3K lower than the lowest measured in the orchards in this study. Chilling lowered productivity on about 7 of the 23 analyzed in detail. In addition, another 7 days had decreased mean net CO_2 exchange because of low PFD so that productivity was actually lower than the potential on 14 of the 23 days. Of importance though, is that chilling effectively doubled the number of days with reduced productivity.
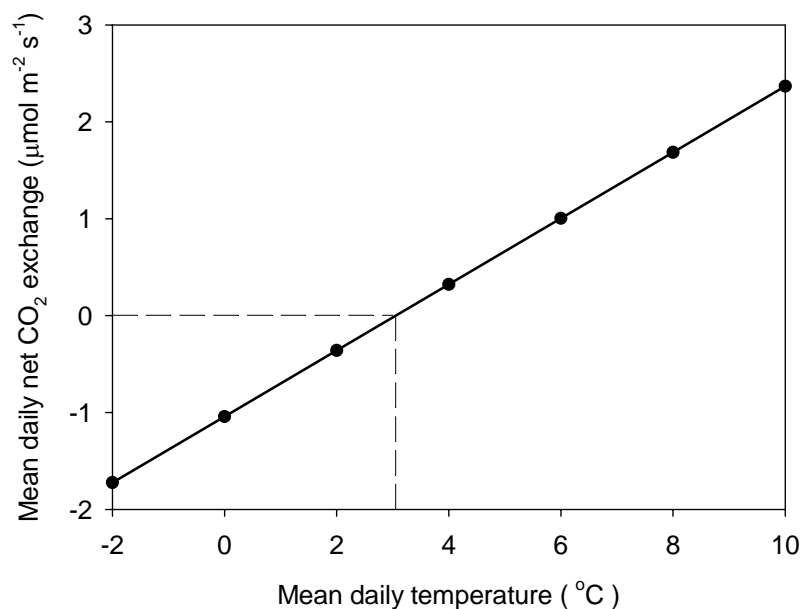
Figure 5.2   Modelled relationship between mean daily net CO2 exchange and mean daily air temperature, from the diel gas exchange results. Fitted line is significant ($p < 0.0001$) for the original data. Zero net CO2 exchange occurs at about 3C. The line is modelled only for days on which saturating PFD occourred.

5.4   Conclusions

- Avocado trees suffer decreased net photosynthesis on days with a mean daily temperature below about 10°C. The decrease can be severe and, at 6°C, the lowest mean temperatures measured, net CO_2 exchange was only 44% of that at 10°C.

- The decrease in photosynthesis appears to be due to a direct effect on the carbon reduction pathway.

- The decreased photosynthesis follows an unusual pattern in that full recovery seems to occur at some time during the day.

- No photodamage of significance was found and the avocado seems to be highly protected against high light when photosynthesis is inhibited.

- Leaf yellowing is not caused by photodamage following depressed photosynthesis.

105

- A new hypothesis is proposed which suggests that leaf yellowing is produced by the re-allocation of nitrogen from leaves during cold weather during flowering. It is suggested that the chilled leaves are seen as unproductive, old or shaded leaves by the plant.

- A foliar application of nitrogen and magnesium was able to increase leaf nitrogen by 29% and reverse leaf yellowing after 20 days, but had no discernable improvement on leaf function.

- Avocados in the major New Zealand growing areas seem to suffer considerable loss in productivity due to chilling. Chilling seems to double the number of days with reduced productivity above those caused by low PFD alone.

5.5 Recommendations for future work:

This thesis was focussed on a hypothesis to explain leaf yellowing that appeared at the start to be reasonable. The original hypothesis was not sustained whilst significant loss of productivity due to chilling was found. It is suggested that:

a. Leaf yellowing be further investigated using the new hypothesis suggested here as the structure for the research.

b. That some form of orchard recording be introduced to better understand the timing and severity of leaf yellowing.

c. It is recommended that the leaf treatment trial be repeated, ensuring all leaves are similar prior to spray application, that more than one orchard is utilised and at the very first signs of leaf yellowing.

d. There is considerable scope to further investigate the degree of net photosynthesis depression by chilling temperatures and also to clarify the protection methods being used by the trees to avoid leaf photodamage.

References

Alexander, A. (1985). *Foliar Fertilization* (Vol. 22). Dortrecht: Martinus Nijhoff Publishing.

Allen, D. J., & Ort, D. R. (2001). Impacts of chilling temperatures on photosynthesis in warm-climate plants. *Trends in Plant Science, 6*(1), 36-42.

Allen, J. A., Ratner, K., Gillner, Y. E., Gussakovsky, E. E., Shahak, Y., & Ort, D. R. (2000). An overnight chill induces a delayed inhibition of photosynthesis at midday in mango (*Mangifera indica* L.). *Journal of Experimental Botany, 51*, 1893-1902.

Arpaia, M. L., Meyer, J. L., Witney, G. W., Bender, G. S., Stottlemyer, D. S., & Robinson, P. R. (1996). The Cashin creek nitrogen fertilizer trial - What did we learn? *California Avocado Society 1996 Yearbook, 80*, 85-98.

Avocado Industry Council. (2006a). *Annual report statistics*. Tauranga: Avocado Industry Council.

Avocado Industry Council. (2006b). *Growers' manual*: Avocado Industry Council.

Aziz, A. B. A., Desouki, I., El-Tanahy, M. M., Abou-Aziz, A. B., & Tanahy, M. (1975). Effect of nitrogen fertilization on yield and fruit oil content of avocado trees. *Scientia Horticulturae, 3*(1), 89-94.

Bar, Y., Lahav, E., & Kalmar, D. (1987). Seasonal changes in nitrogen concentration in avocado leaves associated with leaf age and fertilisation regime. *South African avocado growers' association Yearbook, 10*, 57-58.

Bergh, B. O. (1985). Persea Americana. In A. H. Halevy (Ed.), *Handbook of flowering* (Vol. 5, pp. 253-268). Florida: CRC Press.

Bergh, B. O. (1992). The origin, nature and genetic improvement of the avocado. *California Avocado Society 1992 Yearbook, 76*, 61-75.

Björkman, O., & Demmig, B. (1987). Photon yield of O_2 and chlorophyll fluorescence characteristics at 77k among vascular plants of diverse origins. *Planta, 170*(4), 489-504.

Blanke, M. M., & Lovatt, C. J. (1993). Anatomy and transpiration of the avocado inflorescence. *1993 California Avocado research symposium*, 12-14.

Bower, J. P. (1978a). *Ecophysiological studies of three cultivars of Persea americana (Mill.) emphasising photosynthsis and internal water relations.* Unpublished Masters, University of Natal, Pietermaritzburg.

Bower, J. P. (1978b). The effects of shade and water relations in the avocado cv Edranol. *South African avocado growers' association research report, 2*, 59-61.

Bower, J. P., Wolstenholme, B. N., & de Jager, J. M. (1977). Incoming solar radiation and internal water status as stress factors in avocado, *Persea americana* (Mill.) cv Enranol. *South African avocado growers' association Proceedings of the technical committee, 1*, 35-40.

Briggs, R. M., Hall, G. J., Harmsworth, G. R., Hollis, A. G., Houghton, B. F., Hughes, G. R., et al. (Cartographer). (1996). *Geology of the Tauranga area*

Cameron, S. H., Mueller, R. T., & Wallace, A. (1952). Nutrient composition and stomatal losses of avocado trees. *California Avocado Society 1952 Yearbook, 37*, 201-209.

Chartzoulakis, K., Patakas, A., Kofidis, G., Bosabalidis, A., & Nastou, A. (2002). Water stress affects leaf anatomy, gas exchange, water relations and growth of two avocado cultivars. *Scientia Horticulturae, 95*(1-2), 39-50.

Dixon, H. H., & Joly, J. (1895). On the ascent of sap. *Philosophical Transactions of the Royal Society of London, 186*, 563-576.

Dixon, J. (2006). Investments in science. *Avoscene, September 2006,* 18-19.

Groom, Q. J., & Baker, N. R. (1992). Analysis of light-induced depressions of photosynthesis in leaves of a wheat crop during winter. *Plant Physiology, 100*, 1217-1223.

Guo, Y., & Cao, K. (2004). Effect of night chilling on the photosynthesis of two coffee species grown under diffrent irradiances. *Journal of Horticultural Science and Biotechnology, 79*, 713-716.

Hall, D. O., & Rao, K. K. (1999). *Photosynthesis* (6th ed.). Cambridge: Cambridge university press.

Halliwell, B., & Gutteridge, J. M. C. (1989). *Free radicals in biology and medicine* (2nd ed.). Oxford: Oxford University Press.

Hass, R. G. (1935). United States of America Patent No. Plant Patent 139.

Heath, R., Arpaia, M. L., & Mickelbart, M. (2005). Avocado tree physiology - Understanding the basis of productivity. *Proceedings of the California Avocado Research Symposium*, 65-88.

Hewitt, A. E. (1998). *New Zealand soil classification* (2nd ed.): Landcare Research Science Series 1.

Hunt, S. (2003). Measurements of photosynthesis and respiration in plants. *Physiologia Plantarum, 117*, 314-325.

Kimelmann, R. (1979). *The influence of diffrent temperature an light intensities on gas exchange of avocado leaves (Persea americana Mill.).* Hebrew University of Jerusalem, Jerusalem.

Körner, C. (2000). Biosphere responses to CO_2 enrichment. *Ecological applications, 10*, 1590-1619.

Krezdorn, A. H. (1970). Evaluation of cold-hardy avocados in Florida. *Proceedings of the Florida State Horticulture Society, 83*, 382-386.

Krezdorn, A. H. (1973). Influence of rootstock on cold hardiness of avocados. *Proceedings of the Florida State Horticulture Society, 88*, 346-348.

Lawlor, D. W. (2002). Limitation to photosynthesis in water-stressed leaves: stomata vs. metabolism and the role of ATP. *Annuals of Botany, 89*, 871-885.

Li, Y. C., Crane, J. H., Davenport, T. L., & Balerdi, C. F. (1997). Preliminary findings on the effects of foliar-applied urea and boron on plant nutrition, fruit set and yield of avocado trees. *Proceedings of the Florida State Horticulture Society, 110*, 136-138.

Long, S. P., Farage, P. K., & Garcia, R. L. (1996). Measurement of leaf and canopy photosynthetic CO_2 exchange in the field. *Journal of Experimental Botany, 47*(304), 1629-1642.

Lovatt, C. J. (1994). Improving fruit set and yeild of 'Hass' avocado with a spring application of boron and/or urea to the bloom. *California Avocado Society 1994 Yearbook, 78*, 167-173.

Lovatt, C. J. (1996). Nitrogen allocation within the 'Hass' avocado. *California Avocado Society 1996 Yearbook, 80*, 75-83.

Lovatt, C. J. (2001). Properly timed soil-applied nitrogen fertilizer increases yield and fruit size of 'Hass' avocado. *Journal of the American Society for Horticultural Science, 126*(5), 555-559.

Lui, X., Hofshi, R., & Arpaia, M. L. (1999). 'Hass' Avocado leaf growth, abscission, carbon production and fruit set. *Proceedings of the Avocado Brainstorming '99*, 52-55.

Lui, X., Mickelbart, M., Robinson, P. W., Hofshi, R., & Arpaia, M. L. (2002). Photosynthetic Characteristics of Avocado Leaves. *IS on Trop. & Subtrop. Fruits*, 856 - 874.

Mackintosh, L. (2000). Summary climate data information for selected New Zealand locations. *Climate Data Sheets*

Madeira, A. C., Ferreira, A., Varennes, A. d., & Vieira, M. I. (2003). SPAD meter versus tristimulus colorimeter to estimate chlorophyll content and leaf color in sweet pepper. *Communication in soil and plant analysis, 34*(17 & 18), 2461-2470.

Maxwell, K., & Johnson, G. N. (2000). Chlorophyll fluorescence—a practical guide. *Journal of Experimental Botany, 51*, 659-668.

McKellar, M. A., Buchanan, D. W., & Campbell, C. W. (1983). Cold hardiness of two cultivars of avocado and a mango. *Proceedings of the Florida State Horticulture Society, 96*, 212-215.

McKellar, M. A., Buchanan, D. W., Ingram, D. L., & Campbell, C. W. (1992). Freezing tolerance of avocado leaves. *HortScience, 27*(4), 314-343.

Mickelbart, M. V., & Arpaia, M. L. (2002). Rootstock influences changes in ion concentrations, growth, and photosynthesis of 'Hass' avocado trees in response to salinity. *Journal of the American Society for Horticultural Science, 127*(4), 649-655.

Mickelbart, M. V., Miller, R., Parry, S., Arpaia, M. L., & Heath, R. (2000). Avocado leaf surface morphology. *California Avocado Society 2000 Yearbook, 84*, 139-150.

Minolta. (1989). Chlorophyll meter SPAD-502 instruction manual. Tokyo, Japan.

Minolta. (2003). Chroma meter CR-200b manual. Osaka: Minolta Camera Co. Ltd.

Nevin, J. M., & Lovatt, C. J. (1990). Problems with urea-N foliar fertilization of avocado. *Summary of Avocado Research, 1*, 15-16.

Newett, S. D. E. (2005). *Little evidence to support the use of foliar applied nutrients in avocado*: University of California Cooperative extension.

Newett, S. D. E., Crane, J. H., & Balerdi, C. F. (2002). Cultivars and rootstocks. In A. W. Whiley, B. Schaffer & B. N. Wolstenholme (Eds.), *The avocado: botany, production and uses* (pp. 161-187). Oxon: CAB Publishing.

NIWA National Climate Centre. (2006a). *National climate summary - Autumn 2006*. Auckland: NIWA.

NIWA National Climate Centre. (2006b). *National climate summary - Spring 2006*. Auckland: NIWA.

NIWA National Climate Centre. (2006c). *National climate summary - Summer 2005/06*. Auckland: NIWA.

NIWA National Climate Centre. (2006d). *National climate summary - Winter 2006*. Auckland: NIWA.

Porra, R. J., Thompson, W. A., & Kriedemann, P. E. (1989). Determination of accurate extinction coefficients and simultaneous equations for assaying chlorophylls a and b extracted with four different solvents: verification of the concentration of chlorophyll standards by atomic absorption spectrometry. *Biochim Biophys Acta, 975*, 384-394.

Praloran, J. C. (1970). Le Climat des Aires d'origene des avocatiers. *Fruits, 25*, 543-557.

Ramadasan, A. (1980). Gas exchange in the avocado leaves under water stress and recovery. *California Avocado Society 1980 Yearbook, 64*, 147-152.

Rijkse, W. C., & Cotching, W. E. (1995). Soils and land use of part - Tauranga County, North Island, New Zealand. *Landcare Research Technical Record*.

Schaffer, B. (2006). Effects of soil oxygen deficiency on avocado (*Persea americana* Mill.) trees. *Seminario International: Manejo del Riego y Suelo en el Cultivo del Palto La Cruz, Chile*.

Schaffer, B., & Ploetz, R. C. (1989). Net Gas exchange as a damage indicator for phytophthora root rot of flooded and nonflooded avocado. *HortScience, 24*(4), 653-655.

Schaffer, B., & Whiley, A. W. (2002). Environmental physiology. In A. W. Whiley, B. Schaffer & B. N. Wolstenholme (Eds.), *The avocado: Botany, production and uses* (pp. 135-160): CAB.

Schaffer, B., & Whiley, A. W. (2003). Environmental regulation of photosynthesis in avocado trees - A mini-review. *Proceedings of the V world avocado congress*, 335-342.

Schaffer, B., Whiley, A. W., & Kohli, R. R. (1991). Effects of leaf age on gas exchange characteristics of avocado (*Persea americana* Mill.). *Scientia Horticulturae, 48*, 21-28.

Scholander, P. F., Hammel, H. T., Bradstreet, E. D., & Hemmingsen, E. A. (1965). Sap pressure in vascular plants. *Science, 148*(3668), 339-346.

Scholefield, P. B., Walcott, J. J., Kriedemann, P. E., & Ramadasan, A. (1980). Some environmental effects on photosynthesis and water relations on avocado leaves. *California Avocado Society 1980 Yearbook, 64*, 96-106.

Schreiber, U., Bilger, W., & Neubauer, C. (1994). Chlorophyll fluorescence as a nonintrusive indicator for rapid assessment of in vivo photosynthesis. In *Ecophysiology of photosynthesis* (pp. 49-70). New York: Springer.

Scorza, R. S., & Wiltbank, W. J. (1975). Evaluation of avocado cold hardiness. *Proceedings of the Florida State Horticulture Society, 88*, 496-499.

Sharon, Y., Bravdo, B., & Bar, N. (2001). Aspects of the water economy of avocado trees (*Persea americana, cv. Hass*). *South African avocado growers' association Yearbook, 24*, 55-59.

Smith, G. S., Buwalda, J. G., Green, T. G. A., & Clark, C. J. (1989). Effect of oxygen supply and temperature at the root on the physiology of kiwifruit vines. *New Phytologist, 113*, 431-437.

Soil Survey Staff. (1999). *Soil taxonomy* (Vol. 436): USDA Natural resources conservation service.

Storey, W. B., Bergh, B. O., & Zentmyer, G. A. (1986). The origin, indigenous range, and dissemination of the avocado. *California Avocado Society 1986 Yearbook, 70*, 127-133.

Tyree, M. T. (1997). The Cohesion-Tension theory of sap ascent: current controversies. *Journal of Experimental Botany, 48*(315), 1753-1763.

van Kooten, O., & Snel, J. F. H. (1990). The use of chlorophyll fluorescence nomenclature in plant stress physiology. *Photosynthesis research, 25*, 147-150.

von Caemmerer, S., & Farquhar, G. (1981). Some relationships between the biochemistry of photosynthesis and gas exchange of leaves. *Planta, 154*, 376-387.

von Willert, D. J., Matyssek, R., & Herppich, W. (1995). *Experimentelle pflanzenokologie*. Stuttgart: Thieme.

Wei, C., Steudle, E., & Tyree, M. T. (1999). Water ascent in plants: do ondoing controversies have a sound basis? *Trends in Plant Science, 4*(9), 372-375.

Whiley, A. W. (1991, November/December). 'Hass' - Past, present and future. *Talking Avocados,* 5-6.

Whiley, A. W. (1994). *Ecophysiological studies and tree manipulation for maximisation of yeild potential in avocado (Persea americana Mill.).* Unpublished PhD, University of Natal, Pietermaritzburg.

Whiley, A. W., Saranah, J. B., Cull, B. W., & Pegg, K. G. (1988). Manage avocado tree growth cycles for productivity gains. *Queensland agricultural journal, 114*, 29-36.

Whiley, A. W., & Schaffer, B. (1994). Avocado. In B. Schaffer & P. C. Anderson (Eds.), *Handbook of environmental physiology of fruit crops. Vol 2. Sub-tropical and tropical crops* (Vol. 2, pp. 3-35). Boca Raton, Florida: CRC Press.

Whiley, A. W., Searle, C., Schaffer, B., & Wolstenholme, B. N. (1999). Cool orchard temperatures or growing trees in containers can inhibit leaf gas exchange of avocado and mango. *Journal of the American Society for Horticultural Science, 124*(1), 46-51.

Williams, L. O. (1976). The botany of the avocado and its relatives. *Proceedings of the First International Tropical Fruit Short Course: The Avocado*, 9-15.

Witney, G. W., & Arpaia, M. L. (1991). Tree recovery after the December 1990 freeze. *California Avocado Society 1991 Yearbook, 75*, 63-70.

Wolstenholme, B. N. (2004). Nitrogen- the manipulator element: Managing inputs and outputs in diffrent environments. *South African avocado growers' association Yearbook 2004, 27*, 45-61.

Wolstenholme, B. N., & Whiley, A. W. (1999). Ecophysiology of the avocado tree (*Persea americana* Mill.) tree as a basis for pre-harvest management. *Revista Chapingo Serie Horticultura*(5), 77-88.

Zentmyer, G. A. (1991). The genus *Persea*. *California Avocado Society 1991 Yearbook, 75*, 119-123.

Zilkah, S., Klein, I., & Feigenbaum, S. (1987). Translocation of foliar-applied urea ^{15}N to reproductive and vegetive sinks of avocado and its effect on initial fruit set. *Journal of the American Society for Horticultural Science, 112*(6), 1061-1065.

Zilkah, S., Wiesmann, Z., Klein, I., & David, I. (1996). Foliar applied urea improves freezing protection to avocado and peach. *Scientia Horticulturae, 66*, 85-92.